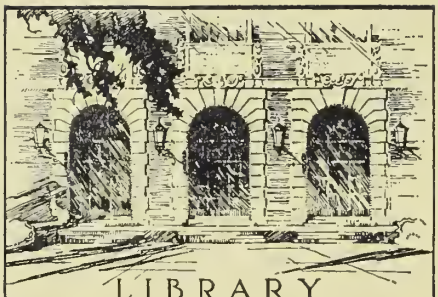

Math

Report No. 352

AN ANALYSIS OF SOME EULERIAN METHODS FOR ONE DIMENSIONAL, INVISCID, COMPRESSIBLE HYDRODYNAMICS

by

Stanley J. Flowerdew

September 22, 1969

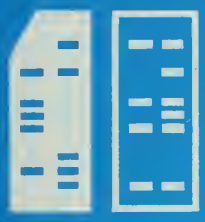

DEPARTMENT OF COMPUTER SCIENCE
UNIVERSITY OF ILLINOIS AT URBANA-CHAMPAIGN · URBANA, ILLINOIS

Report No. 352

AN ANALYSIS OF SOME EULERIAN METHODS FOR ONE DIMENSIONAL, INVISCID, COMPRESSIBLE HYDRODYNAMICS

by

Stanley J. Flowerdew

September 22, 1969

Department of Computer Science
University of Illinois at Urbana-Champaign
Urbana, Illinois 61801

*This work was supported in part by the Advanced Research Projects Agency as administered by the Rome Air Development Center under Contract No. US AF 30(602)4144 and submitted in partial fulfillment of the requirements for the degree of Master of Science in Computer Science, August, 1969.

ACKNOWLEDGMENT

I wish to thank Professor D. L. Slotnick and D. E. McIntyre for directing this thesis. I should like to express my gratitude and appreciation to David McIntyre especially, for contributing many ideas and providing much encouragement during the preparation of this thesis.

Finally, I wish to thank Miss Ramona Andrews for an excellent job of typing this thesis.

ABSTRACT

The description and comparison of several explicit differencing schemes for the solution of the inviscid, non-thermal-conducting, single-material, one-dimensional equations of compressible hydrodynamics is included in this report. The comparison was based on the plots obtained from a series of one dimensional test problems which are included in APPENDIX A.

TABLE OF CONTENTS

Page

1. INTRODUCTION

A shock is a surface discontinuity in a fluid which moves through the fluid. The concept of a discontinuous change in the fluid quantities at the shock position is convenient although, due to viscous effects, the discontinuity is actually replaced by a very narrow region in which the fluid parameters change rapidly. The presence of a shock usually makes the theoretical treatment of the fluid behavior quite difficult. This is because the shock is a moving boundary, along which boundary conditions can be supplied, but whose motion is not a priori known. As a result, analytical solutions in the presence of variable shocks can be obtained only in a few special cases.

The numerical solution of the hydrodynamics equations is also greatly complicated by the presence of shocks. Very smooth flows can be numerically handled in a fairly straight forward manner. However, with most simple numerical methods, oscillations, negative energies and other difficulties arise in the presence of shocks. Another difficulty with shocks is that the gradients are very steep and any refinement of the mesh tends to make the gradients even steeper. One of the standard artifices for handling shocks is artificial viscosity. This method has met with a reasonable degree of success. However, the use of artificial viscosity is almost an art rather than a science for the following reasons:

1. A modification of the original equations is being solved rather than the original equations themselves.

2. There are many different types of artificial viscosity e.g. linear, quadratic, combination of linear and quadratic.
3. The parameters in all artificial viscosity methods are chosen empirically.
4. Artificial viscosity is applied in some regions and subtracted in others, depending on the particular type of artificial viscosity used.

In general, the above make it very hard for a novice to use codes which include artificial viscosity.

The purpose of this report is to compare several differencing schemes which do not use artificial viscosity for solving one dimensional, fluid flows containing shocks. These schemes may be considered logical extensions of the familiar Particle-in-Cell method[1] to the case of a continuous fluid. The differencing schemes are compared by using each of them to approximate the fluid behavior in some special cases when analytical solutions are known and then comparing the results with the analytic solutions.

The selected test problems are identical to those used by Hicks[2,3], who compared the Lax-Wendroff Lagrangian scheme with PUFF (a Lagrangian scheme which uses the Von Neumann-Richtmyer technique of artificial viscosity). Thus, this report enables a simple yet thorough comparison of all five schemes. The test problems include compression waves and rarefaction waves created by the motion of a piston, the collision of two shocks, the overtaking of one shock by another and the shock tube problem.

2. PRELIMINARY THEORY

2.1 Lagrangian and Eulerian Methods

The equations of hydrodynamics are usually written in either the Lagrangian form or the Eulerian form. These two forms are theoretically equivalent although truncated finite difference approximations to them may not be. For each representation, the spatial mesh imposed by the finite difference scheme divides the fluid into cells.

In the Lagrangian formulation, the co-ordinate system is fixed in the fluid and moves with it. The cells of the fluid correspond to elements of mass, and the boundaries of the cells follow the paths of the fluid elements. The equations representing the behavior of an inviscid fluid in a one-dimensional Lagrangian coordinate system are:

$$\frac{\partial V}{\partial t} - \frac{1}{\rho_o}\frac{\partial U}{\partial x} = 0 \qquad (1)$$

$$\frac{\partial U}{\partial t} + \frac{1}{\rho_o}\frac{\partial P}{\partial x} = 0 \qquad (2)$$

$$\frac{\partial I}{\partial t} + P\frac{\partial V}{\partial t} = 0 \qquad (3)$$

$$\frac{\partial x}{\partial t} = U$$

and $$P = f(\rho, I)$$

where V is specific volume, P is pressure, I is specific internal energy, ρ is density, ρ_o is initial density, x is the Lagrangian spatial co-ordinate

and f is a function. The first three equations are the conservation of mass, momentum and energy, respectively, and the fourth is the equation of state.

It has been found that Lagrange calculations work very well for certain types of problems. In particular, in following the motion of thin plates or thin ribbons which move many times their own thickness, Lagrangian codes are very appropriate. In general, fine resolution is found in shock regions at the expense of resolution in rarefaction regions. Also, the motion of material interfaces is closely followed. However, two dimensional Lagrangian codes behave very poorly when turbulence, slip surfaces and other severe distortions exist in the fluid.

The Eulerian formulation describes the variation with time of conditions at a point fixed in space. The fluid can be thought of as flowing through a mesh of cells which is fixed in space. The equations in Eulerian form are

$$\frac{\partial \rho}{\partial t} + \frac{\partial \rho U}{\partial x} = 0$$

$$\frac{\partial U}{\partial t} + U\frac{\partial U}{\partial x} + \frac{1}{\rho}\frac{\partial P}{\partial x} = 0$$

$$\frac{\partial I}{\partial t} + U\frac{\partial I}{\partial x} + \frac{P}{\rho}\frac{\partial U}{\partial x} = 0$$

and $P = f(\rho, I)$

It is possible to transform the Eulerian representation to the equivalent Lagrangian one using the operator $\frac{D}{dt} = \frac{\partial}{\partial t} + U\frac{\partial}{\partial x}$ where $\frac{D}{dt}$ represents the total time variation as "seen" by a particle moving with the fluid. The important property of an Eulerian calculation is that it proceeds without difficulty when there are large distortions of the fluid. However, material interfaces are poorly handled and, in general, it is difficult to resolve small features of the flow moving with the fluid, since the mesh is fixed in space. The use of massless trace particles can partially alleviate this difficulty. Trace particles play no part in the hydrodynamics of the problem. Initially, they are imbedded in the fluid at important locations e.g. along interfaces. The motion of each trace particle is calculated at the end of every time step using a locally assigned velocity for each particle. Thus, the trace particles can be used to follow the motion of Lagrangian interfaces. Another disadvantage with Eulerian methods is that the mesh size is not automatically reduced in areas undergoing compression as it is with Lagrangian methods.

The methods described in this report possess features of both the Lagrangian and Eulerian representations.

2.2 The Particle-in-Cell Method

The particle in cell method (often abbreviated to PIC) was developed at Los Alamos in 1955 by Francis Harlow specifically for the solution of complicated problems in fluid dynamics. It is based on a simple physical model which is mathematically rigorous. PIC is a mixed Lagrangian and Eulerian method retaining some of the advantages

of each. It competes more successfully with two dimensional methods mainly because it handles both severe distortions (an Eulerian property) and material interfaces (a Lagrangian property) well. A brief description of PIC for a single material problem follows.

In PIC, the region through which the fluid moves is divided into a finite mesh of Eulerian cells which are fixed relative to the observer. Associated with the center of each cell is a velocity, an internal energy and the total mass of material in the cell. In addition, as shown in Figure 1, the fluid itself is represented by Lagrangian mass points, or particles, which can move through the Eulerian mesh, thus representing the motion of the fluid. The density of a cell is calculated as the sum of the masses of the individual particles in the cell divided by the volume of the cell. A particle is assumed to have the velocity of the cell in which it resides. The mass of a particle does not change, once a problem has begun and, in one dimension, all particles usually have the same mass.

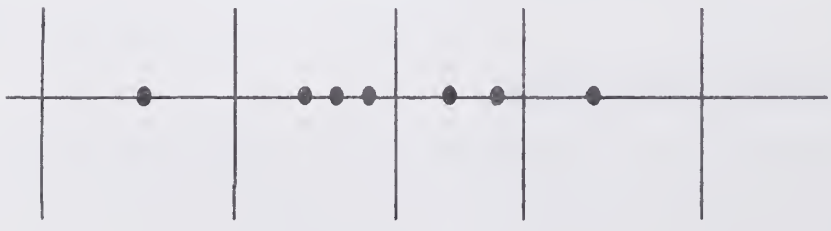

Figure 1. PIC in One Dimension

The first part of the calculation is essentially Lagrangian. Equation (2) is differenced to yield

$$\tilde{U}_j^n = U_j^n - \frac{(P_{j+1}^n - P_{j-1}^n)}{2\Delta x} \frac{\Delta t}{\rho_j^n}$$

where $\tilde{U}_j^n$ is the velocity of the fluid at time $(n+1)\ \Delta t$ and at the position of the fluid which was at the center of cell j at time $n\ \Delta t$. Similarly, $\tilde{I}_j$ is calculated by differencing equation (3). Each particle is then displaced or transported a distance $U_{eff}\ \Delta t$ where U_{eff} is an interpolated value of fluid velocity at the Eulerian position of the particle.

During the transport, each particle is assumed to carry with it the tilde values of velocity and energy of the cell from which it came. The movement of some of the particles across cell boundaries causes a redistribution of mass, momentum and internal energy to take place. This procedure is very much like a Lagrangian time advance followed immediately by a conservative rezone to the original undistorted Eulerian grid.

The diffusion of particles across cell boundaries gives rise to a dissipative force which stabilizes the difference equations and gives PIC many of its desirable characteristics. This dissipative force is frequently referred to as effective viscosity since it is proportional to the velocity gradient. Low velocity flow has caused some difficulty and has led to the use of artificial viscosity in addition to the effective viscosity. The reader should see section 2.4 for a discussion of this topic.

2.3 Shocks

There are two types of surface discontinuity in a fluid. One is called a contact discontinuity and moves with the fluid. It is present at the boundary between two kinds of fluid, and it may arise within one fluid. It is characterized by the continuity of pressure and of the normal velocity component across it.

The other type of discontinuity, the shock, moves relative to the fluid, changing the state of each element as it sweeps by. For the notation used, see Figure 2 in which the shock is moving to the right.

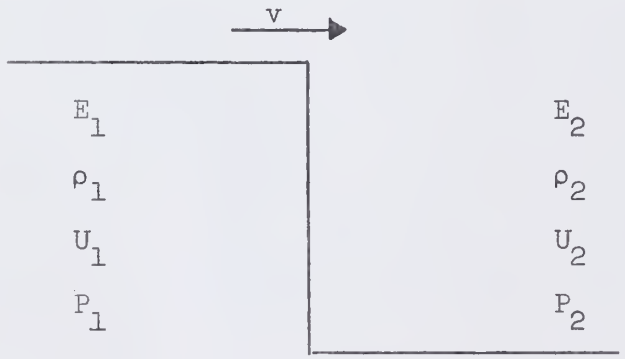

Figure 2. A Shock Moving to the Right

In general, the shock speed, v, is greater than the material speed on either side. Also U_1 is greater than U_2 due to the shock being compressive. The side of the shock front through which the gas enters (the right hand side in Figure 2) will be called the front side of the shock, the other, the back side. The region of flow behind a shock front is frequently called the shock wave. The shock front moves with supersonic speed as observed from the front side, and with subsonic speed as observed

from the back side. There are three equations relating variables on either side of the shock and these are known as the Rankine-Hugoniot conditions.

Rankine-Hugoniot Conditions

These relations are derived by applying the laws of conservation of mass, momentum and energy to the shock.

1 $$m = \rho_2 (v-U_2) = \rho_1 (v-U_1)$$

2 $$m (U_1 - U_2) = P_1 - P_2$$

3 $$m (E_1 - E_2) = P_1U_1 - P_2U_2$$

2.4 Artificial Viscosity

As stated in the introduction, any finite difference scheme to solve the hydrodynamics equations must possess some dissipative mechanism in order to smooth out the discontinuities which occur when shocks are present. Many difficulties in the calculation can arise if no dissipative mechanism is present. In particular, severe oscillations may be obtained. These oscillations remain at approximately the same value as the calculation continues and hence are bounded.

The first dissipative mechanism was introduced by Von Neumann and Richtmyer in 1950 [4] and is known as artificial viscosity because of its similarity to the physical phenomenon. Essentially, they constructed an artificial medium whose final behavior, after experiencing the shock waves, was sufficiently like that of the original medium that it could be used in the hydrodynamics equations in place of the true medium. In their method, the pressure in the momentum and energy equations (2,3) is increased by an artificial viscous term q. In other words p is replaced by p + q where

$$q = -b\ (\Delta x)^2\ \rho\ \frac{\partial U}{\partial x}\ \left|\ \frac{\partial U}{\partial x}\ \right|$$

and b is a constant. This viscous dissipative term causes a diffusion of momentum and energy which has the effect of changing the shock from a discontinuity to a rapid continuous variation of the fluid variables over a narrow region a few mesh spacings wide. This smearing of the shock front dampens oscillations thus enabling calculations to proceed as if there were a smooth flow. Across the narrow region occupied by the shock, the Rankine-Hugoniot equations hold. Artificial viscosity converts kinetic energy into internal energy across shocks thus increasing the entropy.

Artificial viscosity works well in one dimensional codes but has not worked so well in higher dimensions.[5] There are several other types of artificial viscosity in fairly common use e.g. the Landshoff type[6] in which

$$q = q_{NR} + Wq_1 + (1-W)\ q_1$$

where q_{NR} is the Von Neumann-Richtmyer term

and $$q_1 = -\frac{a}{2}\ \rho\Delta x\ U_x$$

$$q_2 = \frac{-(a\rho)^2}{2}\ \frac{\Delta t\ U_x}{\rho_o}$$

with $0 \leq W \leq 1.$

2.5 Effective Viscosity

It has been shown for PIC by Taylor expansions of the difference equations and neglecting higher order terms[1], that solutions to the PIC finite difference equations approximate

$$\rho \frac{\partial U}{\partial t} + \rho U \frac{\partial U}{\partial x} + \frac{\partial P}{\partial x} = \frac{\partial}{\partial x} \left(\lambda' \frac{\partial U}{\partial x}\right) \tag{4}$$

and

$$\rho \frac{\partial I}{\partial t} + \rho U \frac{\partial I}{\partial x} + P \frac{\partial U}{\partial x} = \frac{\partial}{\partial x} \left(\lambda' \frac{\partial I}{\partial x}\right) + \lambda' \left(\frac{\partial U}{\partial x}\right)^2 \tag{5}$$

where $\lambda' = \frac{1}{2} \Delta x \, \rho U$

more closely than

$$\rho \frac{\partial U}{\partial t} + \rho U \frac{\partial U}{\partial x} + \frac{\partial P}{\partial x} = 0$$

and

$$\rho \frac{\partial I}{\partial t} + \rho U \frac{\partial I}{\partial x} + P \frac{\partial U}{\partial x} = 0$$

Some of the terms on the right hand side of equations (4) and (5) are proportional to the velocity gradient and can be related to the physical concept of viscosity. These additional terms arise as a result of the mass transport mechanism and are responsible for producing the dissipative effects that give stability to the method. Thus, PIC and its related methods are a class of codes whose dissipative force is referred

to as effective viscosity or implied viscosity or smoothing. These terms allow PIC to give accurate approximations to high velocity flow. The λ' terms have their principal effectiveness in regions where the velocity gradient is large or where fluctuations occur in high speed flow. At low fluid speeds or in regions of near stagnation, the velocity gradients are small and hence the effective viscosity terms are not large enough to make the dissipative force effective so that oscillations develop. These oscillations will grow until they become comparable to the local sound speed when the effective viscosity terms become large enough to prevent any further growth of the instabilities (as in test problem 6B). Thus, the instabilities are bounded. These difficulties can be alleviated by the use of artificial viscous pressure terms in the equations for momentum and energy (see section 2.4). However, these terms should be added only where the fluid speed is small compared to the local sound speed. If applied in high velocity regions, the artificial viscosity will smear out many features of interest.

Some authors question whether the smoothing scheme in PIC can be directly related to physical concepts.[7,8] They have tried to show that doing so results in many contradictions. For example, the values of the additional terms far exceed the values of the analogous physical terms.

3. DERIVATION OF THE DIFFERENCE EQUATIONS

The region occupied by the fluid is considered to be discretized into a mesh of equal sized cells fixed in space. Each cell is of width Δx and is assigned some index j. Half integer indices are used to denote cell boundaries.

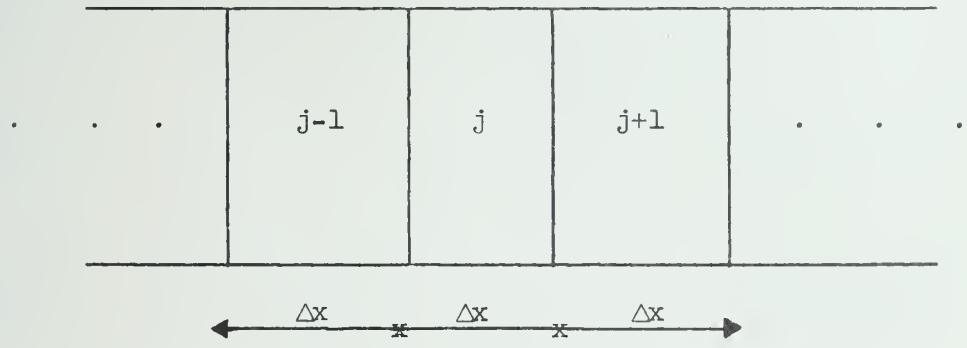

Figure 3. The Mesh of Cells

The fluid is then described at any instant of time by specifying the velocity, density and pressure for each cell. These values are considered to be known at the center of each cell. The calculation advances explicitly in time steps i.e. cell quantities at time $(t + \Delta t)$ are calculated in terms of values of those quantities at t.

The system of equations to be solved is

$$\frac{\partial \rho}{\partial t} + \frac{\partial}{\partial t}(\rho U) = 0 \qquad (6)$$

$$\frac{\partial U}{\partial t} + U\frac{\partial U}{\partial x} + \frac{1}{\rho}\frac{\partial P}{\partial x} = 0 \qquad (7)$$

$$\frac{\partial E}{\partial t} + U \frac{\partial E}{\partial x} + \frac{1}{\rho} \frac{\partial}{\partial x} (PU) = 0 \qquad (8)$$

and $P = f(\rho, I)$

which represent the conservation of mass, momentum and energy and the equation of state, respectively, where the symbols have their usual meanings. As in PIC, the solution is accomplished by performing first a Lagrangian update, then rezoning to the original Eulerian mesh. During the Lagrangian phase, the operator $\frac{\partial}{\partial t} + U\frac{\partial}{\partial x}$ is replaced by $\frac{D}{dt}$, the total derivative. Equations (7) and (8) then become

$$\frac{DU}{dt} + \frac{1}{\rho} \frac{\partial P}{\partial x} = 0 \qquad (9)$$

$$\frac{DE}{dt} + \frac{1}{\rho} \frac{\partial (PU)}{\partial x} = 0 \qquad (10)$$

Equation (10) can be rewritten as

$$\frac{\partial}{\partial t} [I + \tfrac{1}{2}U^2] + \frac{1}{\rho} \frac{\partial}{\partial x} (PU) = 0$$

$$\text{or } \frac{\partial I}{\partial t} + \frac{P}{\rho} \frac{\partial U}{\partial x} + U[\frac{\partial U}{\partial t} + \frac{1}{\rho} \frac{\partial P}{\partial x}] = 0$$

Now, equation (9) implies that

$$\frac{\partial I}{\partial t} + \frac{P}{\rho} \frac{\partial U}{\partial x} = 0 \qquad (11)$$

The intermediate or tilde values of velocity and specific internal energy at the end of the Lagrangian advance are given by the following equations.

3. DERIVATION OF THE DIFFERENCE EQUATIONS

The region occupied by the fluid is considered to be discretized into a mesh of equal sized cells fixed in space. Each cell is of width Δx and is assigned some index j. Half integer indices are used to denote cell boundaries.

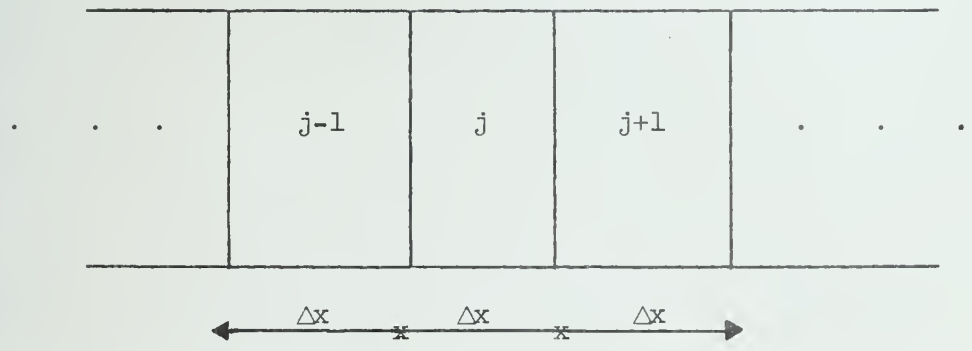

Figure 3. The Mesh of Cells

The fluid is then described at any instant of time by specifying the velocity, density and pressure for each cell. These values are considered to be known at the center of each cell. The calculation advances explicitly in time steps i.e. cell quantities at time $(t + \Delta t)$ are calculated in terms of values of those quantities at t.

The system of equations to be solved is

$$\frac{\partial \rho}{\partial t} + \frac{\partial}{\partial t}(\rho U) = 0 \qquad (6)$$

$$\frac{\partial U}{\partial t} + U\frac{\partial U}{\partial x} + \frac{1}{\rho}\frac{\partial P}{\partial x} = 0 \qquad (7)$$

$$\frac{\partial E}{\partial t} + U \frac{\partial E}{\partial x} + \frac{1}{\rho} \frac{\partial}{\partial x} (PU) = 0 \qquad (8)$$

and $P = f(\rho, I)$

which represent the conservation of mass, momentum and energy and the equation of state, respectively, where the symbols have their usual meanings. As in PIC, the solution is accomplished by performing first a Lagrangian update, then rezoning to the original Eulerian mesh. During the Lagrangian phase, the operator $\frac{\partial}{\partial t} + U\frac{\partial}{\partial x}$ is replaced by $\frac{D}{dt}$, the total derivative. Equations (7) and (8) then become

$$\frac{DU}{dt} + \frac{1}{\rho} \frac{\partial P}{\partial x} = 0 \qquad (9)$$

$$\frac{DE}{dt} + \frac{1}{\rho} \frac{\partial (PU)}{\partial x} = 0 \qquad (10)$$

Equation (10) can be rewritten as

$$\frac{\partial}{\partial t} [I + \tfrac{1}{2}U^2] + \frac{1}{\rho} \frac{\partial}{\partial x} (PU) = 0$$

$$\text{or } \frac{\partial I}{\partial t} + \frac{P}{\rho} \frac{\partial U}{\partial x} + U\left[\frac{\partial U}{\partial t} + \frac{1}{\rho} \frac{\partial P}{\partial x}\right] = 0$$

Now, equation (9) implies that

$$\frac{\partial I}{\partial t} + \frac{P}{\rho} \frac{\partial U}{\partial x} = 0 \qquad (11)$$

The intermediate or tilde values of velocity and specific internal energy at the end of the Lagrangian advance are given by the following equations.

$$\tilde{U}_j^n = U_j^n - (P_{j+1}^n - P_{j-1}^n) \frac{\Delta t}{2 \rho_j^n \Delta x} \tag{12}$$

$$\tilde{I}_j^n = I_j^n - (\bar{U}_{j+1}^n - \bar{U}_{j-1}^n) \frac{P_j^n \Delta t}{2 \rho_j^n \Delta x} \tag{13}$$

where $\bar{U}_j^n = \frac{1}{2} [U_j^n + \tilde{U}_j^n]$

These intermediate values correspond to values at time $(n+1)\,\Delta t$ at the point in the fluid that was at the center of cell j at time $n\,\Delta t$. To first order, the tilde quantities are values at time $(n+1)\,\Delta t$ at the Eulerian point $x_j + U_j^n \Delta t$. The use of time-centered values of velocity $\bar{U}_j^n$ in the equation for $\tilde{I}_j^n$ results in greater stability and better behavior of fluid entropy than if the simple value U_j^n were used.[9] Equation (14) is used to calculate the intermediate value of specific energy.

$$\tilde{E}_j = \tilde{I}_j + \frac{1}{2} (\tilde{U}_j)^2 \tag{14}$$

The distorted Lagrangian mesh is now rezoned back to the original Eulerian mesh. In effect, this is a mass transport across cell boundaries. The mass flow across the interface between cell j and cell $(j + 1)$ is defined by

$$\Delta M_{j+\frac{1}{2}}^n = \rho_{j+\frac{1}{2}}^n \; U_{j+\frac{1}{2}}^{*n} \; \Delta t$$

The quantity $U_{j+\frac{1}{2}}^{*n}$ is known as the weighted velocity.

Three techniques for calculating $U_{j+\frac{1}{2}}^{*n}$ define the three differencing schemes used in this report which are called continuous rezone, OIL and donor. The interface values of density and velocity cannot be calculated by simply

averaging adjacent cell values, because the method obtained is highly unstable and virtually useless. The density weighting and velocity weighting, as they are called, must be done with greater care. The equations for the density weighting and velocity weighting are simply stated in this section but are derived at length in section 3.1. The direction of the flow at the interface between cell j and cell (j+1) is defined by the sign of $\tilde{U}_{j+\frac{1}{2}}^{n}$ where $\tilde{U}_{j+\frac{1}{2}}^{n} = \frac{1}{2}[\tilde{U}_{j}^{n} + \tilde{U}_{j+1}^{n}]$.

Density Weighting for all schemes

If $\tilde{U}_{j+\frac{1}{2}}^{n} > 0$ then $\rho_{j+\frac{1}{2}}^{n} = \rho_{j}^{n}$

If $\tilde{U}_{j+\frac{1}{2}}^{n} = 0$ then $\rho_{j+\frac{1}{2}}^{n} = \frac{1}{2}[\rho_{j}^{n} + \rho_{j}^{n+1}]$

If $\tilde{U}_{j+\frac{1}{2}}^{n} < 0$ then $\rho_{j+\frac{1}{2}}^{n} = \rho_{j+1}^{n}$

Velocity Weighting

(a) continuous rezone

If $U_{j+\frac{1}{2}}^{n} \geq 0$ then $U_{j+\frac{1}{2}}^{*n} = \dfrac{\tilde{U}_{j+\frac{1}{2}}^{n}}{1 + (\tilde{U}_{j+1}^{n} - \tilde{U}_{j-1}^{n})\frac{\Delta t}{2\Delta x}}$

If $\tilde{U}_{j+\frac{1}{2}}^{n} < 0$ then $U_{j+\frac{1}{2}}^{*n} = \dfrac{\tilde{U}_{j+\frac{1}{2}}^{n}}{1 + (\tilde{U}_{j+2}^{n} - \tilde{U}_{j}^{n})\frac{\Delta t}{2\Delta x}}$

(b) OIL

$$U_{j+\frac{1}{2}}^{*n} = \frac{\tilde{U}_{j+\frac{1}{2}}^{n}}{1 + (\tilde{U}_{j+1}^{n} - \tilde{U}_{j}^{n})\frac{\Delta t}{\Delta x}}$$

density for the other two schemes gives fairly good results.

The three velocity weighting schemes used in this report are described below.

3.1.1 Continuous Rezone

Assume that the cell in the diagram is moving from left to right.

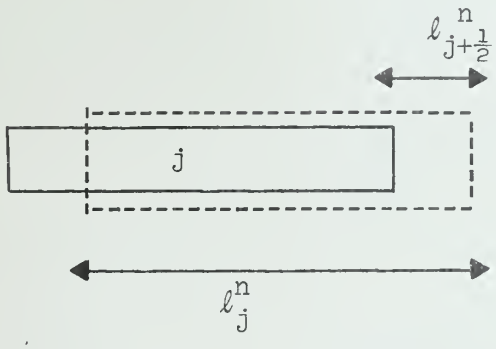

Figure 4. Continuous Rezone

The undashed rectangle in Figure 4 represents the position of cell j at time n. The dashed rectangle represents the position of the same rectangle after the initial Lagrangian flow. The density, specific internal energy and momentum are assumed constant throughout the dashed cell. The velocity and specific internal energy at the center of the dashed cell are given by equations (12) and (13) respectively. The quantity of mass which is in the dashed cell and has crossed over into Eulerian cell (j+1) during the rezone is calculated from the fraction

$$\Delta M^n_{j+\frac{1}{2}} = \frac{\ell^n_{j+\frac{1}{2}}}{\ell^n_j} M^n_j \qquad (16)$$

since the density over the dashed cell is assumed constant. The mass of

cell j before the Lagrangian step equalled M_j^n and this obviously equals the mass in the dashed cell after the Lagrangian step. It can be seen that to first order

$$\ell_j^n = \Delta x + (\tilde{U}_{j+\frac{1}{2}}^{n_{\frac{1}{2}}} - \tilde{U}_{j-\frac{1}{2}}^{n_{\frac{1}{2}}}) \Delta t$$

and $$\ell_{j+\frac{1}{2}}^{n_{\frac{1}{2}}} = \tilde{U}_{j+\frac{1}{2}}^{n_{\frac{1}{2}}} \Delta t$$

Hence $$\Delta M_{j+\frac{1}{2}}^{n_{\frac{1}{2}}} = \frac{\tilde{U}_{j+\frac{1}{2}}^{n_{\frac{1}{2}}} \Delta t \, \rho_j^n}{1 + (\tilde{U}_{j+1}^n - \tilde{U}_{j-1}^n) \frac{\Delta t}{2 \Delta x}}$$

Hence from equation (16)

$$U_{j+\frac{1}{2}}^{*n_{\frac{1}{2}}} = \frac{\frac{\tilde{U}_j^n + \tilde{U}_{j+1}^n}{2}}{1 + (\tilde{U}_{j+1}^n - \tilde{U}_{j-1}^n) \frac{\Delta t}{2 \Delta x}}$$

If the flow is from right to left, then a similar analysis yields

$$U_{j+\frac{1}{2}}^{*n_{\frac{1}{2}}} = \frac{\frac{\tilde{U}_j^n + \tilde{U}_{j+1}^n}{2}}{1 + (\tilde{U}_{j+2}^n - \tilde{U}_j^n) \frac{\Delta t}{2 \Delta x}}$$

3.1.2 OIL

The OIL velocity weighting scheme has been in use for some time in two dimensional calculations[10]. The derivation of OIL is similar to that of continuous rezone except that the cell to be followed is centered at the interface between cells j and (j+1), and is Δx in length.

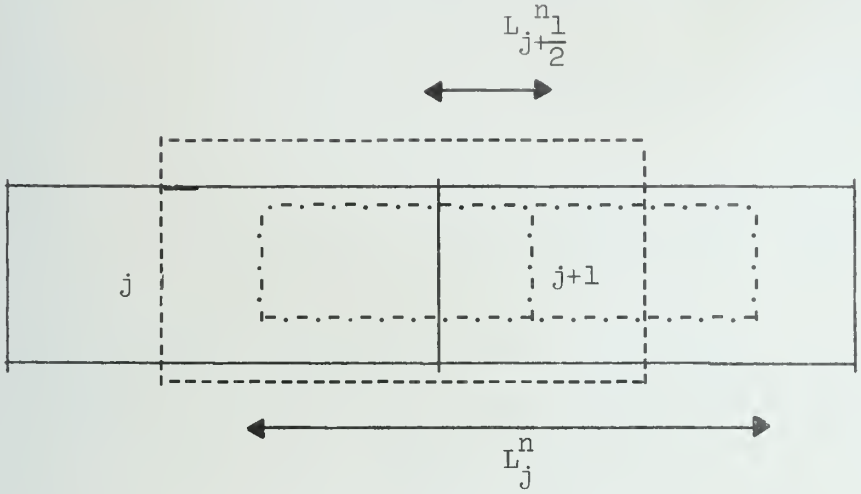

Figure 5. OIL

The mass transported into cell (j+1) by the Lagrangian transport step is

$$\Delta M_{j+\frac{1}{2}}^{n+\frac{1}{2}} = \frac{L_{j+\frac{1}{2}}^{n+\frac{1}{2}} M_j^n}{L_j^n}$$

where $L_j^n = \Delta x + (\tilde{U}_{j+1}^n - \tilde{U}_j^n)\ \Delta t$

and $L_{j+\frac{1}{2}}^{n+\frac{1}{2}} = \tilde{U}_{j+\frac{1}{2}}^{n+\frac{1}{2}}\ \Delta t$

Hence $U_{j+\frac{1}{2}}^{*n+\frac{1}{2}} = \dfrac{\tilde{U}_{j+\frac{1}{2}}^{n+\frac{1}{2}}}{1 + (\tilde{U}_{j+1}^n - \tilde{U}_j^n)\ \frac{\Delta t}{\Delta x}}$

The same analysis holds if the flow is in either direction. Another derivation using Taylor Series expansions can be found in reference [10].

3.1.3 Donor

The value of velocity chosen is simply the tilde velocity of the donor cell. Hence

$$U^{*n}_{j+\frac{1}{2}} = \tilde{U}_j^{\,n} \quad \text{if } \tilde{U}^{n}_{j+\frac{1}{2}} > 0$$

$$U^{*n}_{j+\frac{1}{2}} = 0 \text{ if } \tilde{U}^{n}_{j+\frac{1}{2}} = 0$$

$$U^{*n}_{j+\frac{1}{2}} = \tilde{U}_{j+1}^{\,n} \text{ if } \tilde{U}^{n}_{j+\frac{1}{2}} < 0$$

3.1.4 Rich

This method [11] is included for the sake of completeness although it was not applied to the test problems due to its poor stability properties.

The weighted values of density and velocity are obtained from the first two terms of a Taylor series expansion about the donor cell. Assuming that the flow is from left to right ($\tilde{U}^{n}_{j+\frac{1}{2}} > 0$), and that

$$\tilde{U}^{n}_{j+\frac{1}{2}} = \tilde{U}_j^{\,n} + \frac{\Delta x}{2} \frac{\partial \tilde{U}}{\partial x}\Big|^{n}_{j} = \tilde{U}_j^{\,n} + \frac{\tilde{U}^{n}_{j+1} - \tilde{U}^{n}_{j-1}}{4} > 0$$

$$\text{then} \quad \Delta M^{n}_{j+\frac{1}{2}} = \left[\tilde{U}_j^{\,n} + \frac{\tilde{U}^{n}_{j+1} - \tilde{U}^{n}_{j-1}}{4}\right] \left[\rho_j^{\,n} + \frac{\rho_{j+1} - \rho_{j-1}}{4}\right] \Delta t$$

Similarly, if $\tilde{U}^{n}_{j+\frac{1}{2}} < 0$ and if

$$\tilde{U}^{n}_{j+\frac{1}{2}} = \tilde{U}_{j+1}^{\,n} - \frac{\Delta x}{2} \frac{\partial \tilde{U}}{\partial x}\Big|^{n}_{j+1} = \tilde{U}_{j+1}^{\,n} - \frac{\tilde{U}^{n}_{j+2} - \tilde{U}^{n}_{j}}{4} < 0$$

$$\text{then} \quad \Delta M^{n}_{j+\frac{1}{2}} = \left[\tilde{U}_{j+1}^{\,n} - \frac{\tilde{U}^{n}_{j+2} - \tilde{U}^{n}_{j}}{4}\right] \left[\rho_j^{\,n} - \frac{\rho^{n}_{j+2} - \rho^{n}_{j}}{4}\right] \Delta t$$

Otherwise $\Delta M^{n}_{j+\frac{1}{2}} = 0$

3.2 Conservation of Mass, Momentum and Energy

The change in the mass of cell j between the start and the end of each iteration is

$$\Delta M_j^n = [\rho_j^{n+1} - \rho_j^n] \Delta x$$
$$= \Delta M_{j-\frac{1}{2}}^{n} - \Delta M_{j+\frac{1}{2}}^{n}$$

where the half integer subscripts indicate quantities moving across cell boundaries. Therefore, the change in mass of the entire system is

$$\Delta M^n = \sum_{j=1}^{J} [\Delta M_{j-\frac{1}{2}}^{n} - \Delta M_{j+\frac{1}{2}}^{n}]$$

Note that $\Delta M_{j+\frac{1}{2}}^{n} = \Delta M^{n}_{((j+1)-\frac{1}{2})}$ because the mass transported across the right hand side of cell j equals the mass tranported across the left hand side of cell (j+1). Hence

$$\Delta M^n = \Delta M_{\frac{1}{2}}^{n} - \Delta M_{J+\frac{1}{2}}^{n}$$

Therefore, the only change in mass of the total system occurs by mass crossing the boundaries of the system and hence, mass is conserved.

Redistribution of energy and momentum occurs during the calculation of tilde values and also during the rezoning from the Lagrangian mesh to the Eulerian mesh. During the calculation of tilde values, the changes in energy and momentum are the following

$$\Delta \tilde{E}_T^n = \sum_{j=1}^{J} \rho_j^n [\tilde{E}_j^n - E_j^n] \Delta x$$

$$\Delta \tilde{Mom} = \sum_{j=1}^{J} \rho_j^n [\tilde{U}_j^n - U_j^n] \Delta x$$

Therefore $$\Delta\tilde{M}^n_{om} = \sum_{j=1}^{J} [P_{j-\frac{1}{2}}^{n} - P_{j+\frac{1}{2}}^{n}] \Delta t$$

As before, all terms cancel the first and the last, leaving

$$\Delta\tilde{M}^n_{om} = (P^n_{\frac{1}{2}} - P_{J+\frac{1}{2}}^{n}) \Delta t$$

Also

$$\Delta\tilde{E}^n_T = \sum_{j=1}^{J} \frac{1}{2}[-P^n_j \Delta t (\bar{U}_{j+1}^{n} - \bar{U}_{j-1}^{n}) + \rho^n_j \Delta x (\tilde{U}^n_j + U^n_j)(\tilde{U}^n_j - U^n_j)]$$

$$= \sum_{j=1}^{J} \frac{\Delta t}{2} [-P^n_j (\bar{U}_{j+1}^{n} - \bar{U}_{j-1}^{n}) - \bar{U}^n_j (P_{j+1}^{n} - P_{j-1}^{n})]$$

$$= \frac{\Delta t}{2} [P^n_1 \bar{U}^n_o + \bar{U}^n_1 P^n_o - P^n_J \bar{U}^n_{J+1} - \bar{U}^n_j P_{J+1}^{n}]$$

$$= \Delta t \left[P^n_{\frac{1}{2}} \bar{U}^n_o + \bar{U}^n_{\frac{1}{2}} P^n_o - P^n_o \bar{U}^n_o - P_{J+\frac{1}{2}}^{n} \bar{U}_{J+1}^{n} - \bar{U}_{J+\frac{1}{2}}^{n} P_{J+1}^{n} + P_{J+1}^{n} \bar{U}_{J+1}^{n} \right]$$

Therefore, the only changes in momentum and energy of the system during the calculation of tilde values occurs by momentum and energy crossing the boundaries of the system. Hence, momentum and energy are conserved during this part of the calculation.

The equations for the rezoning phase are directly derived from the equations for conservation of momentum and energy and hence momentum and energy must be conserved during the rezone. The energy and momentum changes of the system occurring during the rezone are

$$\Delta E_R^n = \Delta M_{\frac{1}{2}}^n \tilde{E}_L^n - \Delta M_{J+\frac{1}{2}}^n \tilde{E}_R^n$$

$$\Delta M_{omR}^{\ n} = \Delta M_{\frac{1}{2}}^n \tilde{U}_L^n - M_{J+\frac{1}{2}}^{n_1} \tilde{U}_R^n$$

Thus, the mass, momentum and energy of the system are conserved identically despite finite difference approximations. However, corrections must be made at transmittive boundaries and pistons.

It is interesting that the derivations of the conservation of mass, momentum and energy are independent of the velocity weighting scheme used. This is because the conservation laws are concerned with cell centered quantities but the velocity weighting schemes are defined by interface quantities.

The only discrepancies arising between the theoretical energy of the system and the numerically approximated values are due to round-off errors. The values of system energy obtained for test problem 1A (see section 5.2) which are typical of the values obtained for the rest of the problems are:

Initial system energy 1.1363×10^9 gms.

System energy at .1 seconds minus work done by piston

(a) continuous rezone 1.1360×10^9 gms.

(b) OIL 1.1359×10^9 gms.

(c) donor 1.1353×10^9 gms.

3.3 Order of the Truncation Errors

By applying Taylor's series expansions to the finite difference equations for continuous rezone, OIL and donor, and comparison with the equations of hydrodynamics, the order of the errors involved in the approximations can be found. The methods are of at least the order calculated and might be higher. The derivations are carried out assuming that the flow is from left to right. Combinations of left to right and right to left flow have not been examined. The order of the truncation errors for all three velocity weighting schemes for each of the three equations of hydrodynamics are simply stated in this section and are derived in detail in APPENDIX B.

(a) continuous rezone is $0\ (\Delta x) + 0\ (\Delta t) + 0\ (\frac{\Delta t}{\Delta x}^{2})$ for each of the three conservation equations

(b) OIL is $0\ (\Delta x) + 0\ (\Delta t) + 0\ (\frac{\Delta t^2}{\Delta x})$ for each of the three conservation equations

(c) donor is $0\ (\Delta x) + 0\ (\Delta t)$ for the conservation of mass and momentum, and is $0\ (\Delta t) + 0\ (\Delta x) + 0\ (\frac{\Delta t^2}{\Delta x})$ for the conservation of energy.

Thus, the set of finite difference equations representing each of the three schemes continuous rezone, OIL and donor is of order $0\ (\Delta x) + 0\ (\Delta t) + 0\ (\frac{\Delta t^2}{\Delta x})$

4. TIME STEP CONTROL AND TREATMENT OF BOUNDARIES

4.1 Time Step Control

Three criteria were used for calculating the time step. The first was the familiar Courant-Friedrichs-Lewy stability criterion which states that at any time step n, no signal travelling at the local sound speed C can propagate through more than one cell in one time step. Hence, for each n

$$\Delta t^n \leq \frac{\Delta x}{C_j^n}$$

for all j in the region of interest

$$\text{or } \Delta t^n = F \min_j \left[\frac{\Delta x}{C_j^n}\right]$$

where $0 < F \leq 1$.

F is defined as the Courant-Friedrichs-Lewy number.

The second limitation which applies to supersonic flow problems only, prohibits the transport of mass across more than one cell in one time interval. The fluid model provides no mechanism for transfer of mass between non-adjacent cells. Hence

$$\Delta t^n \leq \frac{\Delta x}{U_j^n}$$

for all j in the region of interest

The third limitation is strictly applicable to the OIL method but was applied to the other schemes as well, enabling all three techniques

to use the same Courant-Friedrichs-Lewy number. Thus, continuous rezone and donor should be able to run faster than OIL.

Suppose Δt is calculated from the Courant-Friedrichs-Lewy criterion. Then

$$\Delta t^n \leq \frac{\Delta x}{V} \quad \text{where } V = \max \left(\max_j \left| U_j^n \right| , c_j^n \right)$$

$$\text{or } \Delta t = \frac{F \Delta x}{V} \quad \text{where } F \leq 1$$

Assuming that the flow is from left to right, suppose that some $\tilde{U}_j^n = V$. Then

$$\tilde{U}_j^n \Delta t = F \Delta x \tag{28}$$

However, the fluid model for OIL prevents the left hand boundary of the cell whose center is at $(j + \frac{1}{2})$ from crossing into cell $(j + 1)$. Hence

$$\tilde{U}_j^n \Delta t \leq \frac{\Delta x}{2} \tag{29}$$

By comparing equations (28) and (29) it can be seen that $F \leq \frac{1}{2}$ is a necessary condition in order to remain consistent with the fluid model. It may also happen that some $\tilde{U}_j^n > V$, in which case $F < \frac{1}{2}$ for stability. It is necessary to show that the condition $\tilde{U}_j^n > V$ can exist to support the hypothesis that $F < \frac{1}{2}$.

Suppose that $\tilde{U}_k^n = V$ for some $j = k$. It is known that

$$\tilde{U}_k^n = U_k^n - \left[\frac{\partial P}{\partial x} \Big|_k + 0 (\Delta x) \right] \frac{\Delta t}{\rho_k^n}$$

Hence, if $\frac{\partial P}{\partial x} \Big|_k < 0$, then $\tilde{U}_k^n > V$.

In the test problems, F was chosen to be equal to .4. This is equivalent to assuming that no $\tilde{U}_j^n$ will increase by more than 25% over V in one time step.

Some authors[10] have experienced difficulties with negative energies and negative volumes and have incorporated additional time step controls to handle them. However, this was not found necessary in this report.

4.2 Treatment of Boundaries

A transmittive boundary at the interface $(j + \frac{1}{2})$ is defined by the following equations:

$$\frac{\partial U}{\partial x}\Big|_{j+\frac{1}{2}} = 0$$

$$\frac{\partial \rho}{\partial x}\Big|_{j+\frac{1}{2}} = 0$$

$$\frac{\partial P}{\partial x}\Big|_{j+\frac{1}{2}} = 0$$

$$\frac{\partial I}{\partial x}\Big|_{j+\frac{1}{2}} = 0$$

For a left hand boundary at $j = \frac{1}{2}$, the above equations are satisfied by using a dummy cell with index 0 and letting $U_o = U_1$, $\rho_o = \rho_1$, $P_o = P_1$ and $I_o = I_1$. A right hand boundary is handled in a similar fashion.

It is necessary to calculate the mass and energy transported across a transmittive boundary in order to check the conservation laws. The conditions at a reflective boundary are the same as above except $U_1 = -U_o$. Moving piston boundaries are complicated by the work terms done on the gas by the piston.

5. DESCRIPTIONS, NUMERICAL VALUES AND DISCUSSIONS OF TEST PROBLEMS

5.1 Introduction

The test problems are intended to exhibit typical behavior of the hydrocodes in a wide variety of situations and are not difficult in themselves. In the report from which the test problems are taken [3], there are seven test problems with a few variations of each, which are designated A, B, C etc. The difference between these variations is in the initial numerical values of one or more of the fluid parameters. The test problems in [3] which were not run with continuous rezone, OIL and donor are described in the next paragraph. The format for the description of each test problem will consist of a brief description, initial numerical values, boundary conditions and plot times together with initial and final plots of pressure, density, specific internal energy and velocity. Sometimes, initial plots are not given if one or more parameters is constant throughout the region of interest. For further details about the test problems, the reader should consult reference [2]. Also, the PUFF, Lax Wendroff and analytic solutions may be found in reference [3].

None of the last three parts of problem two and none of problem four was run due to the presence of a vacuum. When a vacuum arises, the density equals zero and equations using density as a divisor cannot be used. The last part of problem seven was not run, since it is just a scaling down of the first part by a factor of 100 and no new features are introduced. Also, problem three was not run mainly because it is a pure compression problem and in this respect would yield little information not already given by problem one.

The chief difference between the test problems in Hick's reports and the ones in this report are that the latter may be translated in the positive x direction to avoid negative or zero subscripts. This will be clearly stated where appropriate. Also, there might be a slight difference between the total number of cells in the mesh used in this report and in reference [3]. Neither of these differences will change the calculated error norms because the cell sizes in each report are the same and the discrepancy in the total number of cells occurs at the boundaries of the problem where the exact and approximate solutions are equal.

Errors

The analytic solution to the mathematical model of the physical problem is known as the exact solution. The difference between the exact solution and an approximate or hydrocode solution is referred to as the error. For purposes of comparison, the calculated error norms are the same as those used by Hicks and are defined below.

For example, take a variable V whose exact and approximate values in cell j are $V_E(j)$ and $V_A(j)$ respectively. Let V_M be the absolute maximum of $V_E(j)$ where j ranges over the region of interest. For V, make the following definitions:

$$\text{Sum. Abs. Error} = \frac{1}{V_M} \sum_j |V_A(j) - V_E(j)|$$

$$\text{Sum. Sqr. Error} = \frac{1}{V_M^2} \sum_j (V_A(j) - V_E(j))^2$$

$$\text{Maximum Error} = \max_j \frac{|V_A(j) - V_E(j)|}{V_M} \quad \text{sign } (V_A(j_M) - V_E(j_M))$$

where j_M is the index of $\max_j \mid V_A(j) - V_E(j) \mid$.

For each test problem and each of the three schemes, error tables are given containing sum abs. error, sum sqr. error and maximum error. Large values of the maximum error norm can occur at the shock front due to the numerical approximations of the shock being spread over two or three cells. Thus, the maximum error norm is an unreliable norm with which to compare these methods.

For all test problems, a polytropic equation of state is used as in equation (27).

$$P = (\gamma - 1)\, \rho\, I \tag{27}$$

For all test problems, $\gamma = 1.4$.

5.2 Test Problem 1

(a) Description

In this problem, a piston moves into a fluid at constant velocity from left to right. The fluid is consequently compressed. At the start of the problem, a shock moving from left to right exists 50 meters ahead of the piston. The exact solution is two constant states separated by the shock discontinuity as shown in Figure 6.

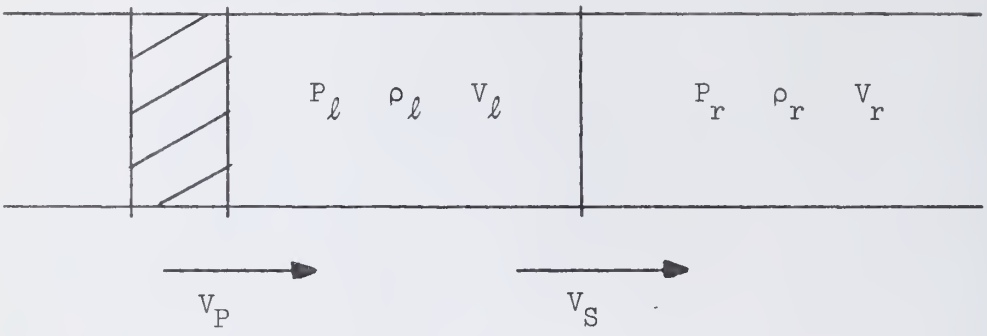

Figure 6. Test Problem 1

C_ℓ = sound speed to the left of the shock

C_r = sound speed to the right of the shock

P_ℓ = pressure to the left of the shock

P_r = pressure to the right of the shock

ρ_ℓ = density to the left of the shock

ρ_r = density to the right of the shock

V_ℓ = velocity to the left of the shock

V_r = velocity to the right of the shock

V_p = piston velocity

V_s = shock velosity

X_s = initial position of shock

V_p = MC_r where M is a positive constant

X_p = initial position of piston

(b) Numerical Values for 1A

$M = 1$

$\Delta x = 1$ meter

$P_r = 10^4$ dynes/cm^2

$\rho_r = 10^{-6}$ gm/cm^3

$V_r = 0$

$V_\ell \simeq 1.18 \times 10^5$ cm/sec

$V_s \simeq 2.08 \times 10^5$ cm/sec

$P_\ell \simeq 3.47 \times 10^4$ dynes/cm^2

$\rho_\ell \simeq 2.30 \times 10^{-6}$ gm/cm^3

$X_s =$ 51 meters in this report and 50 meters in [3]

Right boundary at 300 meters

$X_p =$ 1 meter in this report and 0 meters in [3]

(c) Boundary Conditions

On the right, a transmittive boundary and on the left, a piston starting at 1 meter and moving to the right with velocity V_p.

(d) Plot Times 0. and .1 sec.

(e) Numerical Values for 1B

The same as 1A except

$M = 100$

$V_\ell \simeq 1.18 \times 10^7$ cm/sec

$P_\ell \simeq 1.68 \times 10^8$ dynes/cm^2

$C_\ell \simeq 6.26 \times 10^6$ cm/sec

$V_s \simeq 1.42 \times 10^7$ cm/sec

$\rho_\ell \simeq 5.99 \times 10^{-6}$ gm/sec

(f) Plot Times 0. and 10^{-3} sec.

Table 1. Errors for Test Problem 1A

Problem Time = 10^{-3} Sec.

Continuous Rezone

Computer Time = 100 Sec. Iteration Number = 364

	Sum Abs. Error	Sum Sqr. Error	Maximum Error	Position of Maximum Error
Pressure	.885	.101	.285	current shock position
Density	.655	.056	.201	current shock position
Energy	.465	.019	.122	current shock position
Velocity	.737	.143	.326	current shock position

OIL

Computer Time = 105 Sec. Iteration Number = 364

	Sum Abs. Error	Sum Sqr. Error	Maximum Error	Position of Maximum Error
Pressure	.835	.076	.240	current shock position
Density	.638	.041	.154	current shock position
Energy	.487	.018	.109	current shock position
Velocity	.709	.133	.285	current shock position

Donor

Computer Time = 105 Sec. Iteration Number = 364

	Sum Abs. Error	Sum Sqr. Error	Maximum Error	Position of Maximum Error
Pressure	1.031	.104	-.236	current shock position
Density	.886	.078	-.238	current shock position
Energy	.658	.027	-.115	current shock position
Velocity	1.045	.236	-.390	current shock position

Table 2. Errors for Test Problem 1B

Problem Time = 10^{-3} Sec.

Continuous Rezone

Computer Time = 99 Sec. Iteration Number = 300

	Sum Abs. Error	Sum Sqr. Error	Maximum Error	Position of Maximum Error
Pressure	.945	.119	-.254	current shock position
Density	.963	.100	-.266	current shock position
Energy	.980	.358	-.587	current shock position
Velocity	.828	.326	-.556	current shock position

OIL

Computer Time = 98 Sec. Iteration Number = 299

	Sum Abs. Error	Sum Sqr. Error	Maximum Error	Position of Maximum Error
Pressure	1.113	.171	-.356	current shock position
Density	1.165	.157	-.366	current shock position
Energy	1.229	.463	-.658	current shock position
Velocity	1.005	.443	-.641	current shock position

Donor

Computer Time = 98 Sec. Iteration Number = 300

	Sum Abs. Error	Sum Sqr. Error	Maximum Error	Position of Maximum Error
Pressure	1.569	.312	-.495	current shock position
Density	1.752	.320	-.504	current shock position
Energy	1.715	.658	-.720	current shock position
Velocity	1.370	.6537	-.719	current shock position

(g) Discussion of 1A

For each of the three schemes run, there are spikes at the shock front and slight waves behind the shock front as shown in Figure 7. Although the waves travelling back from the shock front are larger in the donor method, the donor spike obtained at the shock front is smaller than the spike for OIL or continuous rezone.

PUFF has very good shock front definition and slight rarefaction dips behind the shock. Lax Wendroff and PUFF both have spikes in density and internal energy at the initial position relative to the piston, i.e. 50 meters in front of the piston. In addition, Lax Wendroff also has spikes at the shock front for all parameters.

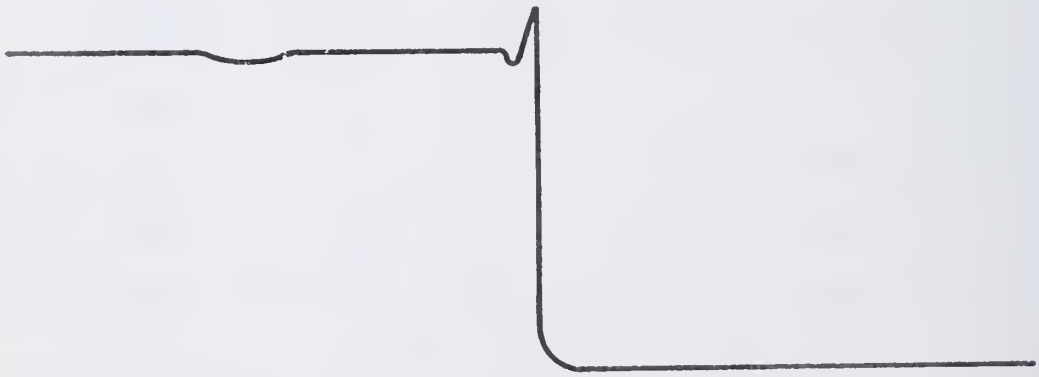

Figure 7. Typical Wareform for Problem 1

(h) Discussion of 1B

Continuous rezone, OIL and donor show the same basic behavior as in 1A. Again, waves travel back from the shock front as in 1A. The largest waves are also obtained in the donor scheme. However, the small waves may be preferable to the very large spikes obtained in PUFF and Lax

Wendroff. PUFF has better shock front definition than any of the three schemes tried here but at the expense of large spikes 50 meters in front of the piston. Lax Wendroff has oscillations both at the piston face and at the shock front.

5.3 Test Problem 2

(a) Description

In this problem, a piston moves with constant velocity from right to left thus evacuating a pipe which initially contains constant state gas at rest as in Figure 8. The motion of the piston creates a rarefaction wave moving to the right.

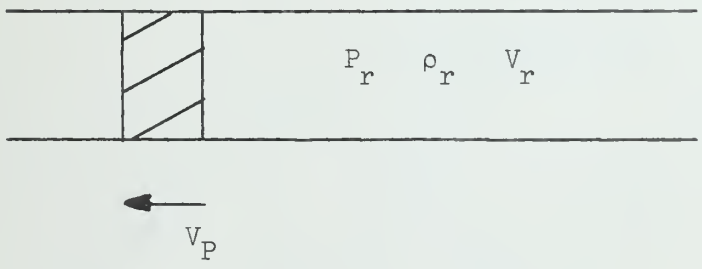

Figure 8. Test Problem 2

(b) Numerical Values for 2A

$P_r = 10^4$ dynes/cm^2

$\rho_r = 10^{-6}$ gm/cm^3

$C_r^2 = 1.4 \times 10^{10}$ cm^2/sec^2

$V_p = - C_r/(\gamma + 1)$

$\Delta x = 100$ cm

$X_p(o)$ = 1300 meters in this report and 100 meters in [3].

X_Q = 1500 meters in this report and 300 meters in [3].

(c) Boundary Conditions

On the right, a transmittive boundary and on the left, a piston moving to the left away from the gas with velocity V_p.

(d) Plot Times .1 seconds

(e) Numerical Values for 2B

the same as 2A except

$$V_p = \frac{-2C_r}{\gamma + 1}$$

Table 3. Errors for Test Problem 2A

Problem Time = .1 Sec.

Continuous Rezone

Computer Time = 92 Sec. Iteration Number = 296 Sec.

	Sum Abs. Error	Sum Sqr. Error	Maximum Error	Position of Maximum Error
Pressure	1.071	.016	-.031	X_R
Density	.821	.011	-.026	X_R
Energy	.456	.003	-.014	X_R
Velocity	2.47	.111	-.088	X_R

OIL

Computer Time = 93 Sec. Iteration Number = 296

	Sum Abs. Error	Sum Sqr. Error	Maximum Error	Position of Maximum Error
Pressure	1.096	.017	-.032	X_R

Density	.848	.011	-.026	X_R
Energy	.470	.003	-.014	X_R
Velocity	2.536	.115	-.089	X_R

Donor

Computer Time = 90 Sec. Iteration Number = 296

	Sum Abs. Error	Sum Sqr. Error	Maximum Error	Position of Maximum Error
Pressure	3.102	.218	.135	rarefaction wave
Density	2.726	.151	.120	rarefaction wave
Energy	1.088	.019	.042	rarefaction wave
Velocity	5.586	.680	.269	rarefaction wave

Table 4. Errors for Test Problem 2B

Problem Time = .1 Sec.

Continuous Rezone

Computer Time = 95 Sec. Iteration Number = 296

	Sum Abs. Error	Sum Sqr. Error	Maximum Error	Position of Maximum Error
Pressure	1.226	.014	-.023	2600 metres
Density	1.052	.011	-.023	2600 metres
Energy	.924	.007	-.017	2600 metres
Velocity	2.034	.055	-.057	2600 metres

OIL

Computer Time = 101 Sec. Iteration Number = 296

	Sum Abs. Error	Sum Sqr. Error	Maximum Error	Position of Maximum Error
Pressure	1.201	.013	-.023	2600 metres

Density	1.024	.011	-.023	2600 metres
Energy	.906	.006	-.017	2600 metres
Velocity	1.998	.053	-.055	2600 metres

Donor

Computer Time = 96 Sec. Iteration Number = 296

	Sum Abs. Error	Sum Sqr. Error	Maximum Error	Position of Maximum Error
Pressure	2.818	.172	.135	2786 metres
Density	2.528	.120	.122	2786 metres
Energy	1.104	.017	.042	2788 metres
Velocity	3.072	.164	.133	2778 metres

(f) Discussion of 2A

The results obtained for continuous rezone and OIL are very good. Donor displays the start of strong instabilities in the rarefaction wave. In continuous rezone, OIL and donor, there is a slight rise in density and slight drop in specific internal energy just in front of the piston as in Figure 9 which seems to have little or no effect on the rarefaction region. This effect is slightly worse in donor than the other two. The reason for this effect might be connected with always choosing the donor value of density in the density weighting. Also, OIL, continuous rezone and donor underround at X_C and at X_R. PUFF and Lax Wendroff show undershoots to the left of X_R. Lax Wendroff even oscillates slightly at the left of X_R.

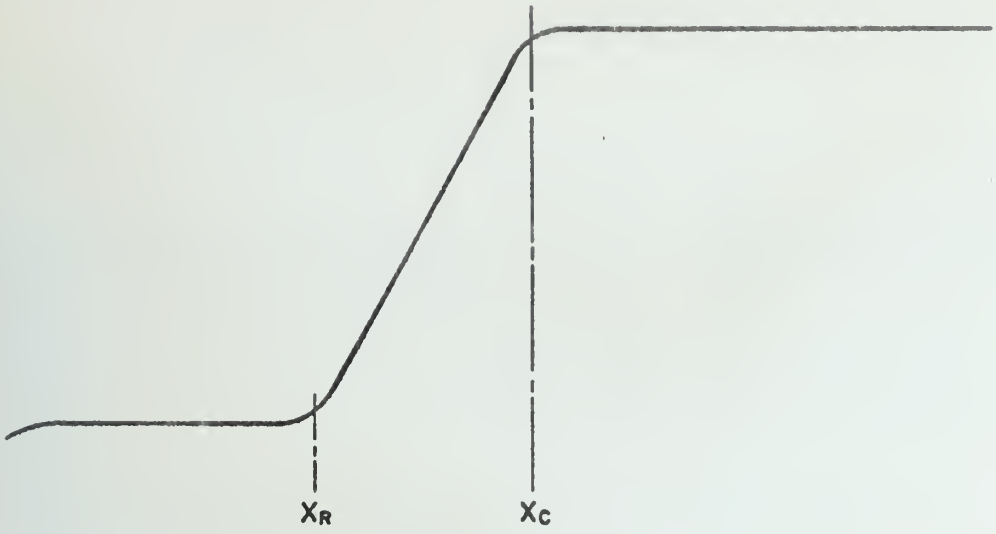

Figure 9. Internal Energy for OIL and Continuous Rezone

(g) Discussion of 2B

The basic behavior of 2B is similar to that of 2A. Again, donor breaks down in the rarefaction wave. PUFF and Lax Wendroff, due to the undershoots obtained to the left of X_R, seem inferior to continuous rezone and OIL for this problem.

5.4 Test Problem 5

(a) Description

This problem is a special case of the Riemann problem and is known as either the shock tube problem or the ruptured membrane problem. The problem is to find the hydrodynamic variables after the removal of a membrane at time t = 0 separating two constant unequal states at rest as in Figure 10. We adopt the convention $P \geq P_r \geq 0$ and investigate the three cases $\rho_\ell > \rho_r, \rho_\ell = \rho_r, \rho_\ell < \rho_r$. When the membrane has been removed, a rarefaction wave travels into the left state and a shock travels into the right state.

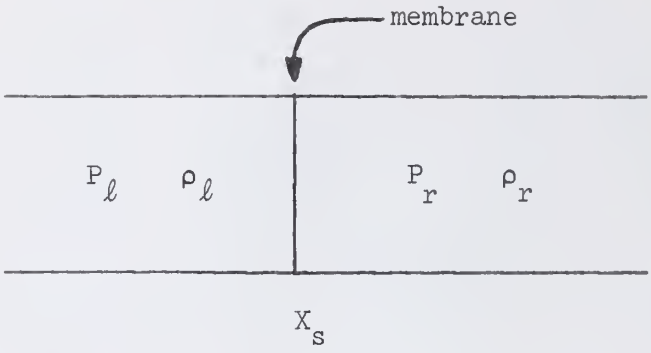

Figure 10. Test Problem 5

(b) Numerical Values for 5A

$X_s(0)$ = 101 metres in this report and 100 metres in [3]

Δx = 1 meter

P_ℓ = 10^8 dynes/cm^2

ρ_ℓ = 10^{-5} gm/cm^3

V_ℓ = 0

P_r = 10^4 dynes/cm^2

ρ_r = 10^{-6} gm/cm^3

V_r = 0

Left boundary at 2 metres in this report and 0 metres in [3].

Right boundary at 252 metres in this report and 250 metres in [3].

(c) Boundary Conditions

Transmittive boundaries exist at both the left hand and right hand boundaries.

(d) Plot Times 2×10^{-3} sec.

(e) Numerical Values for 5B

The same as 5A except

$X_s(0)$ = 251 meters in this report and 250 meters in [3]

ρ = 10^{-6} gm/cm^3

Right boundary at 502 metres in this report and 500 meters in [3].

(f) Numerical Values for 5C

The same as 5A except

$X_s(0)$ = 251 meters in this report and 250 meters in [3]

ρ = 10^{-6} gm/cm^3

ρ_r = 10^{-5} gm/cm^3

Right boundary at 502 metres in this report and 500 meters in [3].

Table 5. Errors for Test Problem 5A

Problem Time = .002 Sec.

Continuous Rezone

Computer Time = 85 Sec. Iteration Number = 202

	Sum Abs. Error	Sum Sqr. Error	Maximum Error	Position of Maximum Error
Pressure	1.480	.037	-.123	X_S
Density	3.199	.293	-.348	X_S
Energy	2.890	.244	-.273	X_S
Velocity	3.357	.927	-.832	X_S

OIL

Computer Time = 86 Sec. Iteration Number = 200

	Sum Abs. Error	Sum Sqr. Error	Maximum Error	Position of Maximum Error
Pressure	1.481	.041	-.137	X_S
Density	3.292	.344	-.392	X_S
Energy	2.911	.254	-.278	X_S
Velocity	3.518	1.088	-.861	X_S

Donor

Computer Time = 88 Sec. Iteration Number = 202

	Sum Abs. Error	Sum Sqr. Error	Maximum Error	Position of Maximum Error
Pressure	1.771	.072	-.140	X_S
Density	3.602	.415	-.403	X_S
Energy	2.804	.268	-.277	X_S
Velocity	3.630	1.229	-.861	X_S

(g) Discussion of 5A

This problem demonstrates very clearly the instabilities which can occur in rarefaction regions with the donor scheme. The instabilities in this particular problem seem to be caused by the slope to the right of X_c on all donor plots being too steep as shown in Figure 11. A general loss of fine detail is also in evidence in all three methods. In particular, there is strong underrounding of the density at X_D and a consequent loss of definition at X_D in the specific internal energy plot. The continuous rezone and OIL plots are essentially identical but for minuscule peaks at X_s on the pressure

and velocity in continuous rezone. PUFF causes less smearing of the density at X_D than in OIL or continuous rezone. However, Puff also has overrounds at X_R which are not in evidence with continuous rezone and OIL. The Lax-Wendroff solution has several spikes.

Table 6. Errors for Test Problem 5B

Problem Time = .002 Sec.

Continuous Rezone

Computer Time = 172 Sec. Iteration Number = 592

	Sum Abs. Error	Sum Sqr. Error	Maximum Error	Position of Maximum Error
Pressure	1.358	.062	-.218	401 meters
Density	7.758	2.084	.4599	376 meters
Energy	9.588	4.136	.649	375 meters
Velocity	3.137	.679	-.736	401 meters

OIL

Computer Time = 176 Iteration Number = 592

	Sum Abs. Error	Sum Sqr. Error	Maximum Error	Position of Maximum Error
Pressure	1.391	.072	-.239	401 meters
Density	7.882	2.157	-.487	401 meters
Energy	9.549	4.103	.648	375 meters
Velocity	3.241	.753	-.760	401 meters

Donor

Donor will not run to .002 sec. due to instabilities.

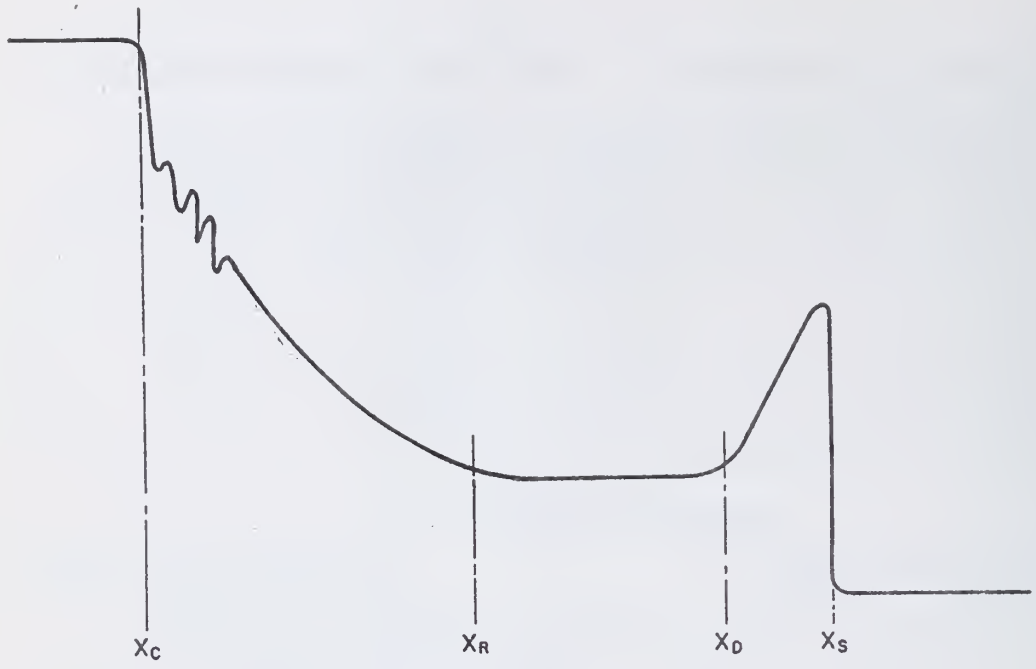

Figure 11. Donor Density in Problem 5A

(h) Discussion of 5B

The instabilities in the rarefaction region for the donor scheme are so bad in 5B that the problem will not run to .002 seconds. Even at .001 seconds, the instabilities in donor are quite bad. As in 5A, continuous rezone and OIL are essentially identical. Also, the general behavior of OIL and continuous rezone is similar to that in 5A. In PUFF, the overshoot in velocity is quite pronounced, although the definition at X_D is still good. The Lax Wendroff solution shows oscillations.

Table 7. Errors for Test Problem 5C

Problem Time = .002 Sec.

Continuous Rezone

Computer Time = 178 Sec. Iteration Number = 592

	Sum Abs. Error	Sum Sqr. Error	Maximum Error	Position of Maximum Error
Pressure	1.343	.140	-.328	312 meters
Density	6.356	2.206	.571	302 meters
Energy	12.111	8.737	.890	301 meters
Velocity	4.040	.655	-.699	312 meters

OIL

Computer Time = 176 Sec. Iteration Number = 592

	Sum Abs. Error	Sum Sqr. Error	Maximum Error	Position of Maximum Error
Pressure	1.394	.148	-.340	312 meters
Density	6.397	2.233	.575	302 meters
Energy	12.101	8.717	.890	301 meters
Velocity	4.208	.682	-.705	312 meters

Donor

Donor will not run to .002 sec. due to instabilities.

(i) Discussion of 5C

As in 5B, donor will not run to .002 seconds due to severe instabilities in the rarefaction region. Overrounding occurs with both continuous rezone and OIL in the pressure and velocity at X_R. The overrounding seems slightly worse in OIL. However, the overrounding at X_R in the PUFF solution seems worse than either continuous rezone

or OIL. The handling of the density at X_D by PUFF is considerably better than continuous rezone or OIL. The Lax-Wendroff solution is very poor with many overshoots and spikes etc.

5.5 Test Problem 6

(a) Description

This problem is another special case of the Riemann problem and involves the collision of two shocks as in Figure 12. The first part of the problem investigates the case when $P_\ell > P_r$. The second part examines the collision of two symmetrical shocks.

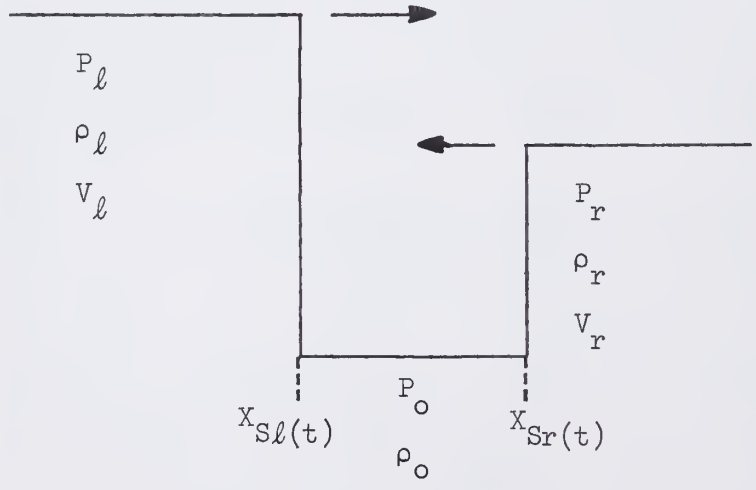

Figure 12. Test Problem 6

(b) Numerical Values for 6A

$$\Delta x = 1 \text{ meter}$$

$$X_{s\ell}(0) = 75 \text{ meters}$$

$$X_{sr}(0) = 125 \text{ meters}$$

$$P_o = 10^4 \text{ dynes/cm}^2$$

$\rho_o = 10^{-6}$ gm/cm^3

$V_o = 0$ cm/sec

$P = 10^8$ dynes/cm^2

$P_r = 10^7$ dynes/cm^2

Left boundary at 70 metres in this report and 0 metres in [3]. Right boundary at 180 metres in this report and 200 metres in [3].

(c) Boundary Conditions

Transmittive boundary conditions are applied at both the left hand and right hand boundaries.

Plot Times 0., and 7×10^{-4} seconds

(d) Numerical Values for 6B

The same as 6A except

$P = P_r = 10^8$ dynes/cm^2

Table 8. Errors for Test Problem 6A

Problem Time = .0007 Sec.

Continuous Rezone

Computer Time = 75 Sec. Iteration Number = 163

	Sum Abs. Error	Sum Sqr. Error	Maximum Error	Position of Maximum Error
Pressure	1.477	.431	.515	X^*_{SR}
Density	1.914	.373	.412	X^*_{SR}
Energy	1.924	.334	.336	X_{col}
Velocity	1.104	.148	-.229	X^*_{S1}

OIL

Computer Time = 75 Sec. Iteration Number = 163

	Sum Abs. Error	Sum Sqr. Error	Maximum Error	Position of Maximum Error
Pressure	1.298	.309	.398	X^*_{SR}
Density	1.784	.293	.307	X^*_{SR}
Energy	1.866	.314	.330	X_{col}
Velocity	1.064	.120	-.226	X^*_{S1}

Donor

Computer Time = 79 Sec. Iteration Number = 164

	Sum Abs. Error	Sum Sqr. Error	Maximum Error	Position of Maximum Error
Pressure	1.315	.369	.465	X^*_{S1}
Density	2.166	.449	-.397	X^*_{SR}
Energy	1.951	.325	.297	X_{col}
Velocity	1.375	.305	-.443	X^*_{SR}

(f) Discussion of 6A

Continuous rezone and OIL both have small overshoots at X^*_{SR} in pressure, density and velocity as shown in Figure 13 while donor has almost no overshoot. Also, there is a general smearing of fine detail as has been noticed in previous problems. The specific internal energy plots for continuous rezone and OIL are slightly better than donor. OIL and continuous rezone are practically identical. PUFF has large spikes in the density and specific internal energy. The Lax-Wendroff solution is barely recognizable due to large oscillatory components.

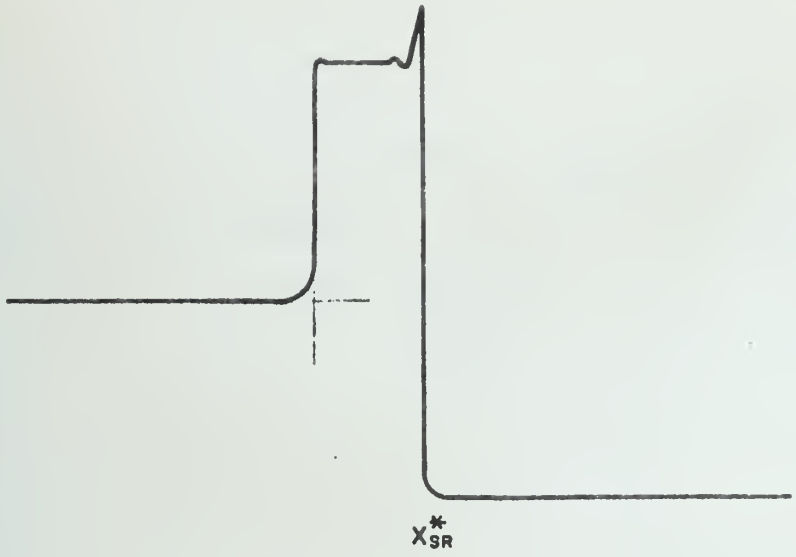

Figure 13. Pressure for Problem 6A

Table 9. Errors for Test Problem 6B

Problem Time = .0007 Sec.

Continuous Rezone

Computer Time = 73 Sec. Iteration Number = 162

	Sum Abs. Error	Sum Sqr. Error	Maximum Error	Position of Maximum Error
Pressure	5.541	1.336	.493	83 metres
Density	4.322	.808	.347	83 metres
Energy	2.571	.429	.382	83 metres
Velocity	30.831	26.560	-.990	76 metres

OIL

Computer Time = 75 Sec. Iteration Number = 162

	Sum Abs. Error	Sum Sqr. Error	Maximum Error	Position of Maximum Error
Pressure	4.923	1.163	.463	83 metres
Density	3.948	.694	.312	83 metres
Energy	2.308	.384	.368	83 metres
Velocity	31.001	26.494	-.990.	76 metres

Donor

Donor will not run to .0007 sec. due to instabilities.

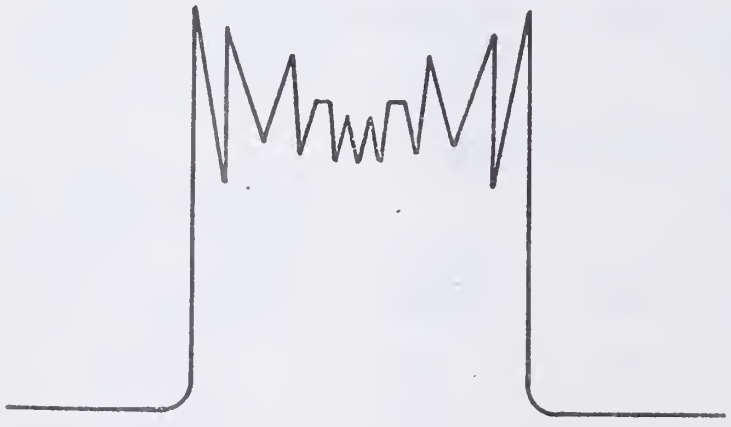

Figure 14. Pressure for Continuous Rezone in Problem 6B

(g) Discussion of 6B

More difficulty was obtained with this problem than any other. The donor scheme for 6B would not run to 7×10^{-4} seconds. The reasons for this difficulty are not, as yet, understood. It cannot be blamed on rarefaction regions, since none exist in this problem. The donor scheme runs up to and just beyond the collision but then 'blows up'. Both OIL and continuous rezone show serious oscillations

soon after collision as in Figure 14. However, no asymmetries were observed. Several variations of the basic continuous rezone scheme were tried not using artificial viscosity, but none of them showed fewer oscillations than the standard method. PUFF shows some large spikes in the density and specific internal energy but the pressure and velocity are very good. The Lax Wendroff solution has instabilities comparable to OIL and continuous rezone. In summary, the collision of two asymmetric shocks works reasonably well but a lot of difficulty is obtained with the collision of two symmetrical shocks. From the plots, it can be seen that the instabilities for continuous rezone and OIL arise in the region where the velocity is supposed to be zero. Hence, in this region the effective viscosity will be close to zero and there will be almost no damping effect for any slight perturbations.

5.6 Test Problem 7

(a) Description

This problem is concerned with the overtaking of one shock wave by another as in Figure 15. When two shock waves are travelling in the same direction, the one behind will always overtake the one in front. This is a consequence of the fact that the front side of a shock is supersonic relative to the shock front and the backside is subsonic. When the overtaking has occurred, a rarefaction wave travels to the left and a stronger shock continues moving to the right.

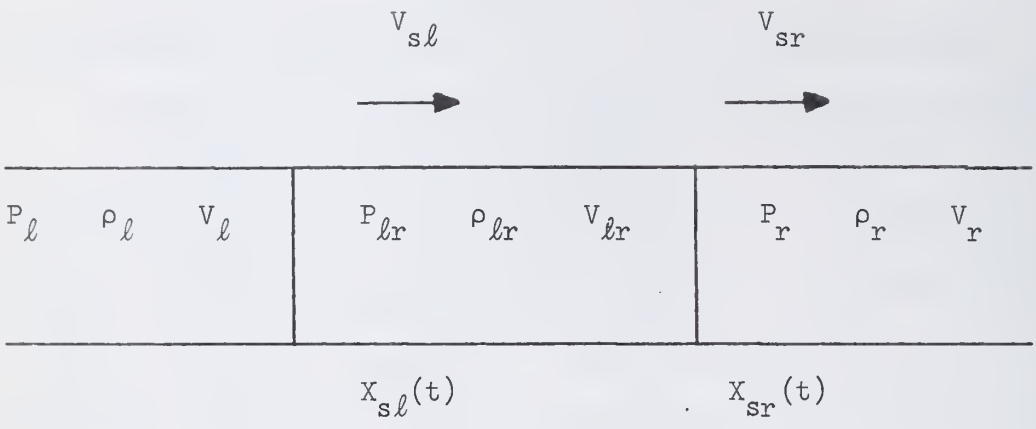

Figure 15. Test Problem 7

(b) Numerical Values for 7A

$\Delta x = 1$ meter

$P_r = 10^4$ dynes/cm^2

$\rho_r = 10^{-6}$ gm/cm^2

$V_r = 0$

$P_{\ell r} = 10^8$ dynes/cm^2

$P_\ell = 10^{12}$ dynes/cm^2

$X_{sl}(0) = 25$ meters

$X_{sr}(0) = 100$ meters

Left boundary at 2 meters in this report and 0 meters in [3]. Right boundary at 200 meters.

(c) Boundary Conditions

Transmittive boundary conditions are applied at both the left hand and right hand boundaries.

(d) Plot Times 0. and 3×10^{-5} seconds

Table 10. Errors for Test Problem 7A

Problem Time = 3. X 10^{-5} Sec.

Continuous Rezone

Computer Time = 98 Sec. Iteration Number = 332

	Sum Abs. Error	Sum Sqr. Error	Maximum Error	Position of Maximum Error
Pressure	2.667	.167	.142	185 meters
Density	3.230	.208	-.135	172 meters
Energy	5.146	1.229	.465	172 meters
Velocity	1.581	.181	-.340	186 meters

OIL

Computer Time = 99 Sec. Iteration Number = 331

	Sum Abs. Error	Sum Sqr. Error	Maximum Error	Position of Maximum Error
Pressure	2.772	.169	.139	185 meters
Density	3.260	.207	-.138	172 meters
Energy	5.376	1.316	.474	172 meters
Velocity	1.687	.214	-.374	186 meters

Donor

Computer Time = 93 Sec. Iteration Number = 331

	Sum Abs. Error	Sum Sqr. Error	Maximum Error	Position of Maximum Error
Pressure	3.024	.177	.155	185 meters
Density	3.330	.202	-.140	172 meters
Energy	5.734	1.430	.485	172 meters
Velocity	1.886	.260	-.397	186 meters

(e) Discussion of 7A

At 3×10^{-5} seconds, there is a slight dip to the left of the rarefaction wave on all plots for each of donor, continuous rezone and OIL at ninety meters as in figure 16. One does not know if these dips are obtained with PUFF and Lax Wendroff since in Hicks report, the plots for this problem start at 115 meters. A general smearing of shock corners is evidenced as in other problems. Continuous rezone has tiny overshoots in the pressure and density at X_s which do not arise in OIL or donor. The plots obtained for velocity and specific internal energy for continuous rezone, OIL and donor, are practically identical. Also, there is very little difference between continuous rezone and OIL in general. PUFF has good overall definition but there are two very large spikes on the density and specific internal energy.

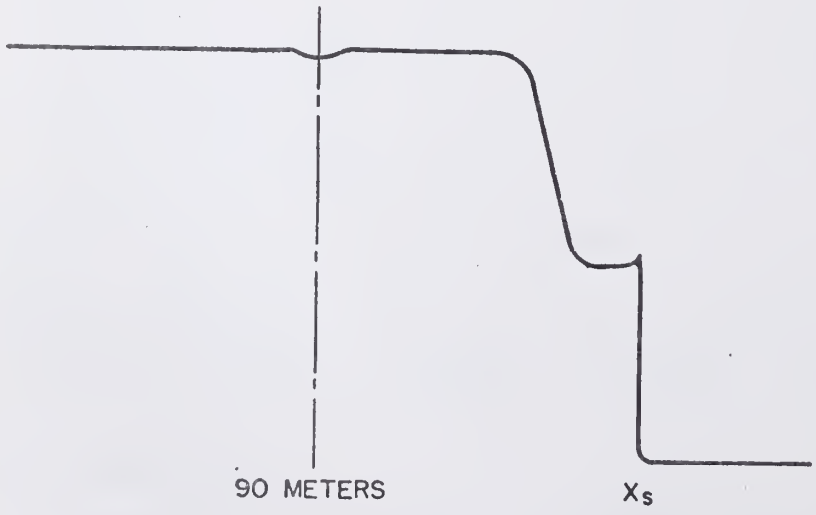

Figure 16. Pressure for Continuous Rezone in 7A

6. GENERAL DISCUSSION

A comparison of the three differencing schemes described in this report with PUFF and Lax Wendroff[3] seems to refute the often asserted statement that Lagrangian codes are overwhelmingly superior to Eulerian codes in one dimension.[12]

In general, donor preserves quite good definition at the shock front but is very unstable in rarefaction regions. Donor also shows waves behind the shock front (on the rarefaction side) which are evidence of the start of instabilities. Continuous rezone and OIL are stable in rarefaction but often have larger overshoots than donor at the shock. For many of the test problems, continuous rezone and OIL are almost indistinguisable. There is a general loss of fine detail in rarefaction regions in all three schemes as is evidenced by problems 5 and 6A.

The mechanism for breakdown of donor in rarefaction is not, as yet, ascertained. In problem 5, instabilities seem to set in at the intersection of two curves of differing gradients, whereas in OIL and continuous rezone there is one continuous curve.

For a general purpose hydrocode, donor, due to its rarefaction problems is less preferable than either OIL or continuous rezone. A hybrid scheme which uses donor at the shock front and one of the other two codes in the rest of the problem is probably best.

APPENDIX A

PLOTS FROM THE TEST PROBLEMS

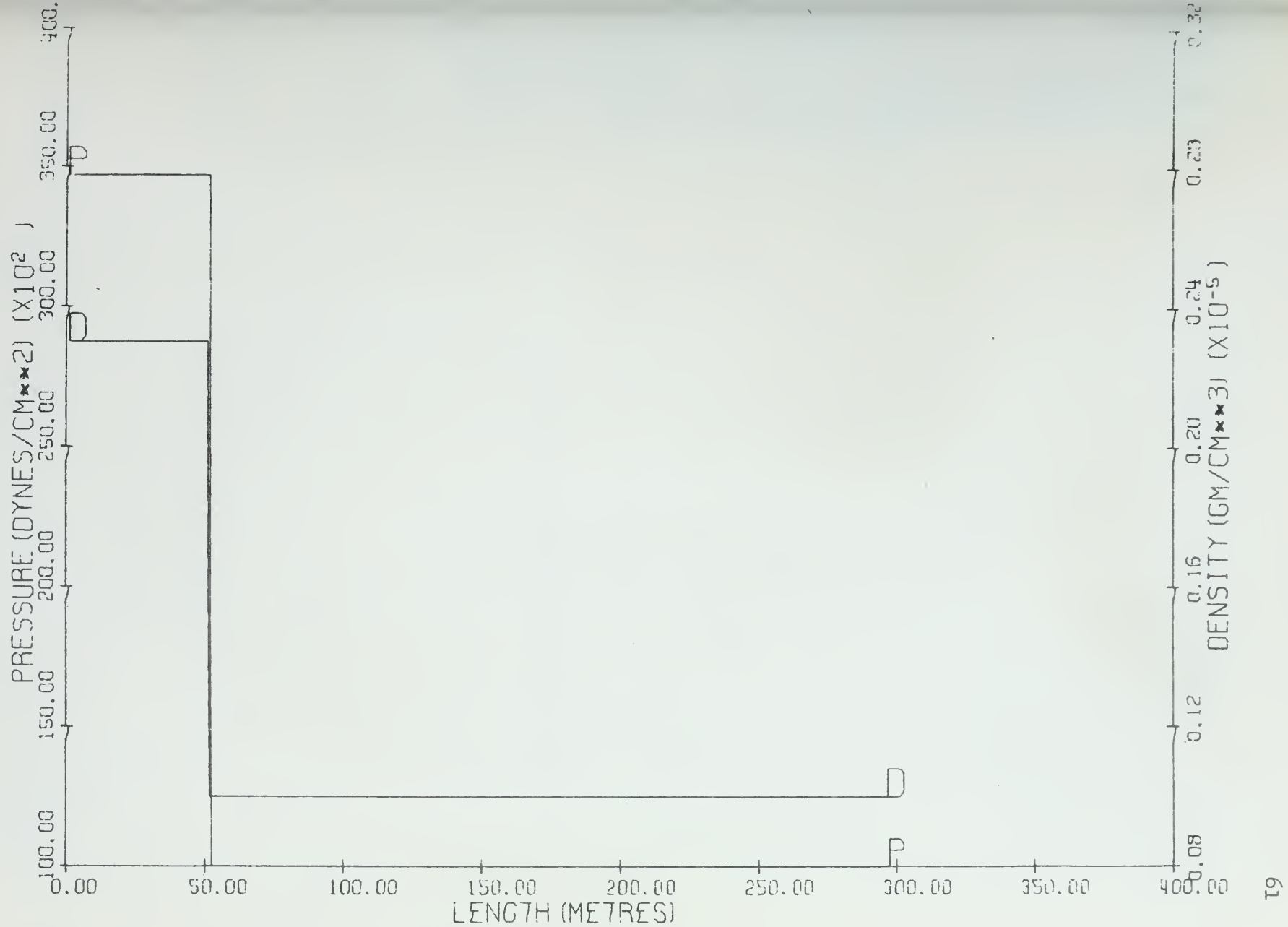

Figure 17. 1A Exact, Time = 0. Sec.

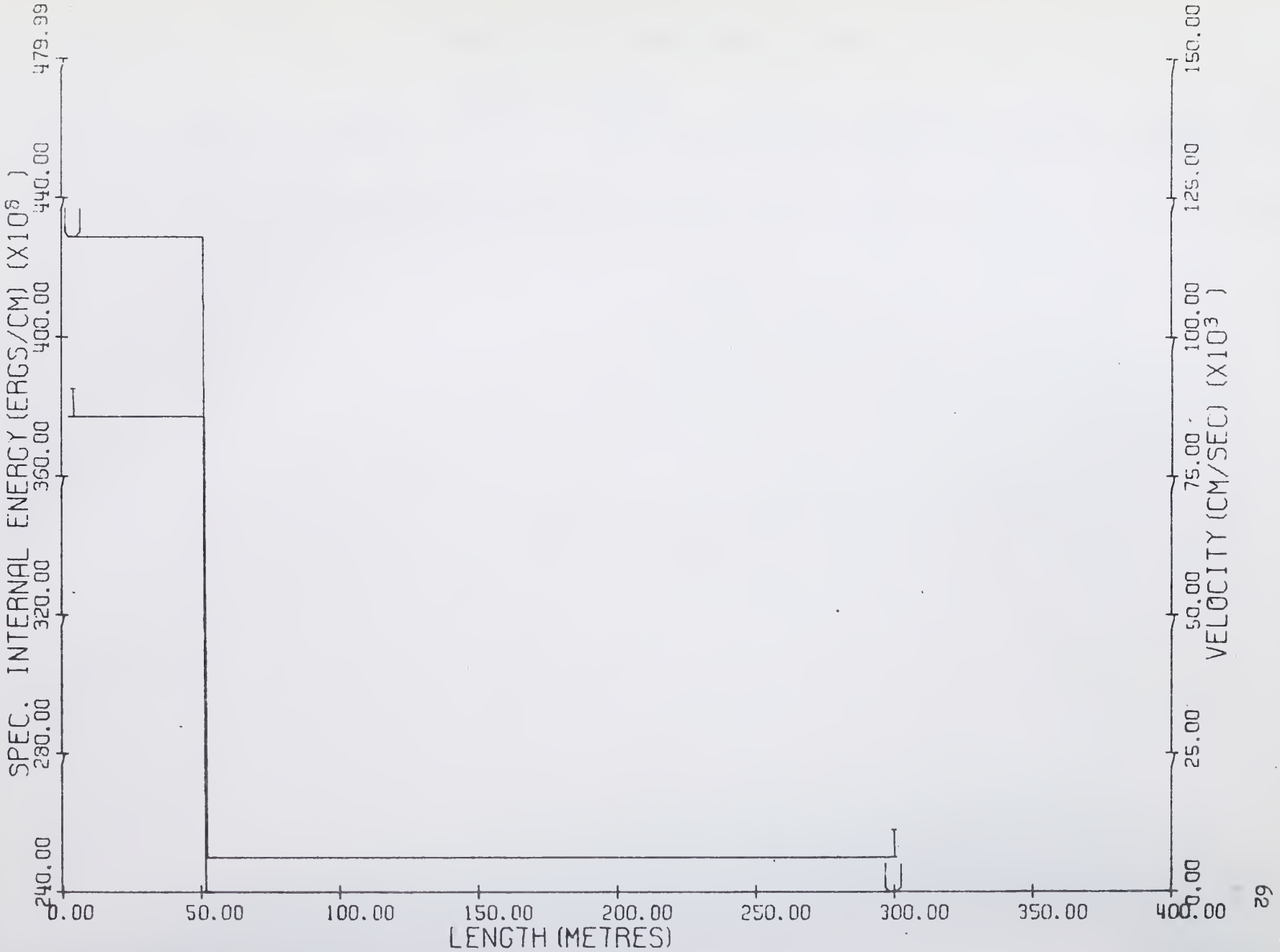

Figure 18. 1A Exact, Time = 0. Sec.

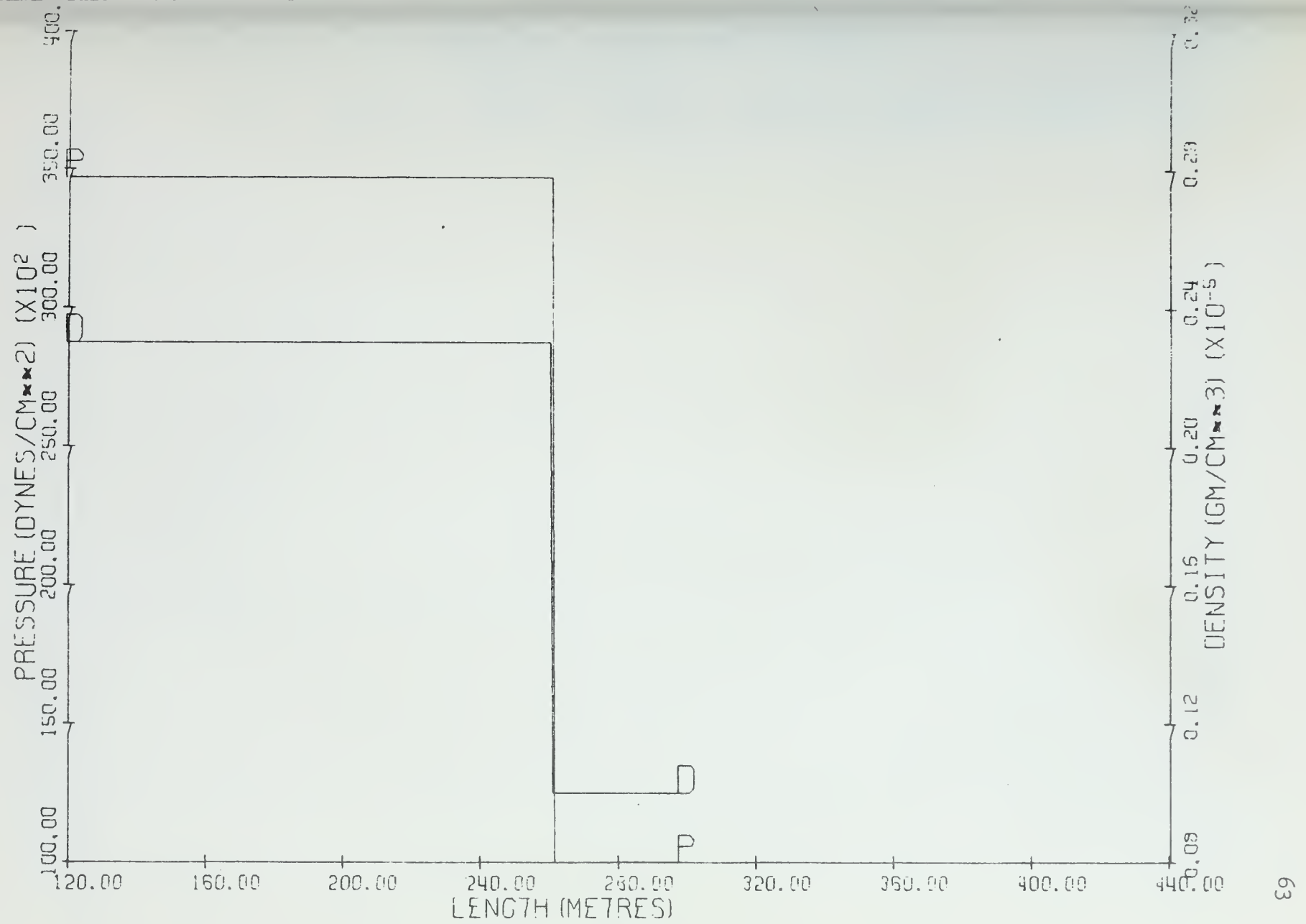

Figure 19. 1A Exact, Time = .1 Sec.

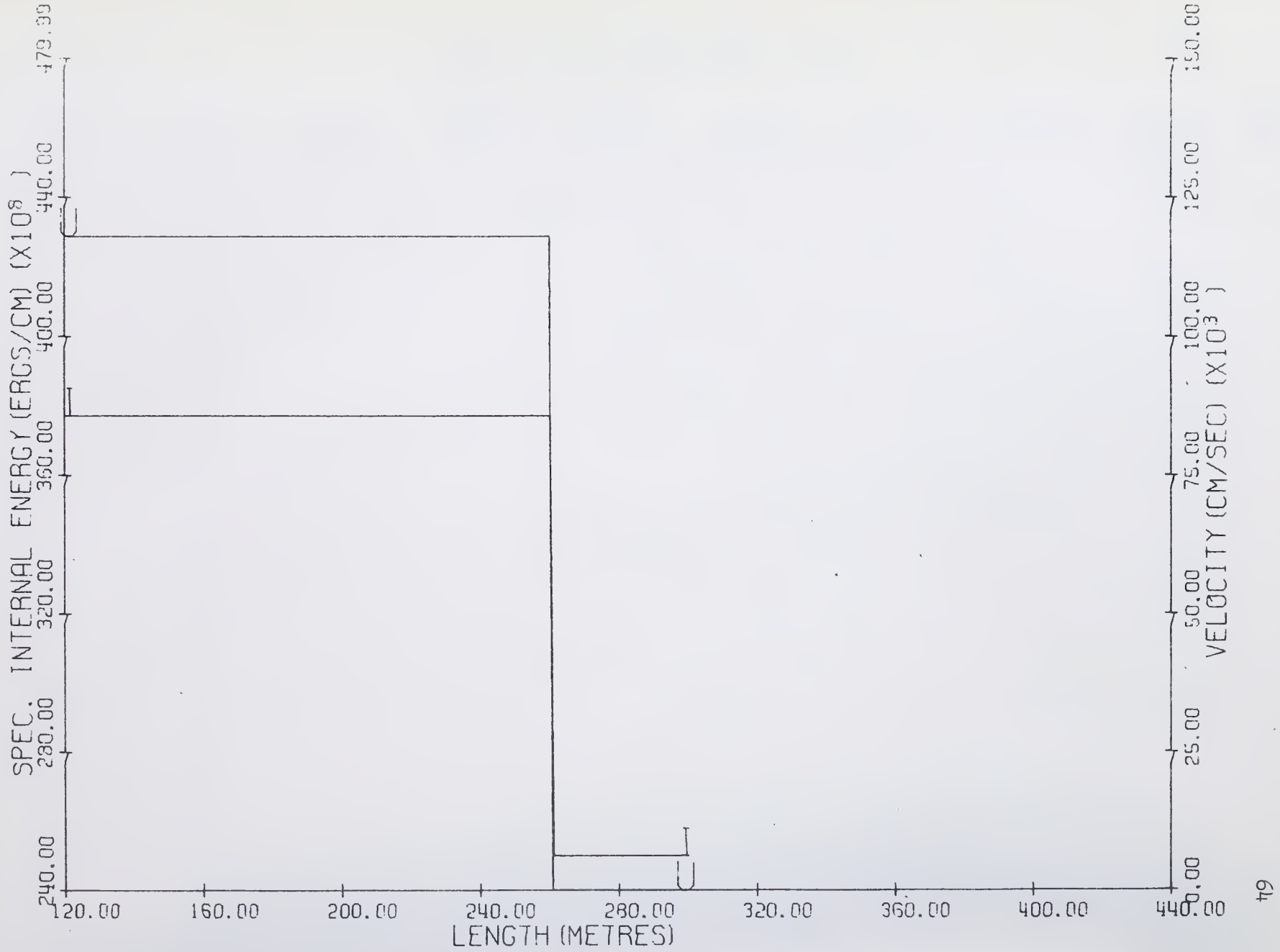

Figure 20. 1A Exact, Time = .1 Sec.

Figure 21. 1A Continuous Rezone, Time = .1 Sec.

Figure 22. 1A Continuous Rezone, Time = .1 Sec.

Figure 23. 1A OIL, Time = .1 Sec.

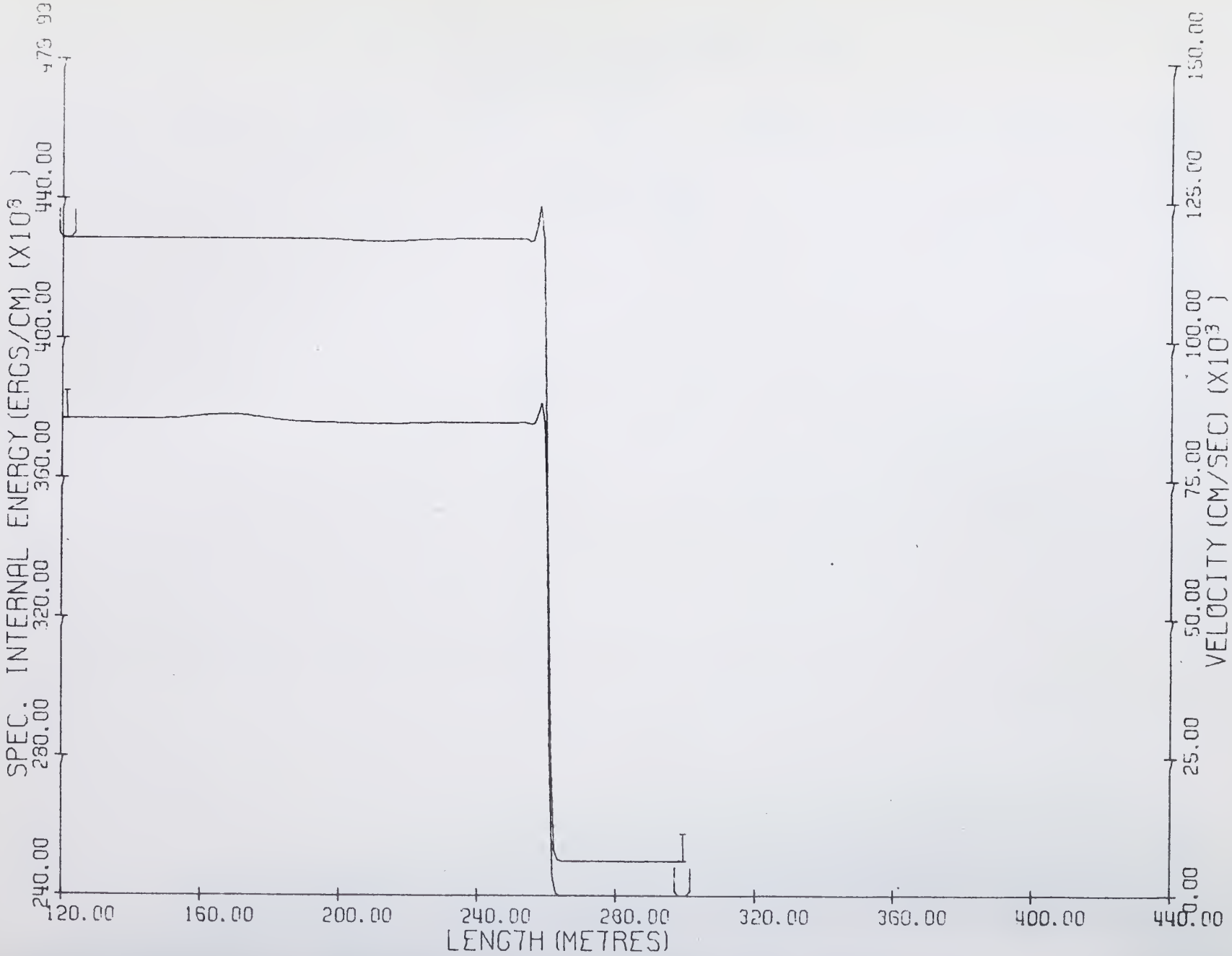

Figure 24. 1A OIL, Time = .1 Sec.

Figure 25. 1A Donor, Time = .1 Sec.

Figure 26. 1A Donor, Time = .1 Sec.

Figure 27. 1B Exact, Time = 0. Sec.

Figure 28. 1B Exact, Time = 0. Sec.

Figure 29. 1B Exact, Time = .001 Sec.

Figure 30. 1B Exact, Time = .001 Sec.

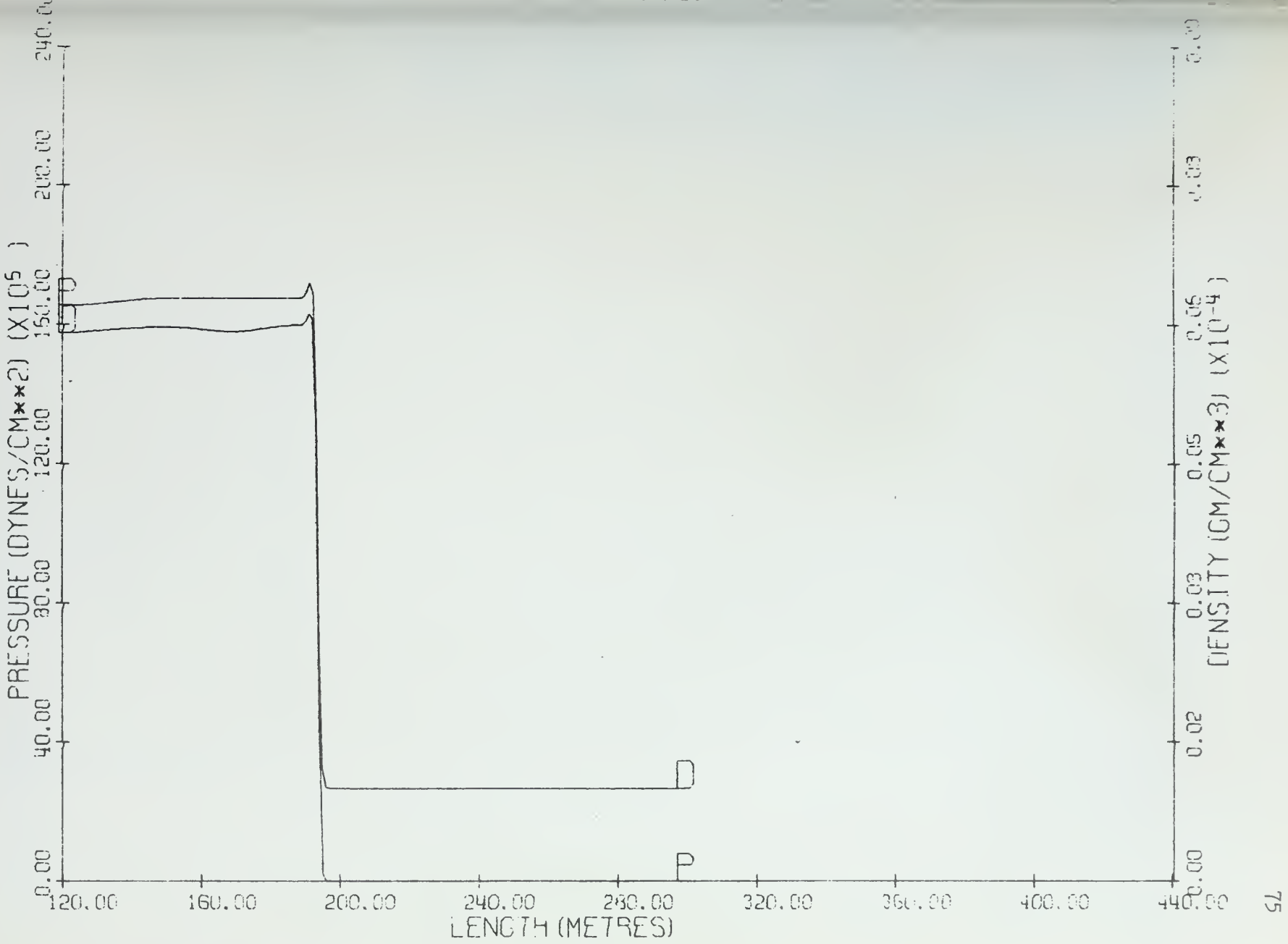

Figure 31. 1B Continuous Rezone, Time = .001 Sec.

Figure 32. 1B Continuous Rezone, Time = .001 Sec.

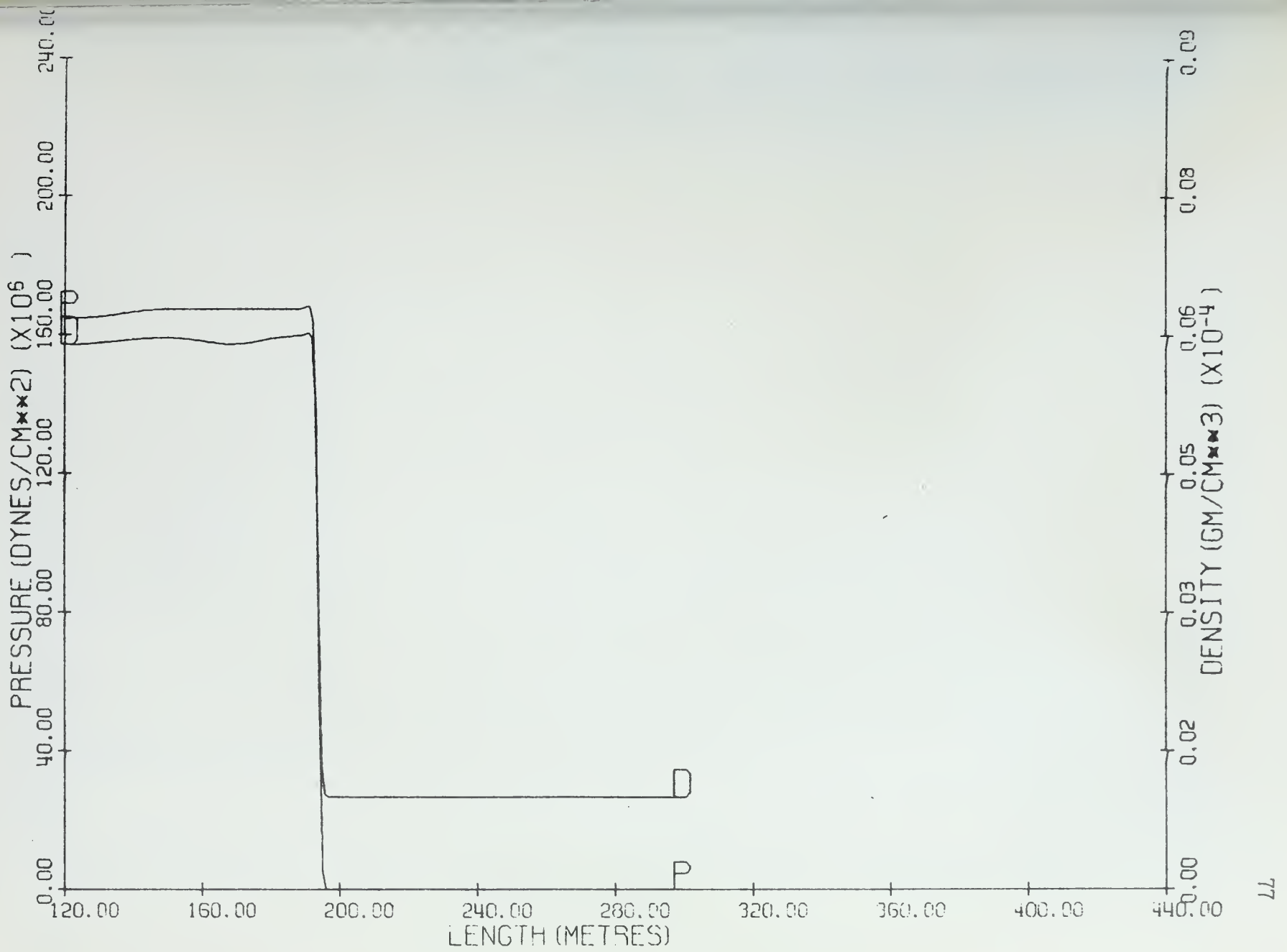

Figure 33. 1B OIL, Time = .001 Sec.

Figure 34. 1B OIL, Time = .001 Sec.

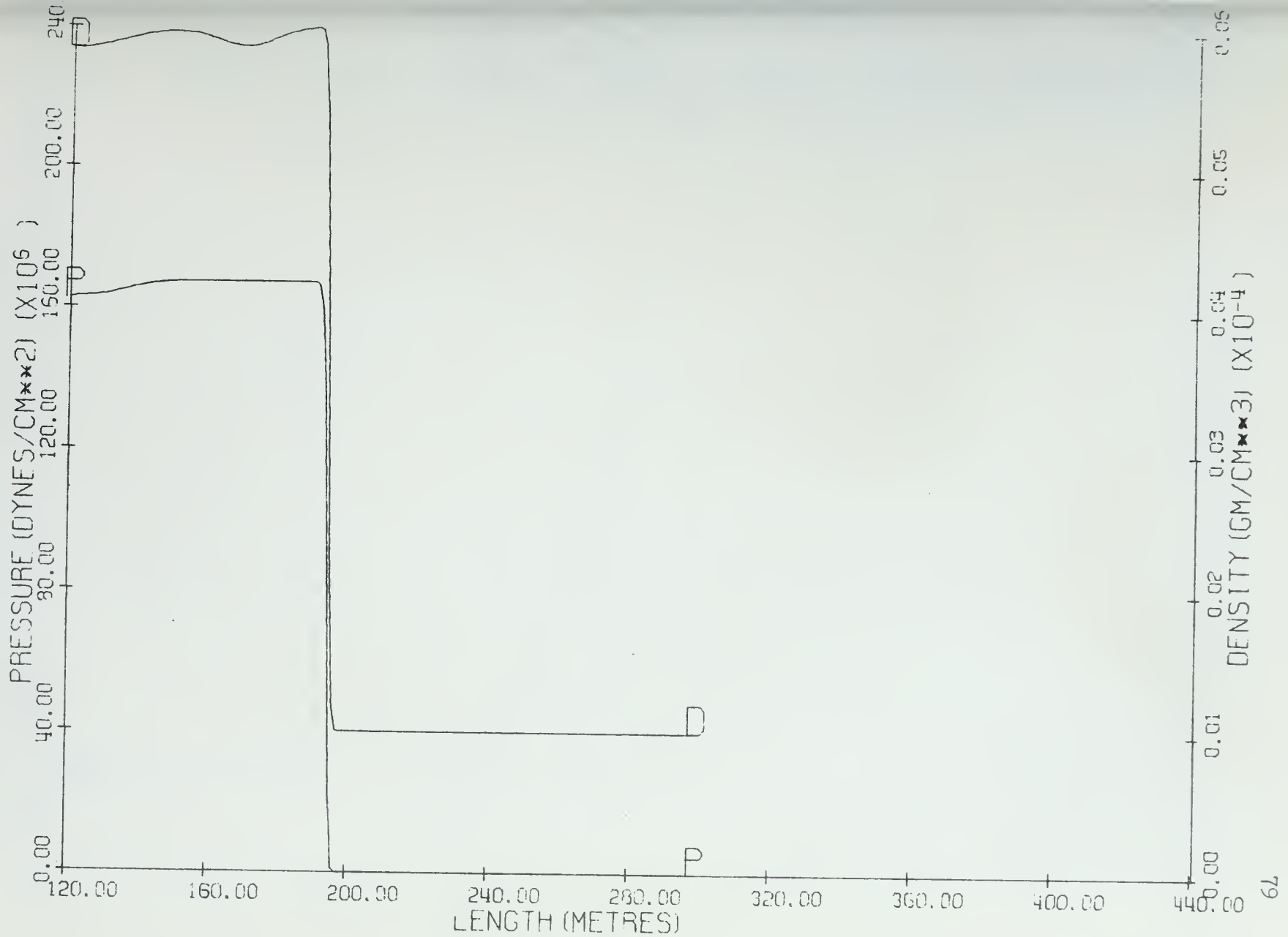

Figure 35. 1B Donor, Time = .001 Sec.

Figure 36. 1B Donor, Time = .001 Sec.

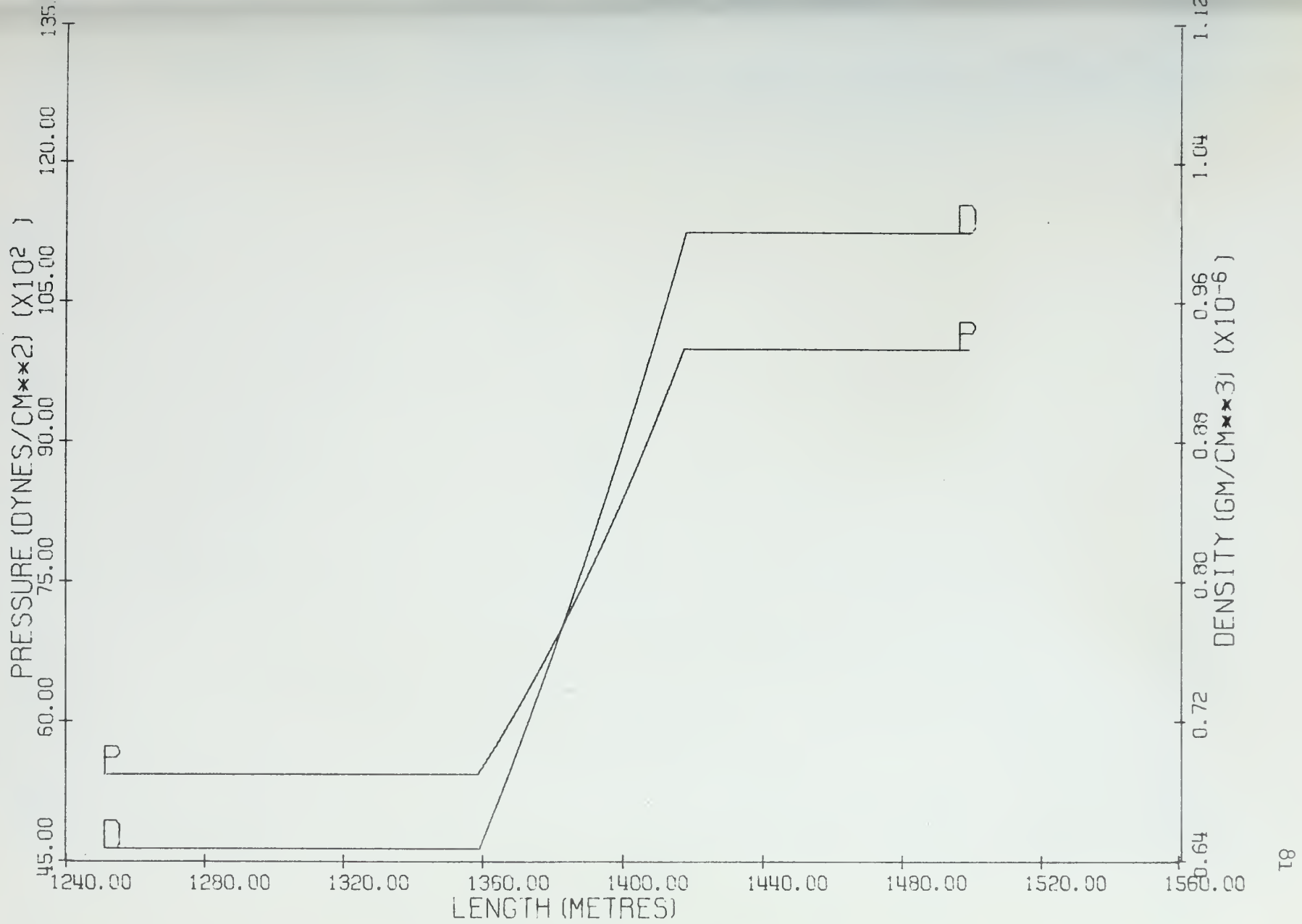

Figure 37. 2A Exact, Time = .1 Sec.

Figure 38. 2A Exact, Time = .1 Sec.

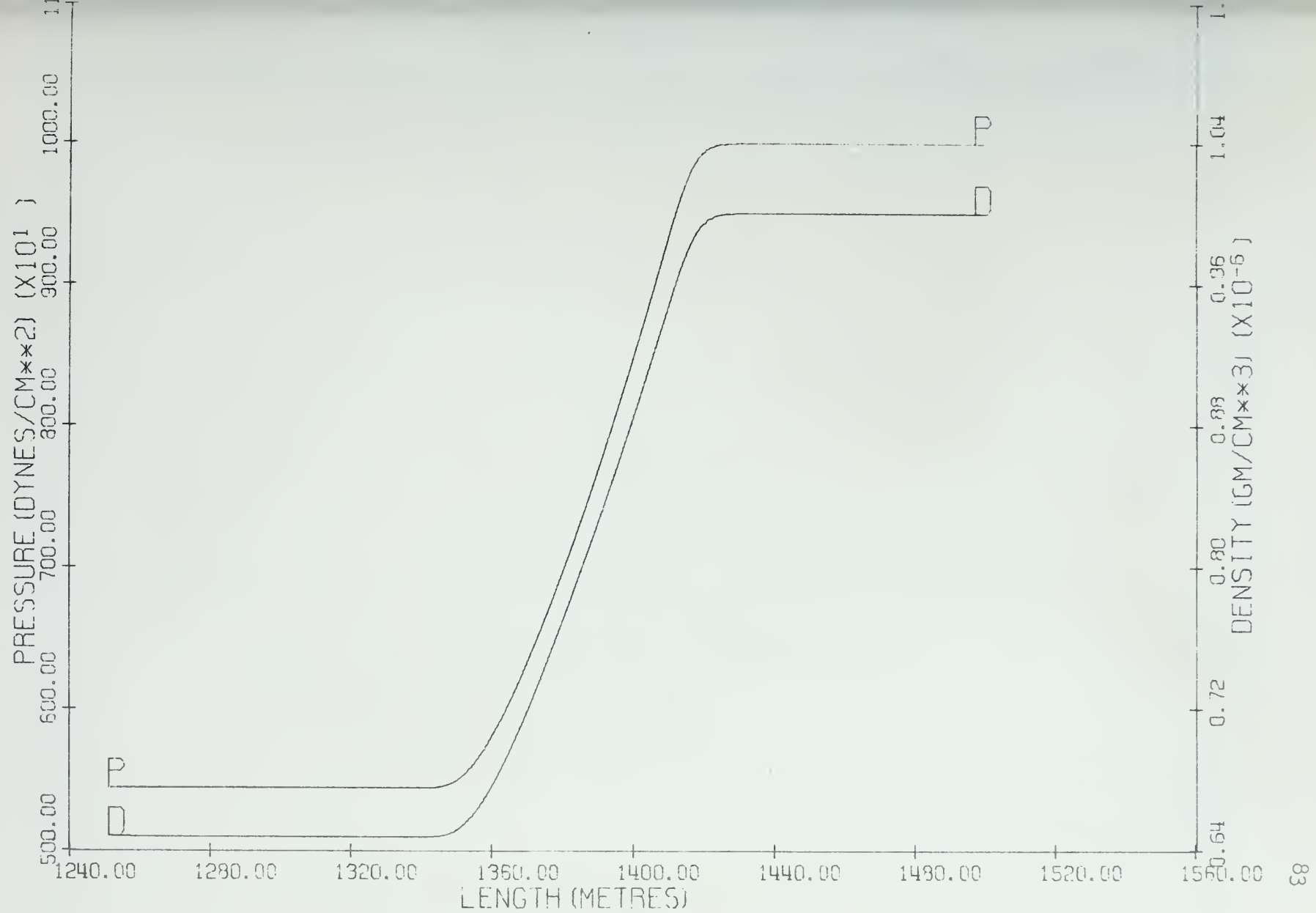

Figure 39. 2A Continuous Rezone, Time = .1 Sec.

Figure 40. 2A Continuous Rezone, Time = .1 Sec.

Figure 41. 2A OIL, Time = .1 Sec.

Figure 42. 2A OIL, Time = .1 Sec.

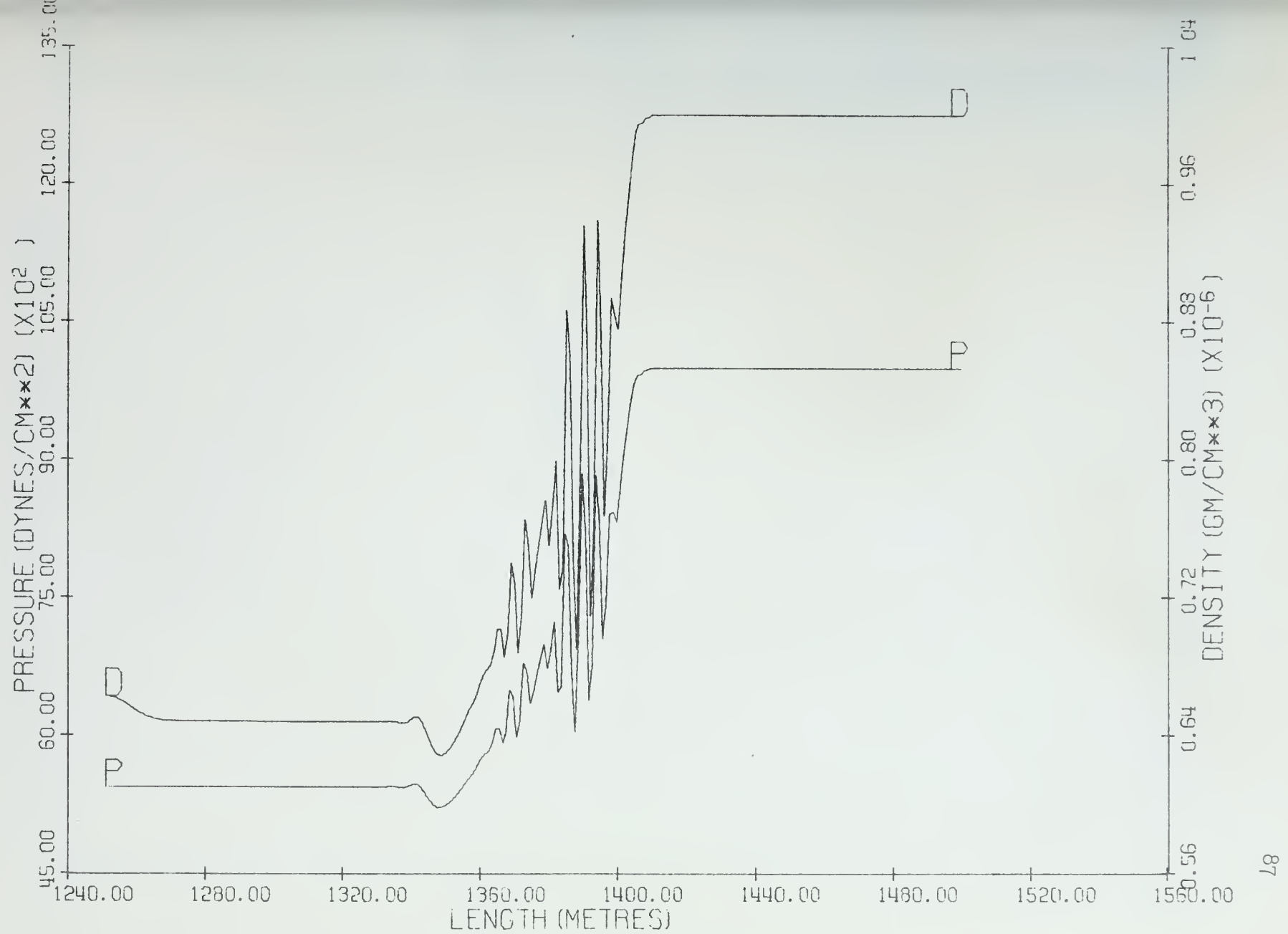

Figure 43. 2A Donor, Time = .1 Sec.

Figure 44. 2A Donor, Time = .1 Sec.

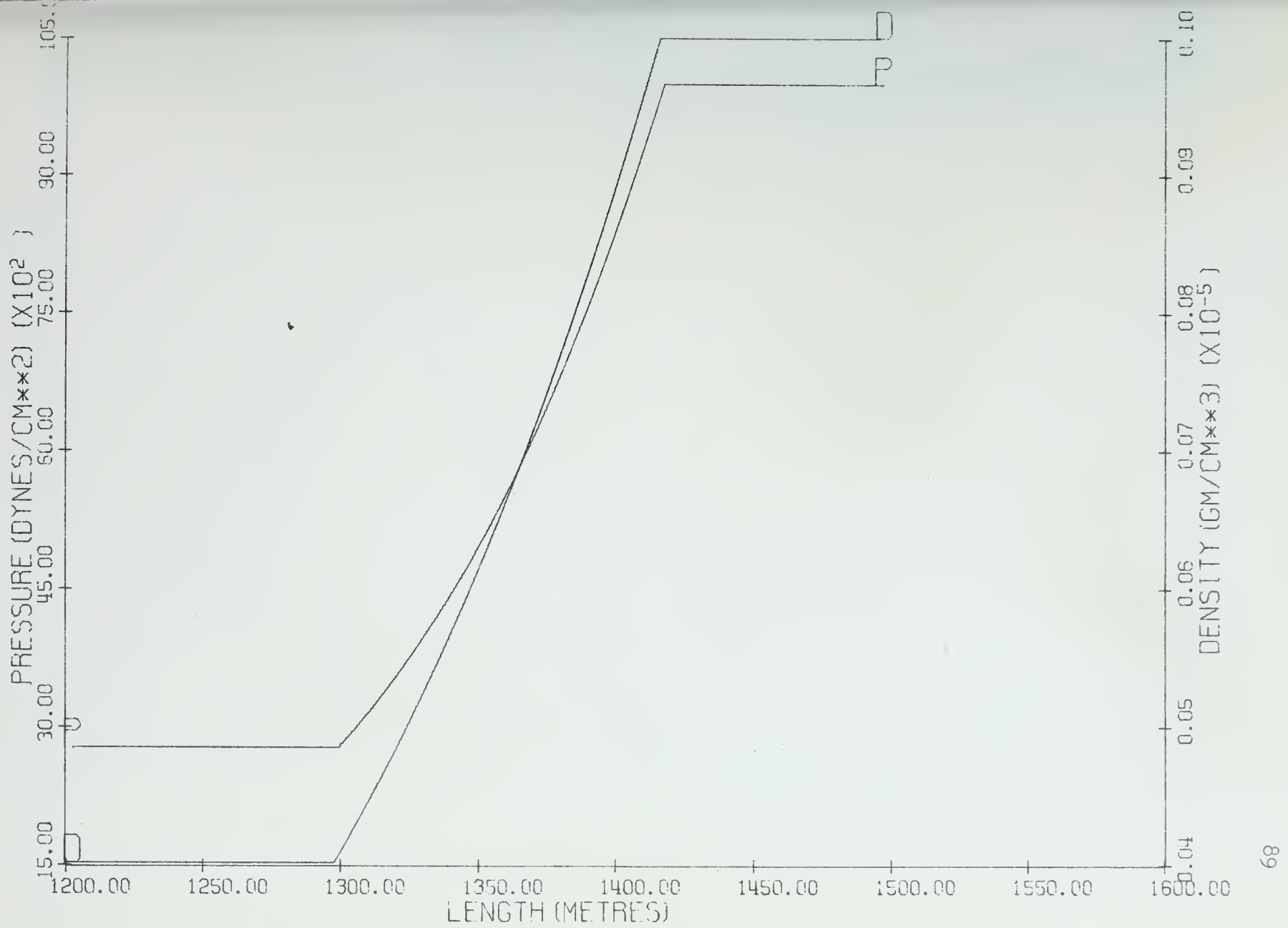

Figure 45. 2B Exact, Time = .1 Sec.

Figure 46. 2B Exact, Time = .1 Sec.

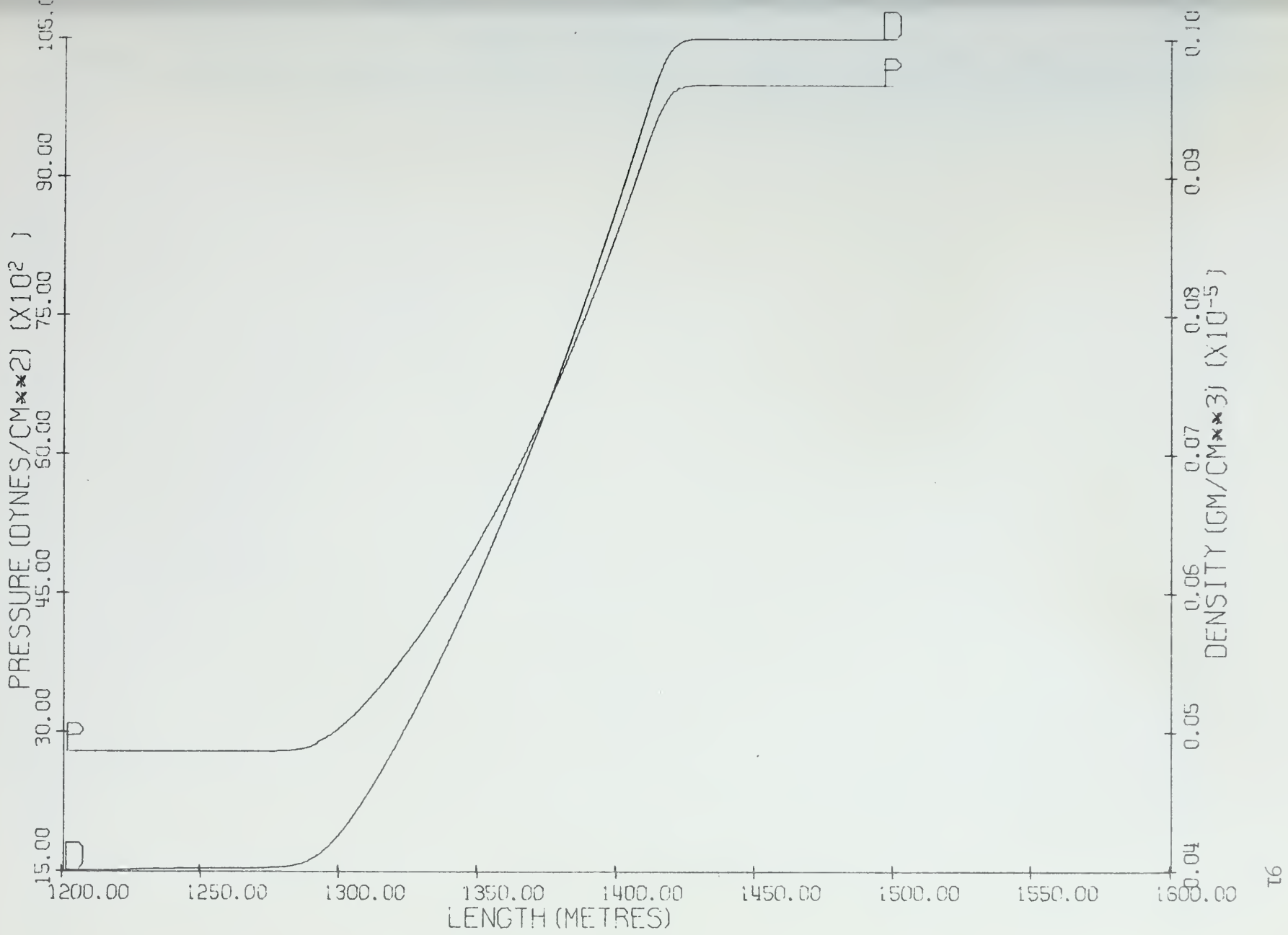

Figure 47. 2B Continuous Rezone, Time = .1 Sec.

Figure 48. 2B Continuous Rezone, Time = .1 Sec.

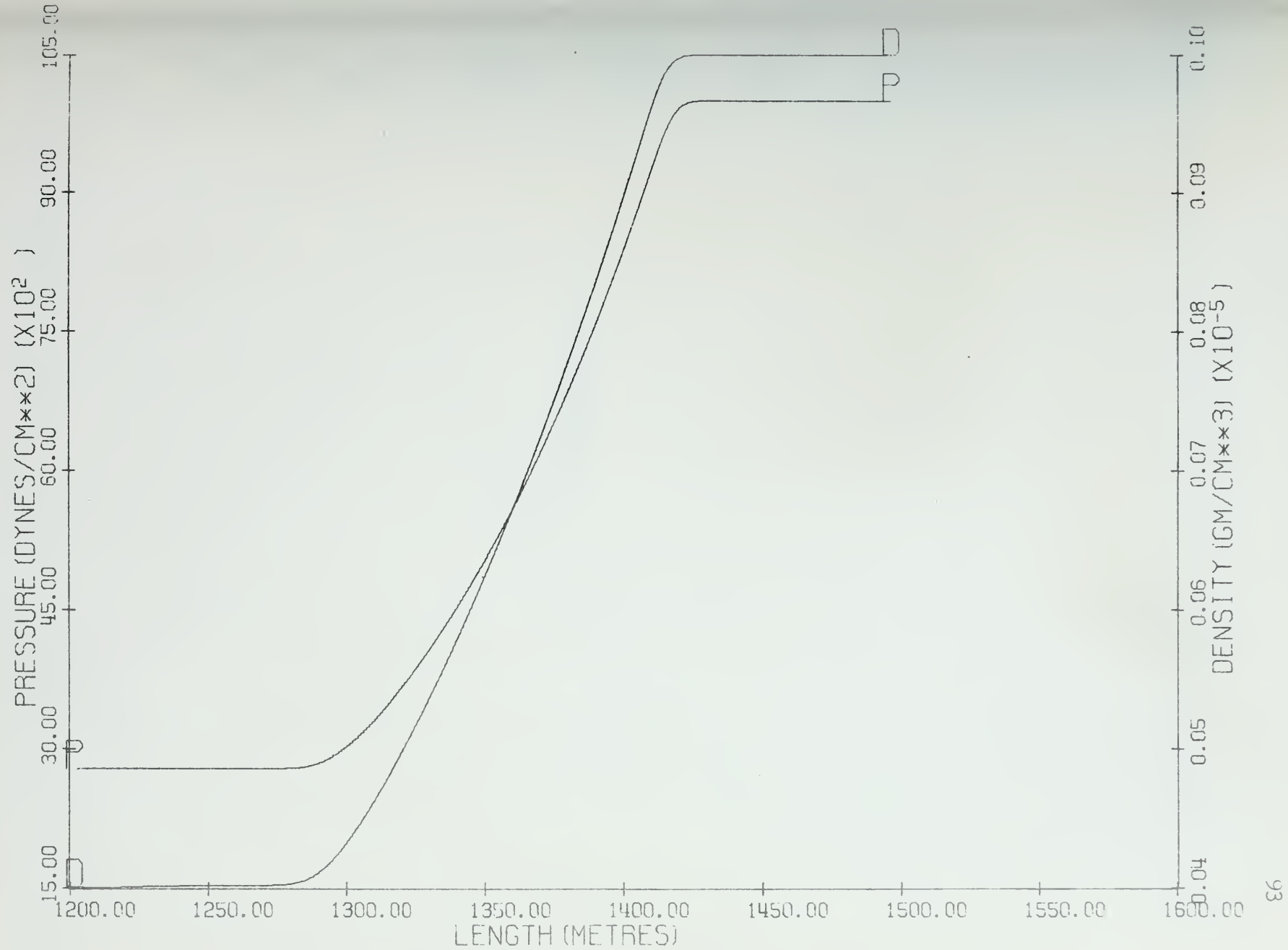

Figure 49. 2B OIL, Time = .1 Sec.

Figure 50. 2B OIL, Time = .1 Sec.

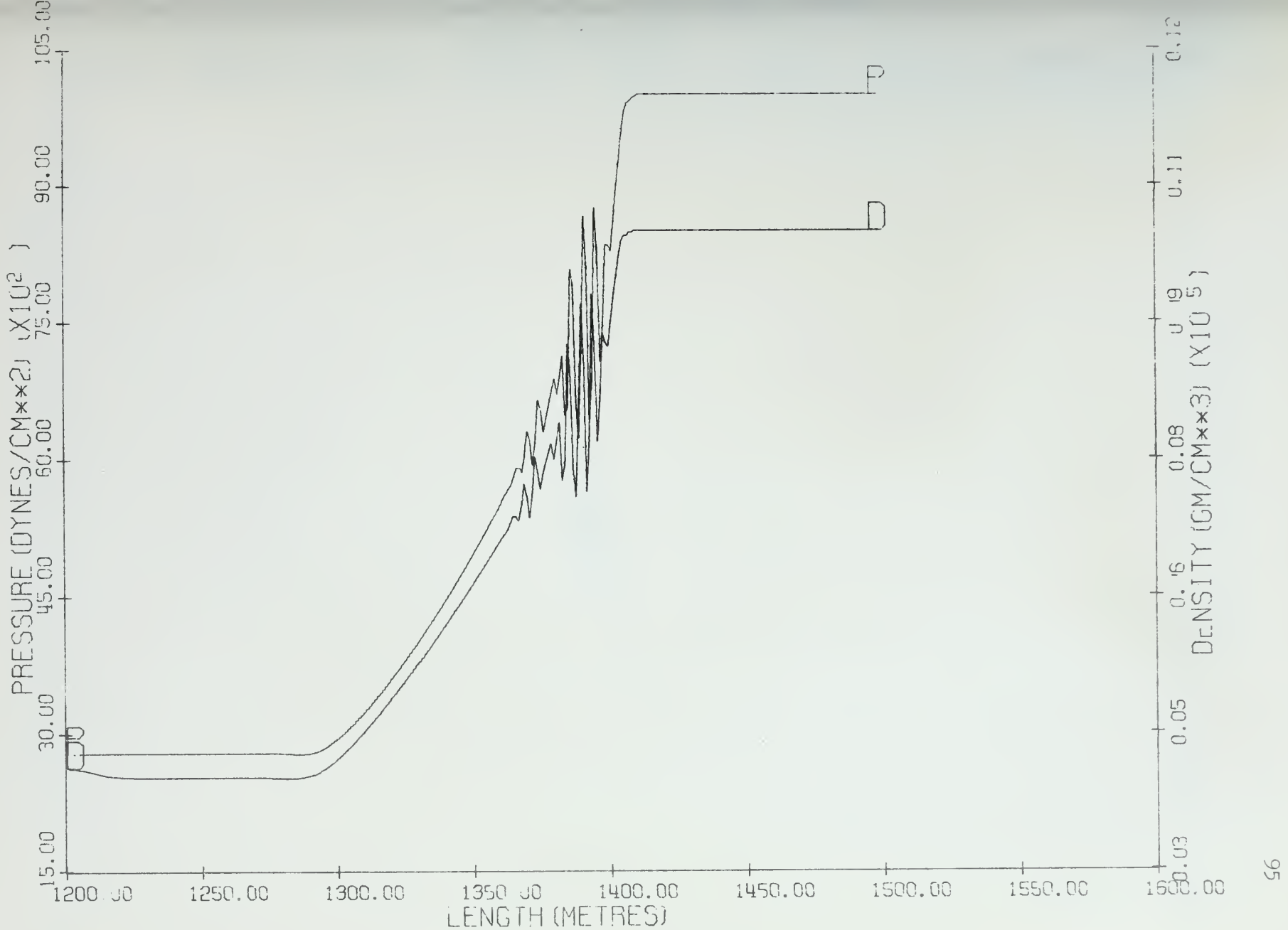

Figure 51. 2B Donor, Time = .1 Sec.

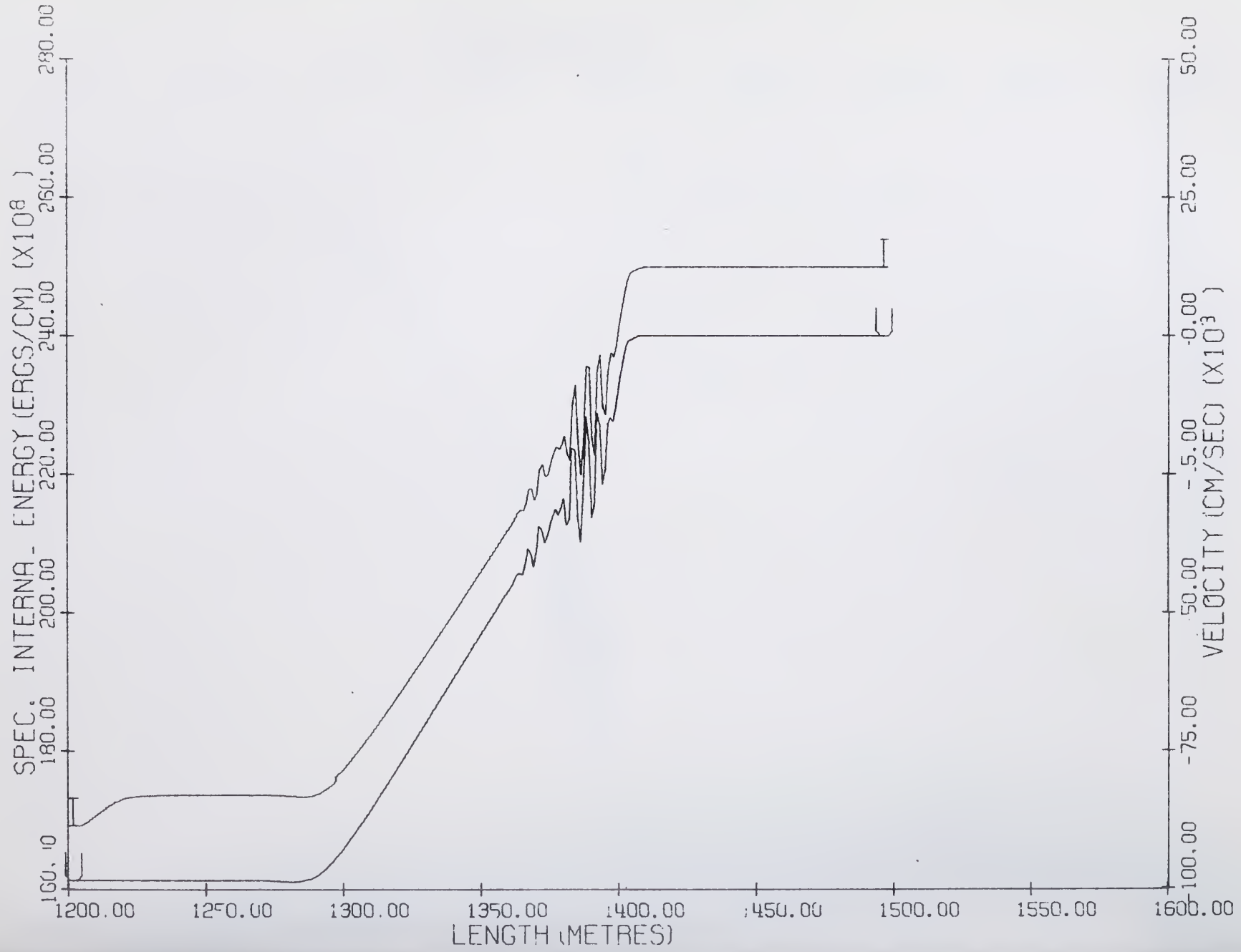

Figure 52. 2B Donor, Time = .1 Sec.

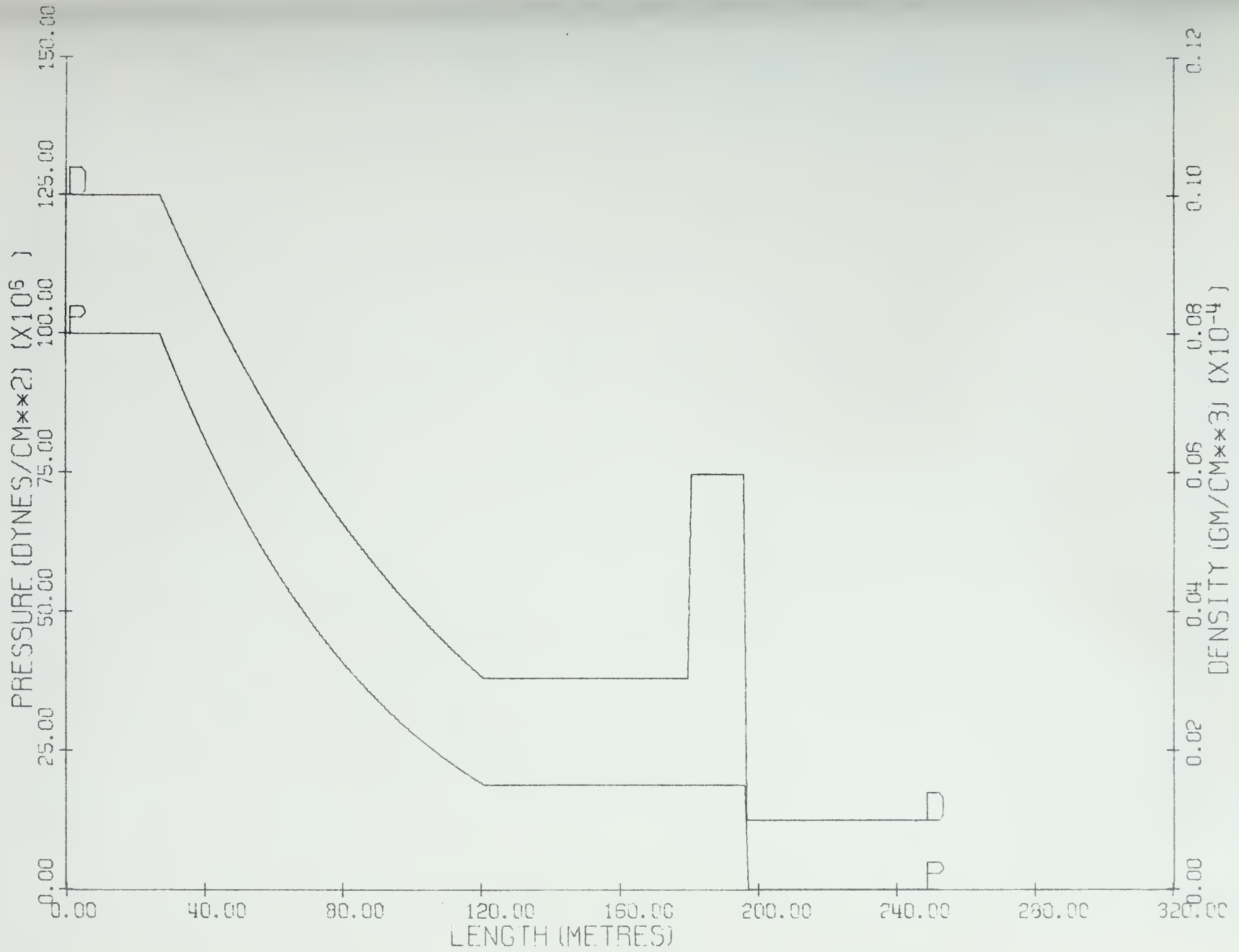

Figure 53. 5A Exact, Time = .002 Sec.

Figure 54. 5A Exact, Time = .002 Sec.

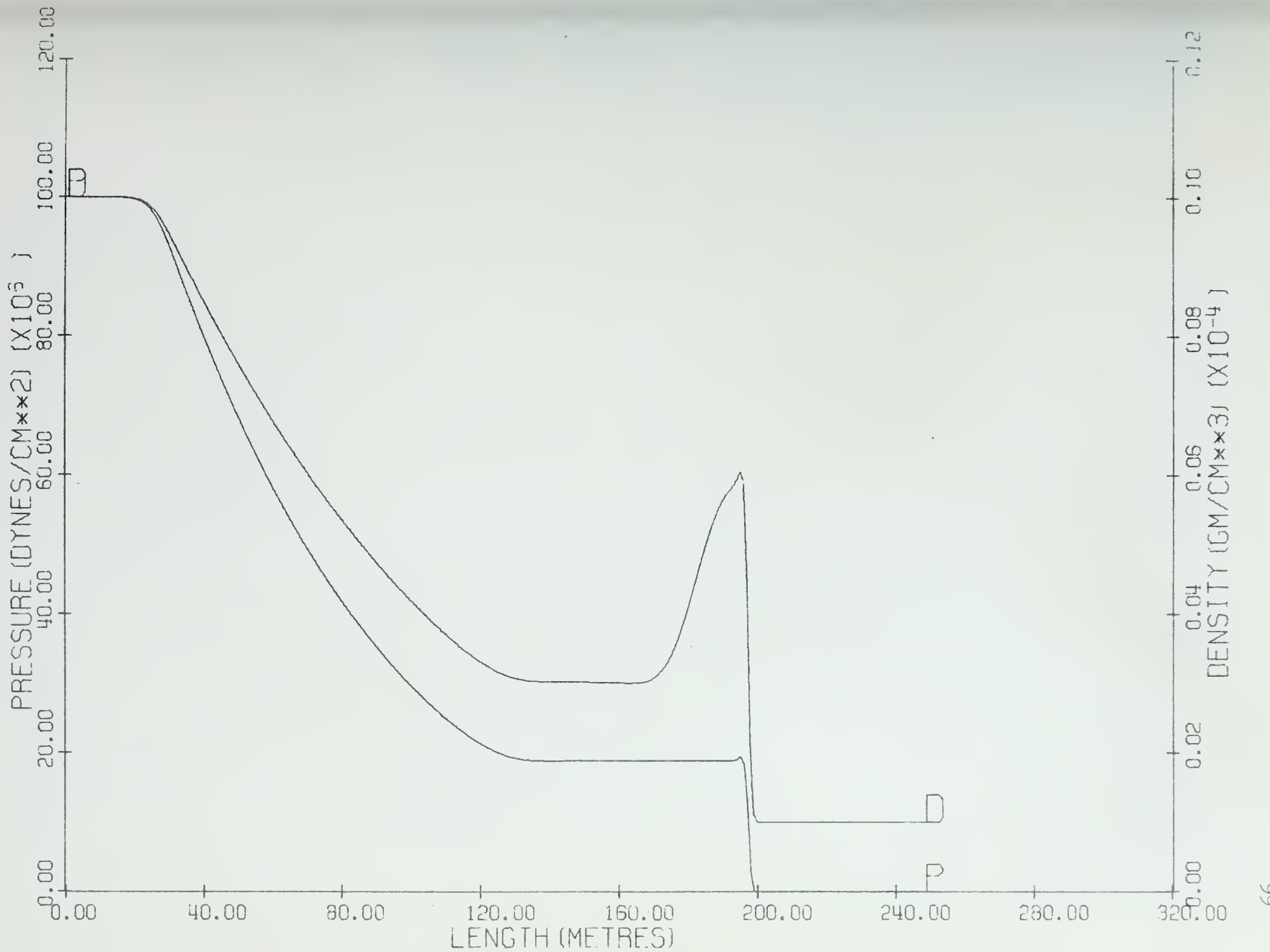

Figure 55. 5A Continuous Rezone, Time = .002 Sec.

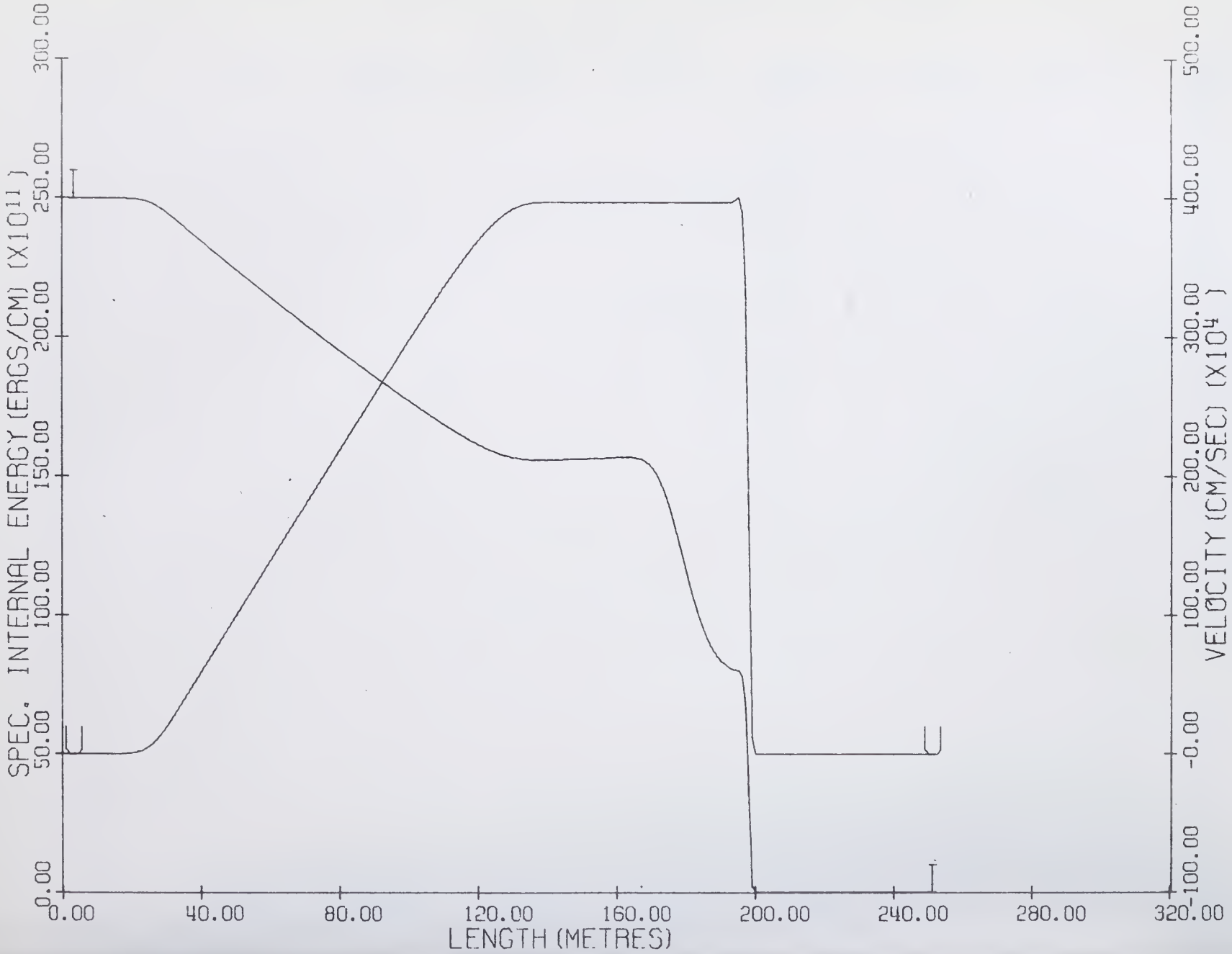

Figure 56. 5A Continuous Rezone, Time = .002 Sec.

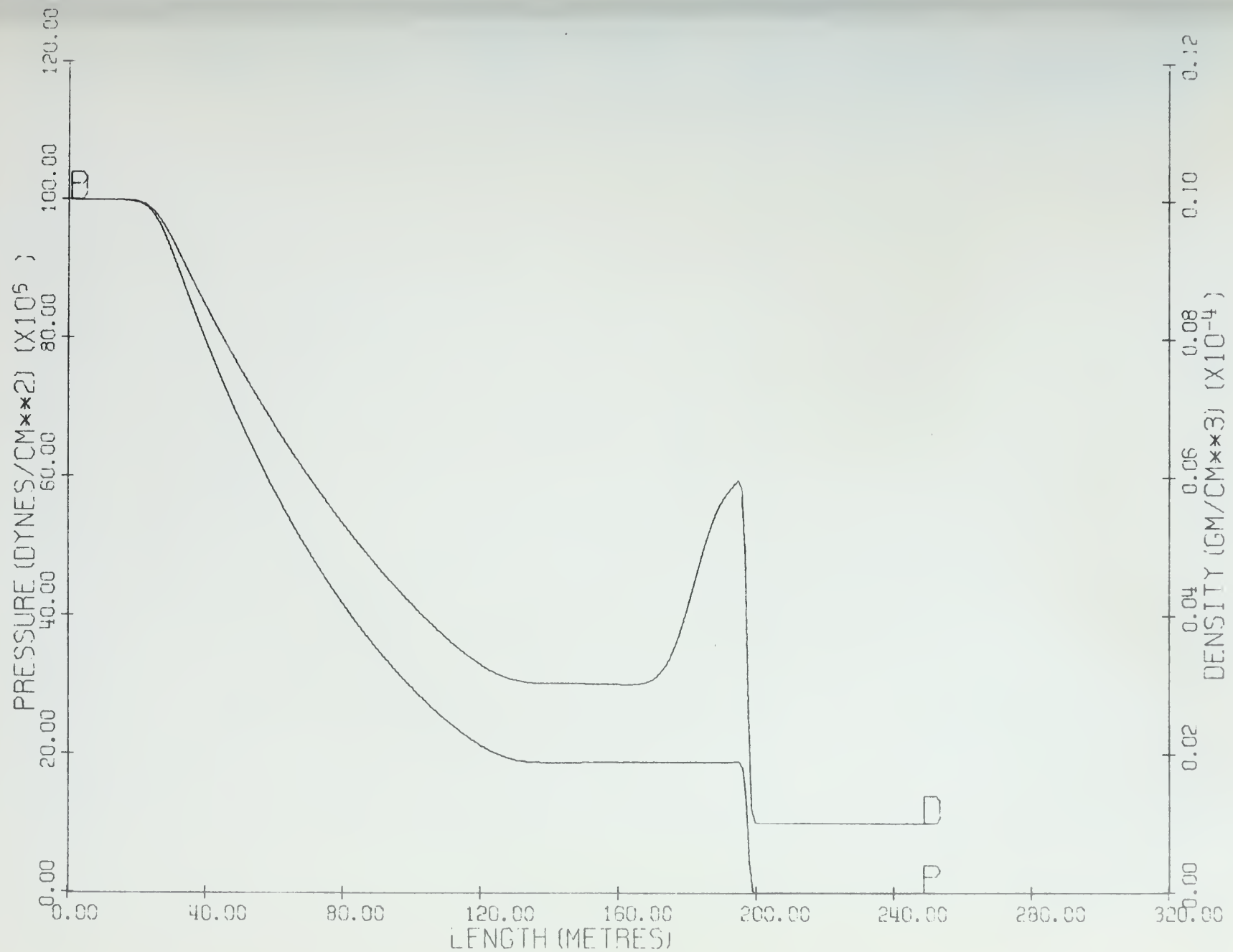

Figure 57. 5A OIL, Time = .002 Sec.

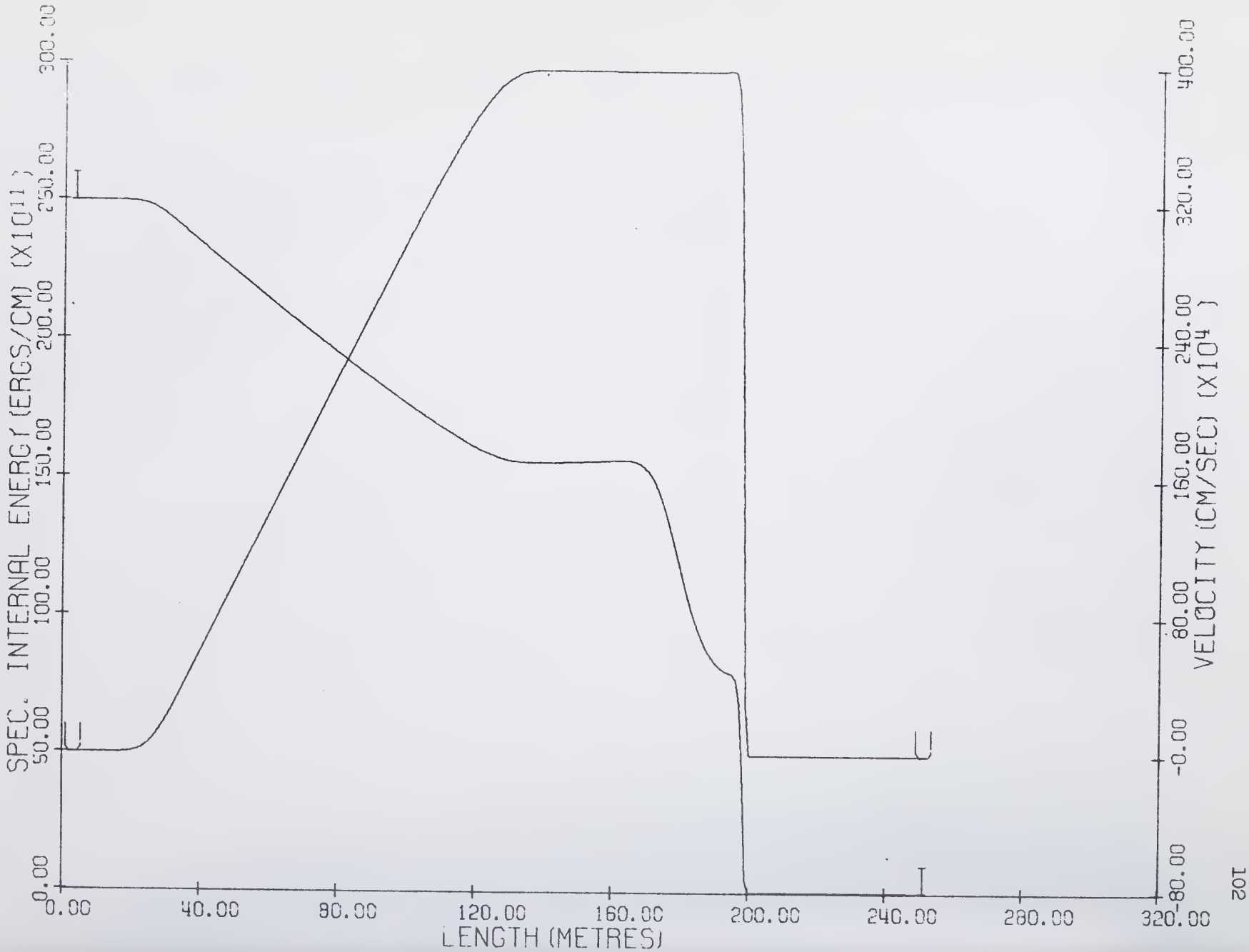

Figure 58. 5A OIL, Time = .002 Sec.

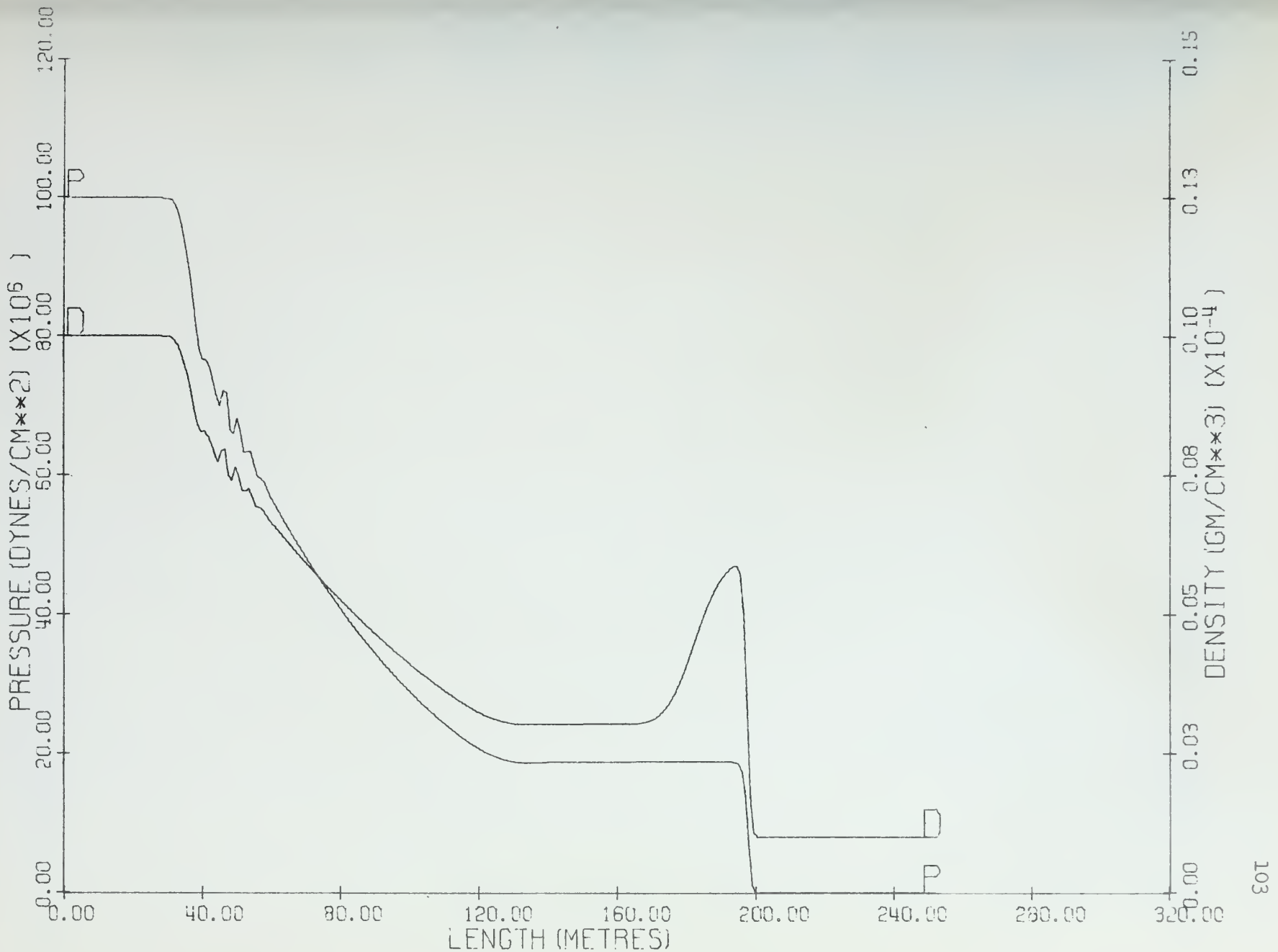

Figure 59. 5A Donor, Time = .002 Sec.

Figure 60. 5A Donor, Time = .002 Sec.

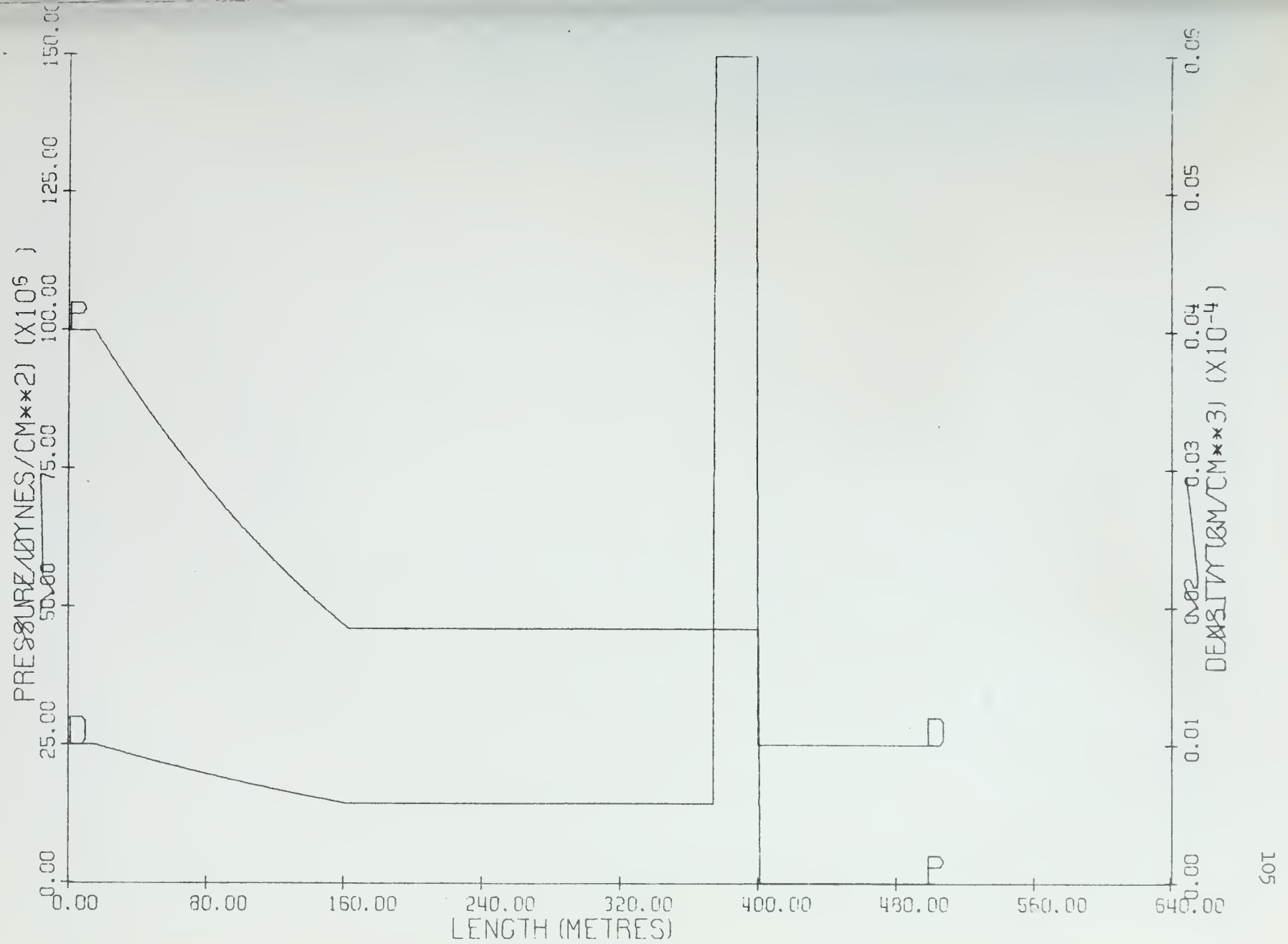

Figure 61. 5B Exact, Time = .002 Sec.

Figure 62. 5B Exact, Time = .002 Sec.

Figure 63. 5B Continuous Rezone, Time = .002 Sec.

Figure 64. 5B Continuous Rezone, Time = .002 Sec.

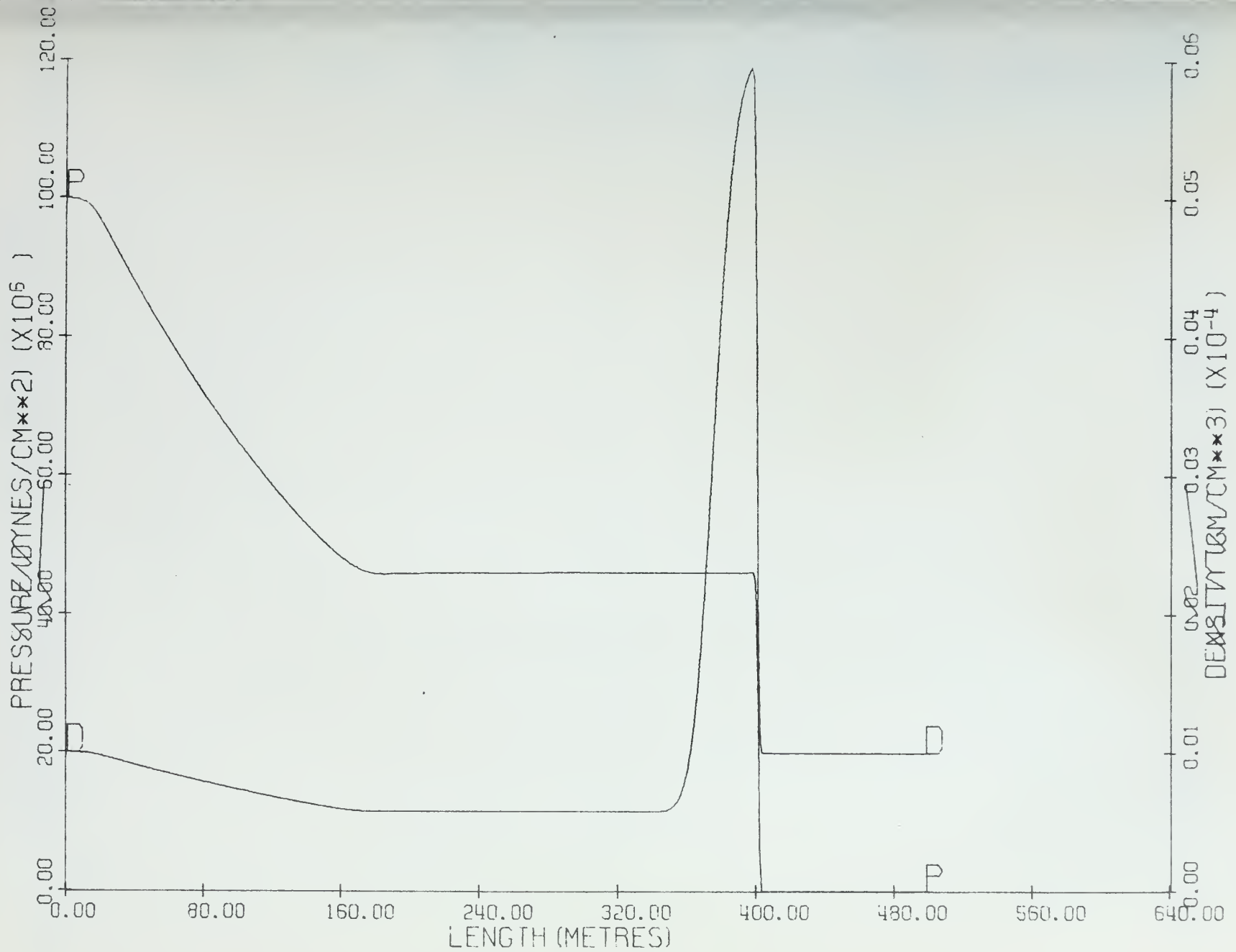

Figure 65. 5B OIL, Time = .002 Sec.

Figure 66. 5B OIL, Time = .002 Sec.

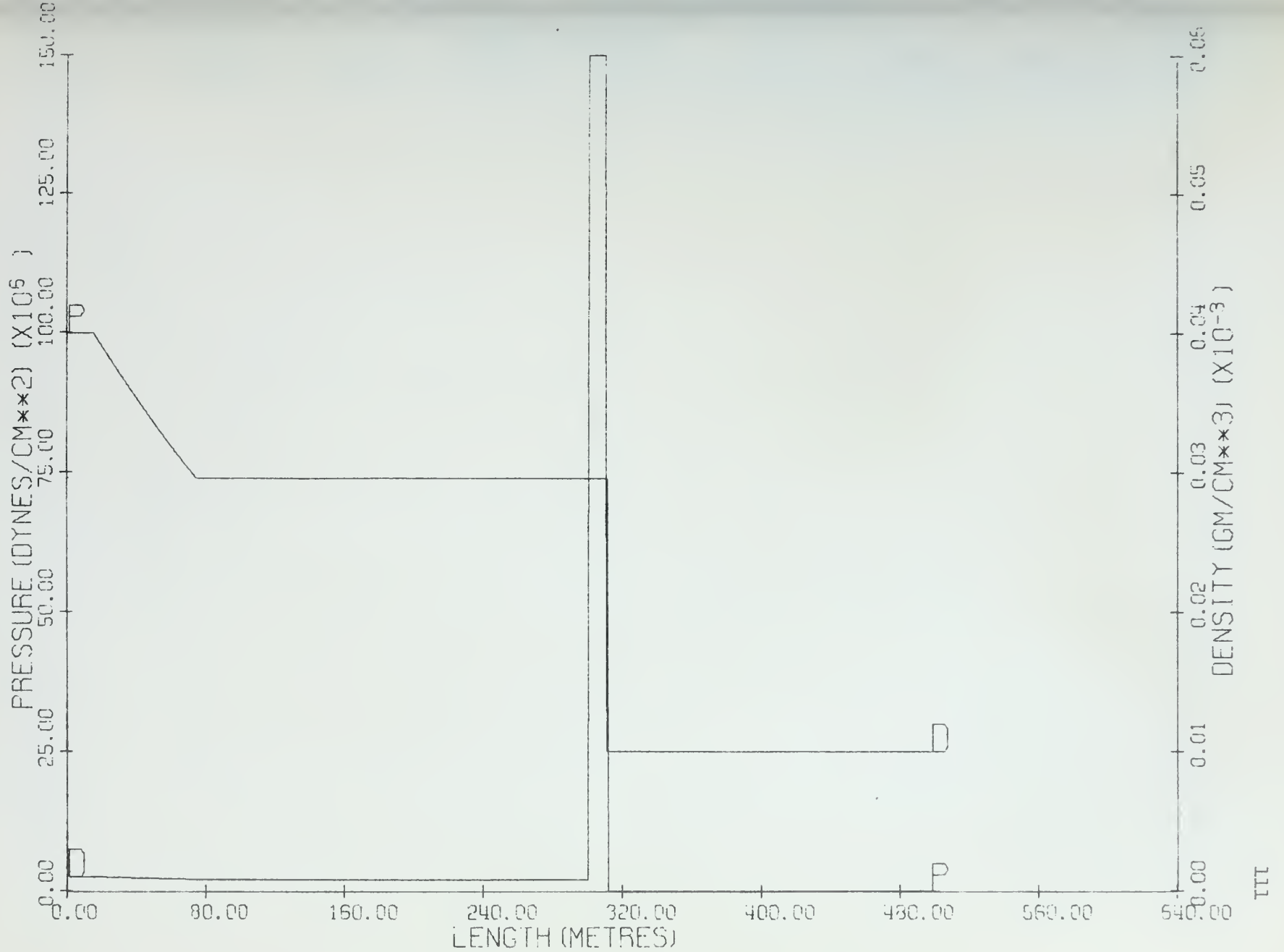

Figure 67. 5C Exact, Time = .002 Sec.

Figure 68. 5C Exact, Time = .002 Sec.

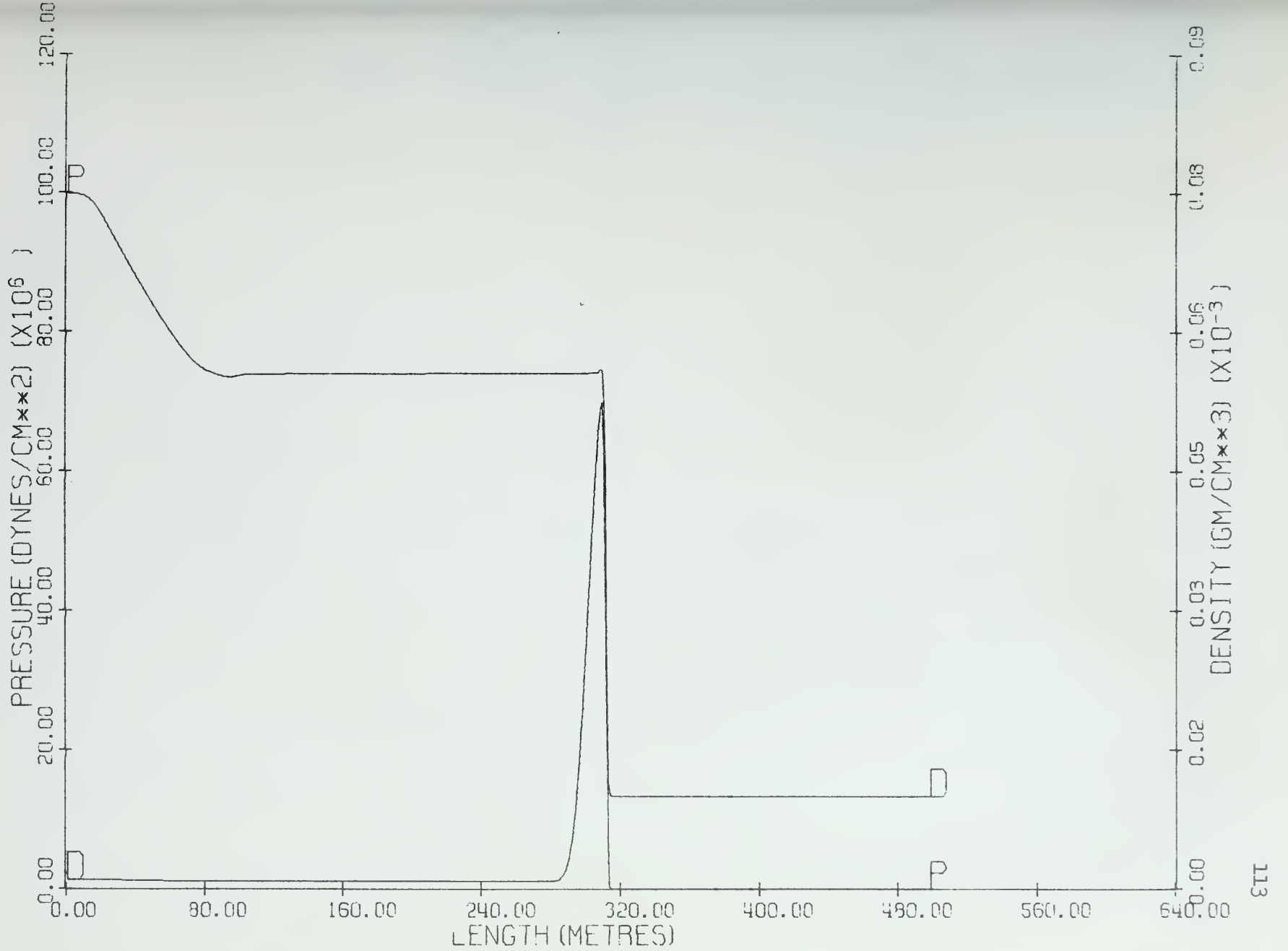

Figure 69. 5C Continuous Rezone, Time = .002 Sec.

Figure 70. 5C Continuous Rezone, Time = .002 Sec.

Figure 71. 5C OIL, Time = .002 Sec.

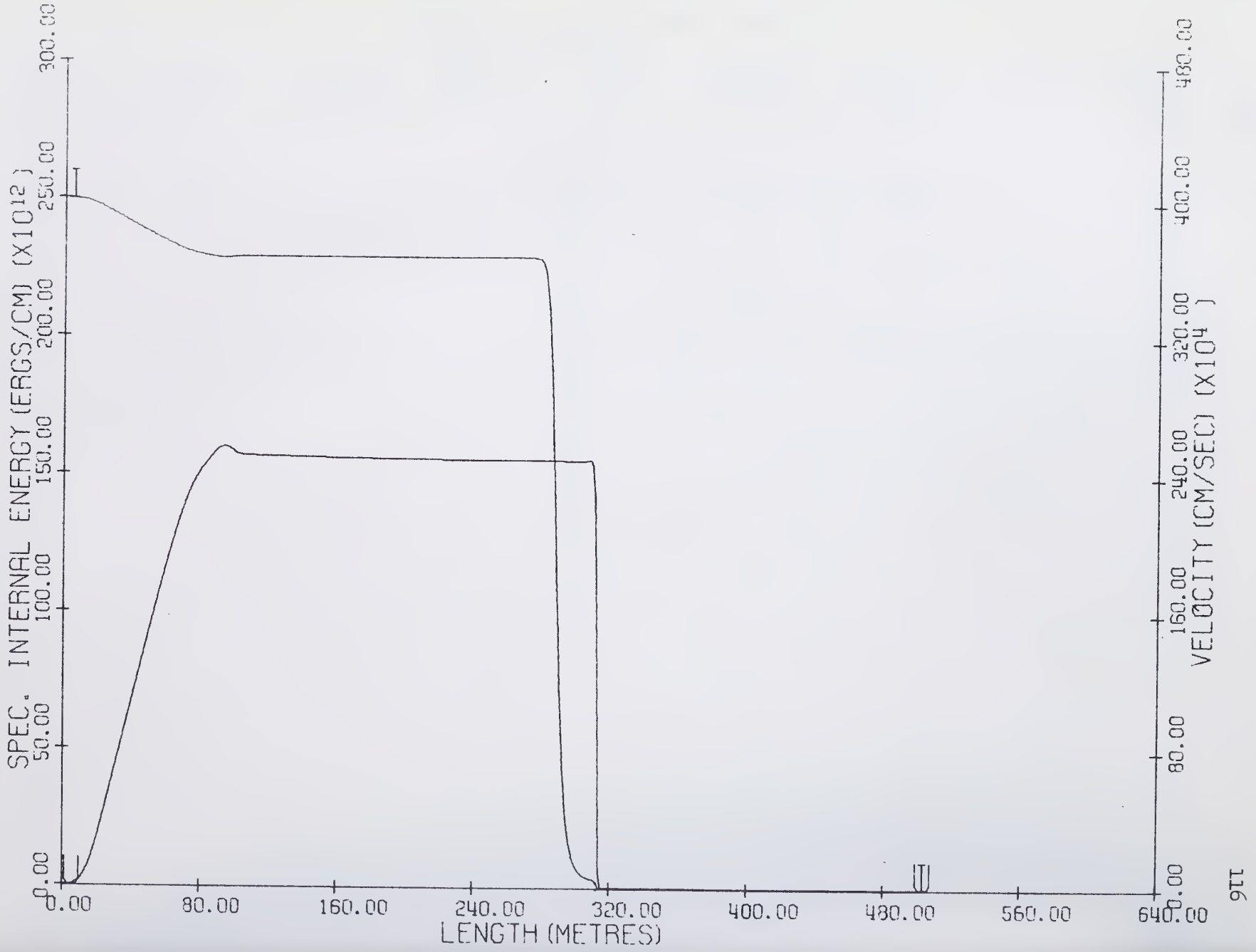

Figure 72. 5C OIL, Time = .002 Sec.

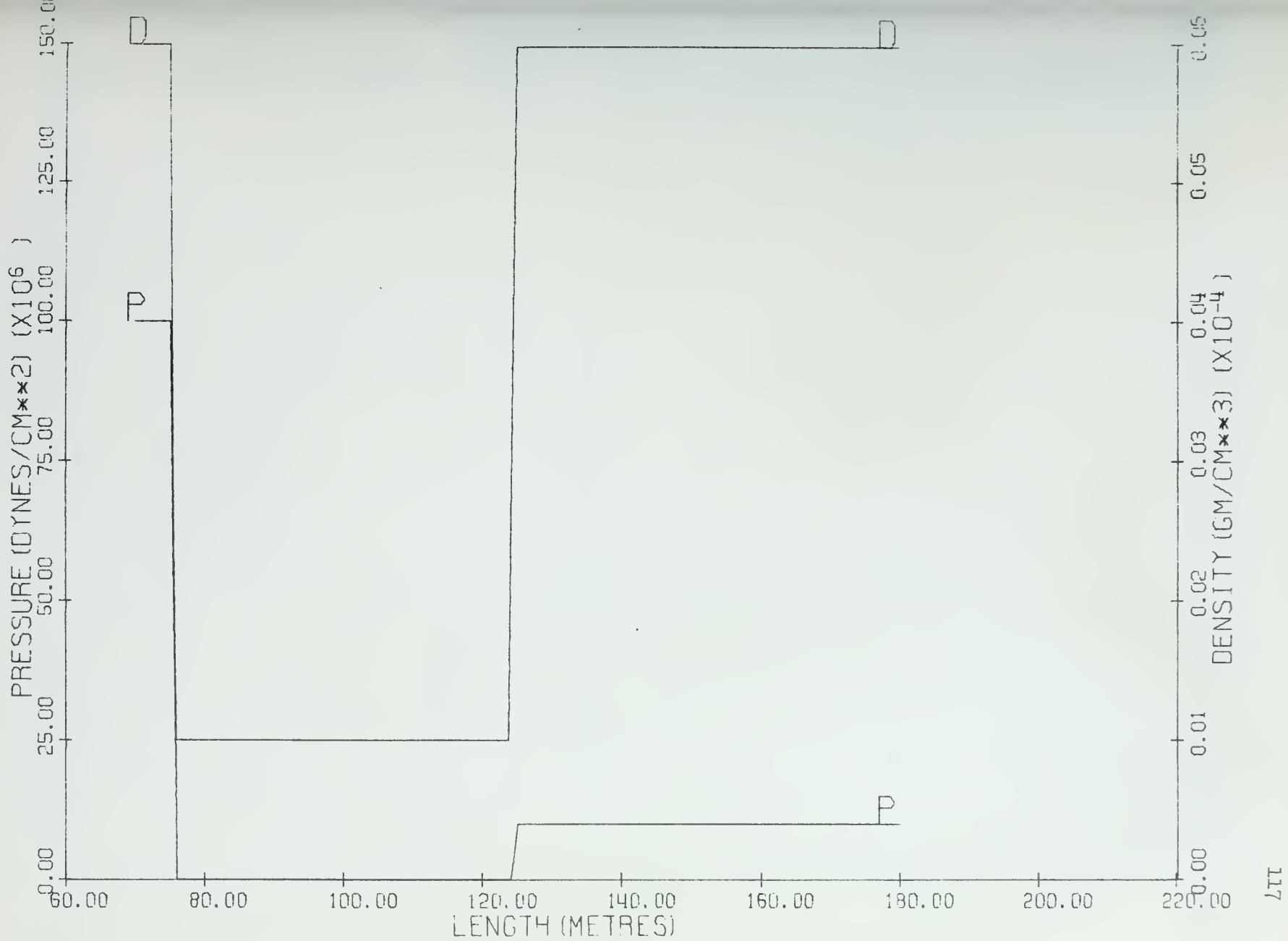

Figure 73. 6A Exact, Time = 0. Sec.

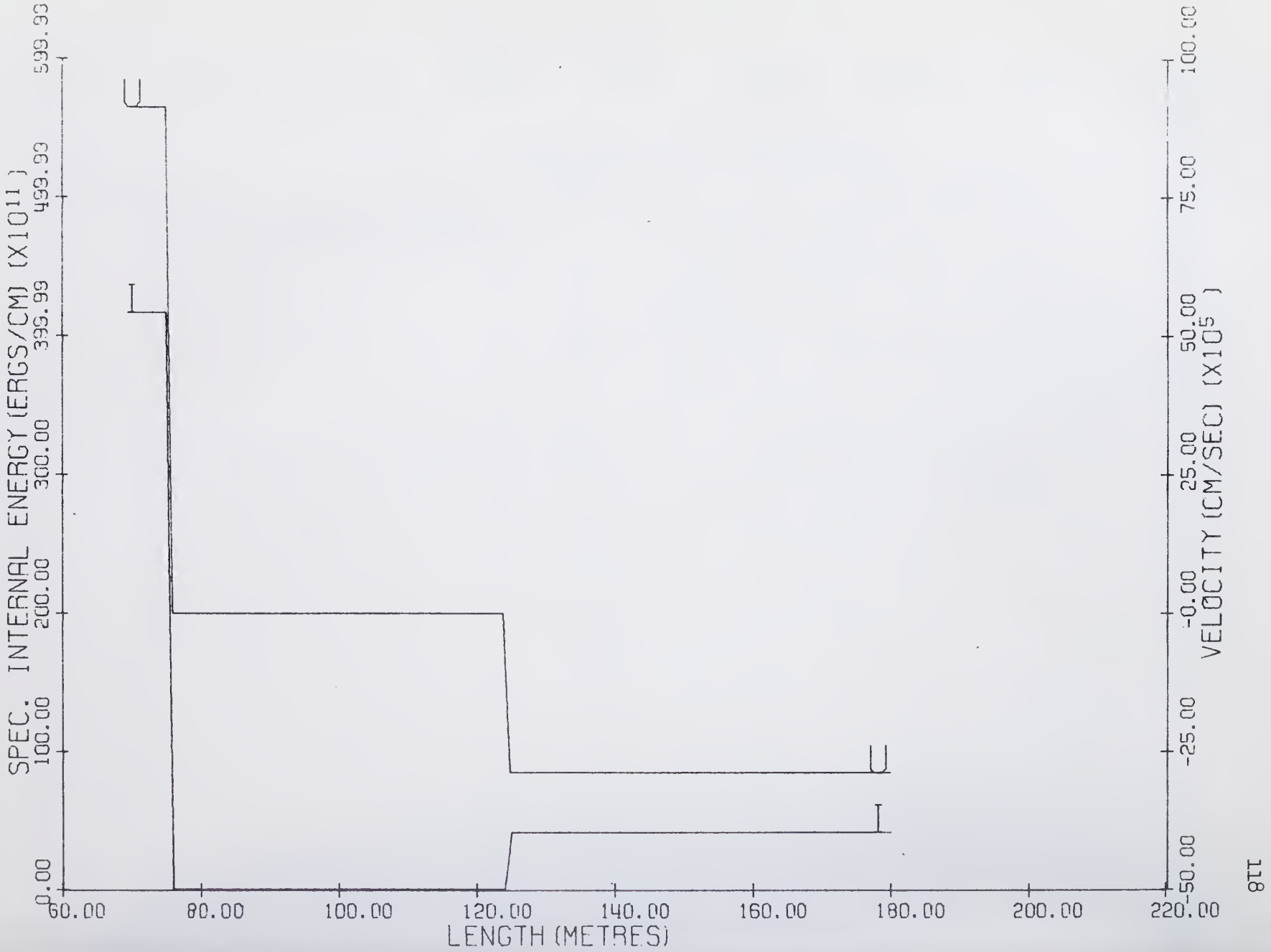

Figure 74. 6A Exact, Time = 0. Sec.

Figure 75. 6A Exact, Time = 7. X 10^{-4} Sec.

Figure 76. 6A Exact, Time = 7. X 10^{-4} Sec.

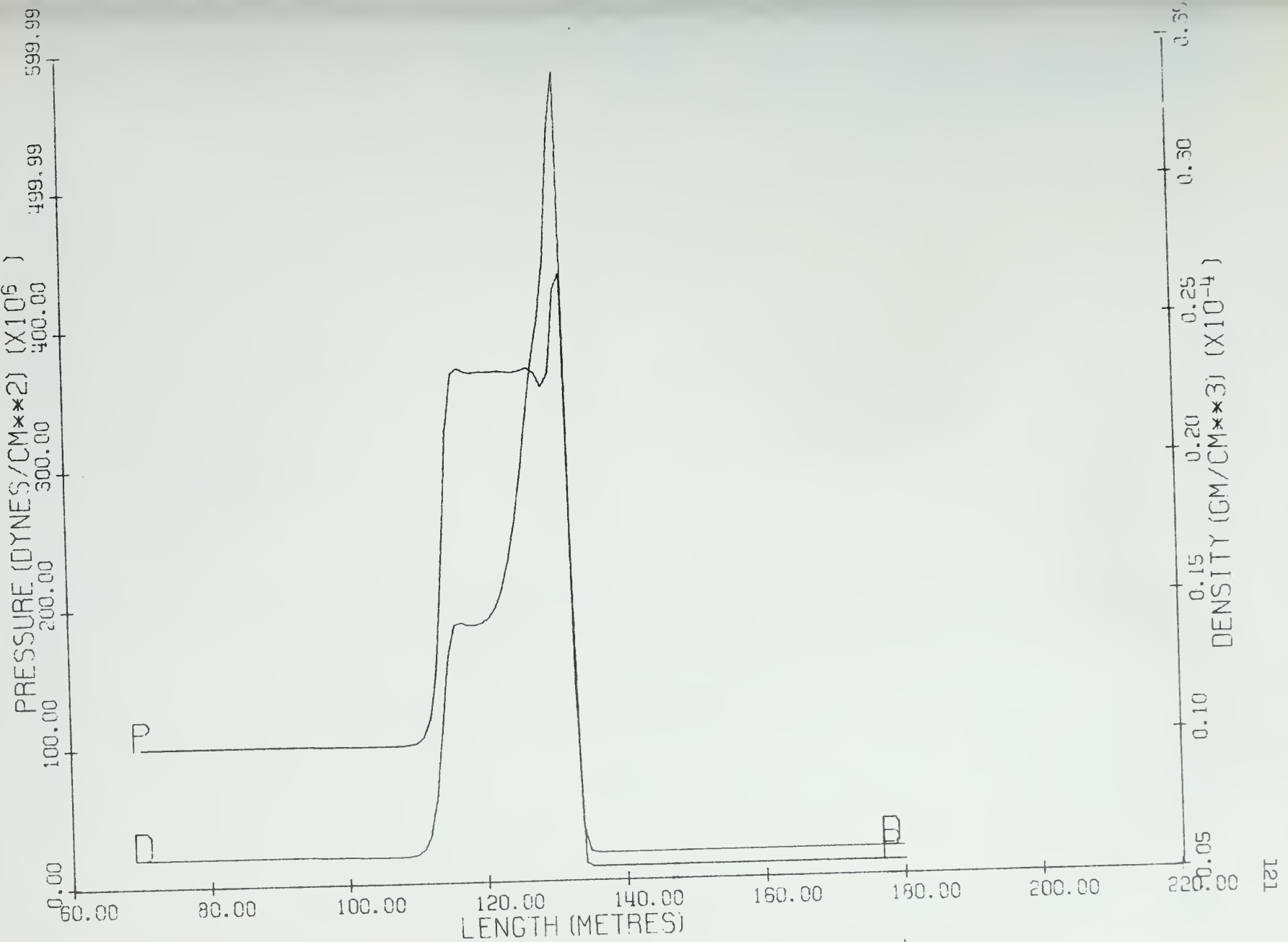

Figure 77. 6A Continuous Rezone, Time = 7. X 10^{-4} Sec.

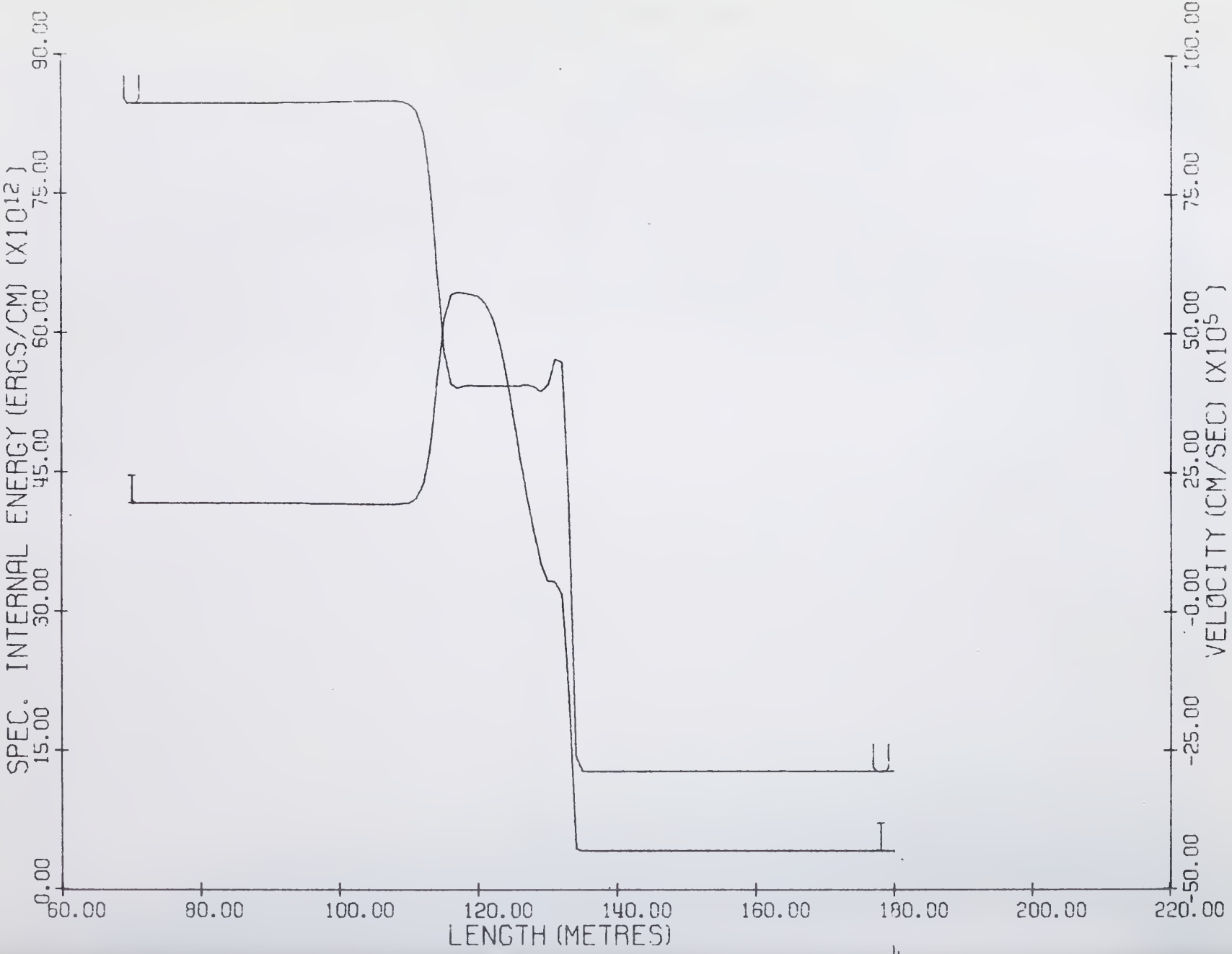

Figure 78. 6A Continuous Rezone, Time = 7. X 10^{-4} Sec.

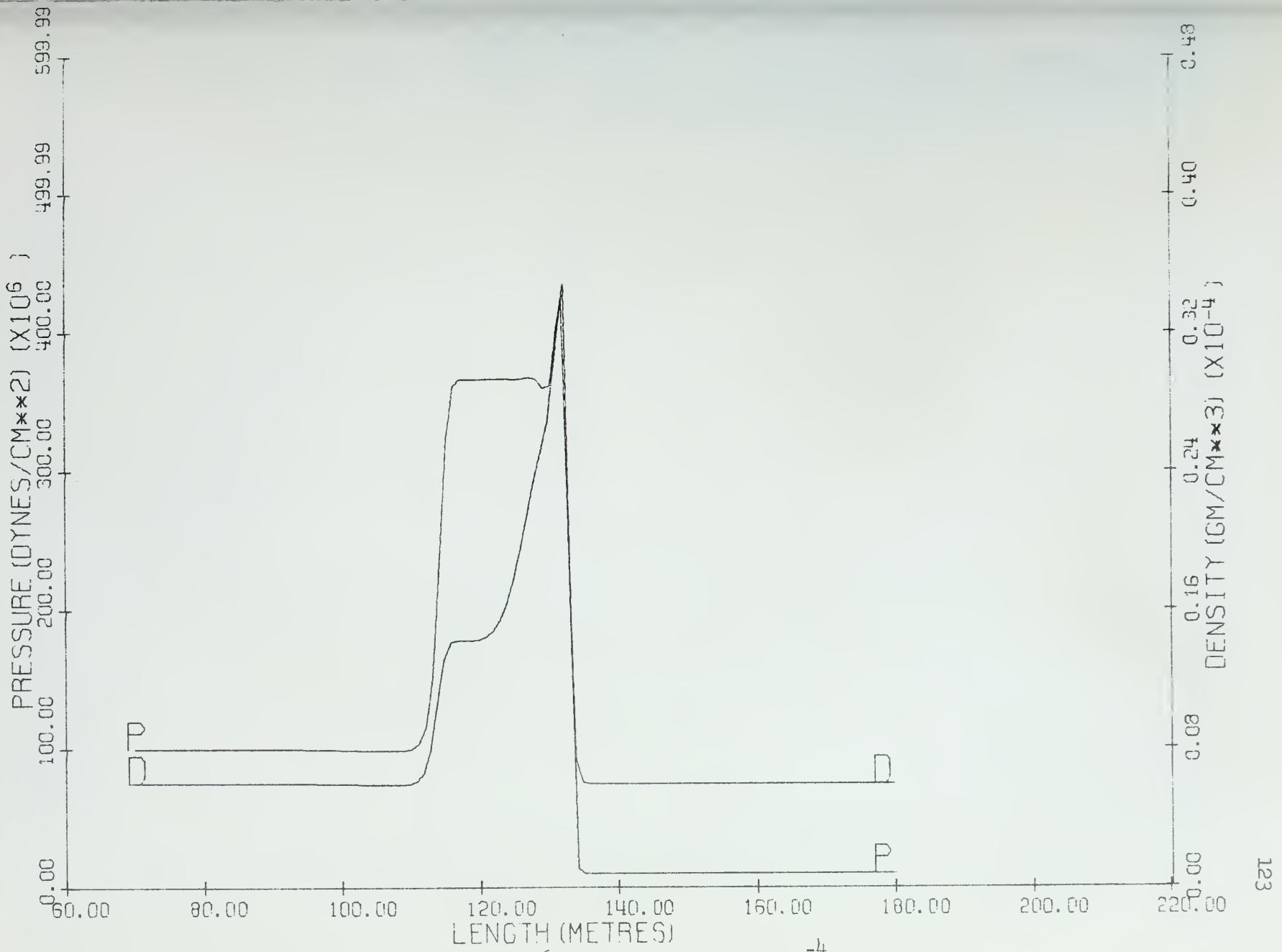

Figure 79. 6A OIL, Time = 7. X 10^{-4} Sec.

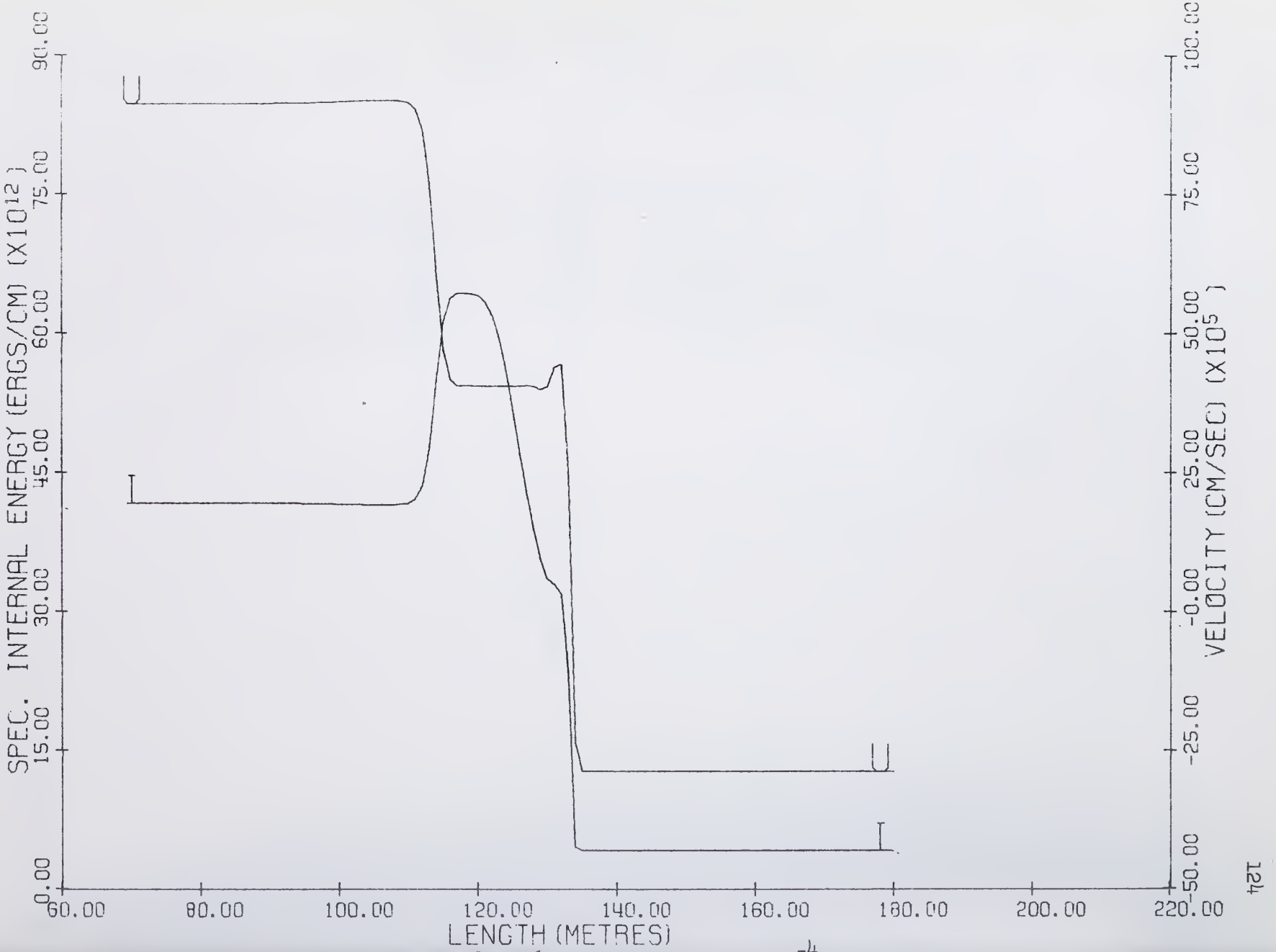

Figure 80. 6A OIL, Time = 7. X 10^{-4} Sec.

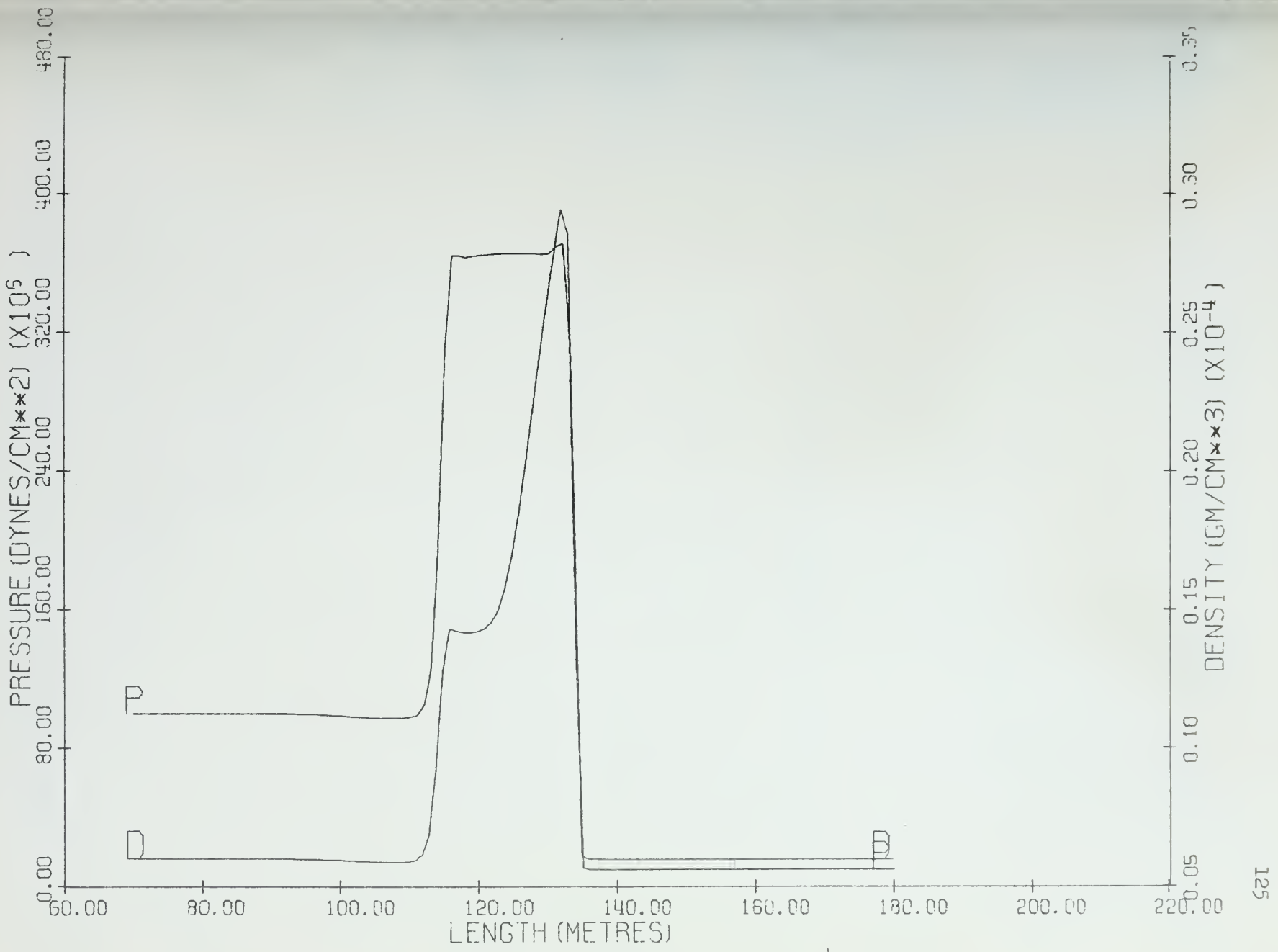

Figure 81. 6A Donor, Time = 7. X 10^{-4} Sec.

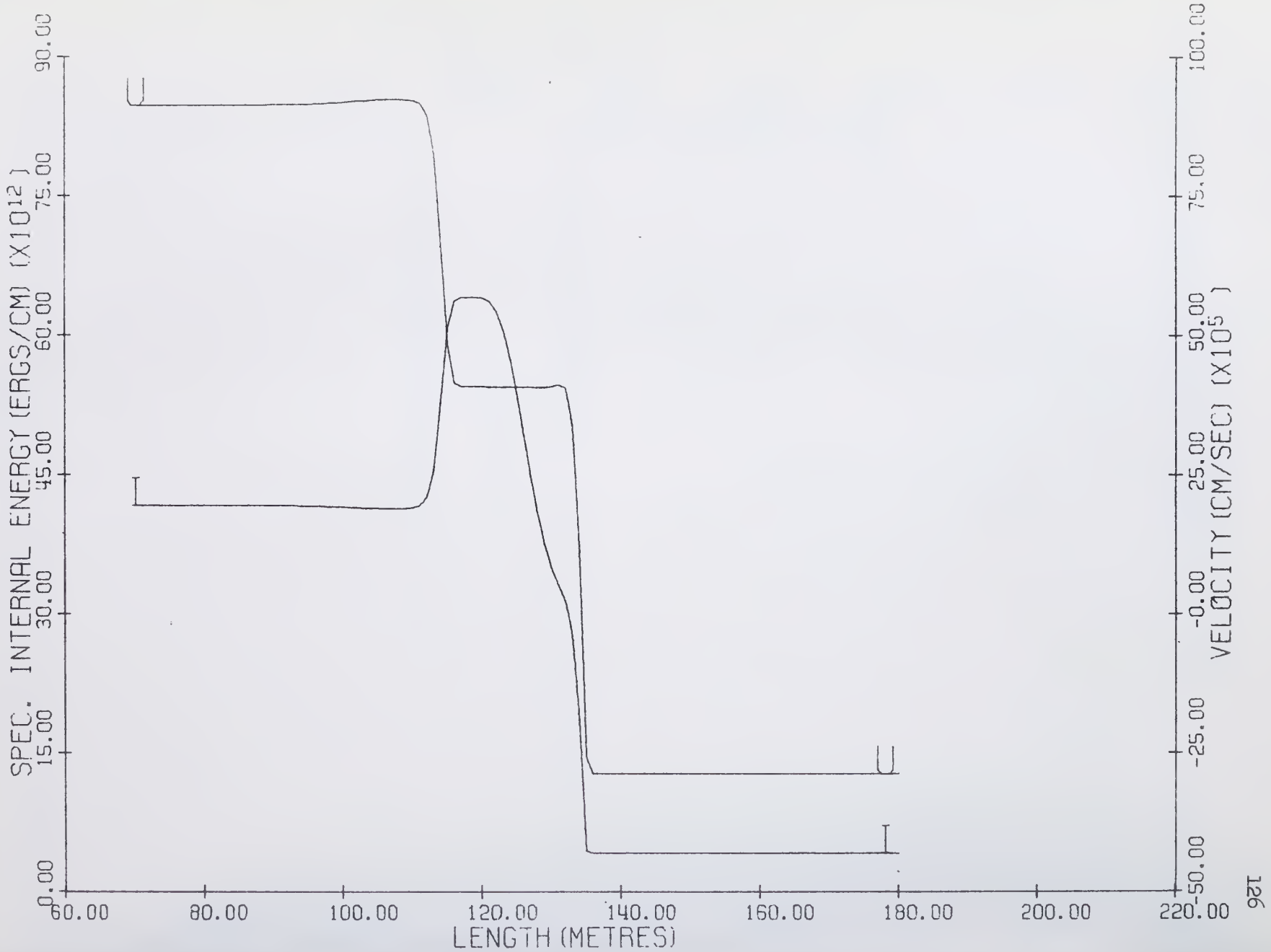

Figure 82. 6A Donor, Time = 7. X 10^{-4} Sec.

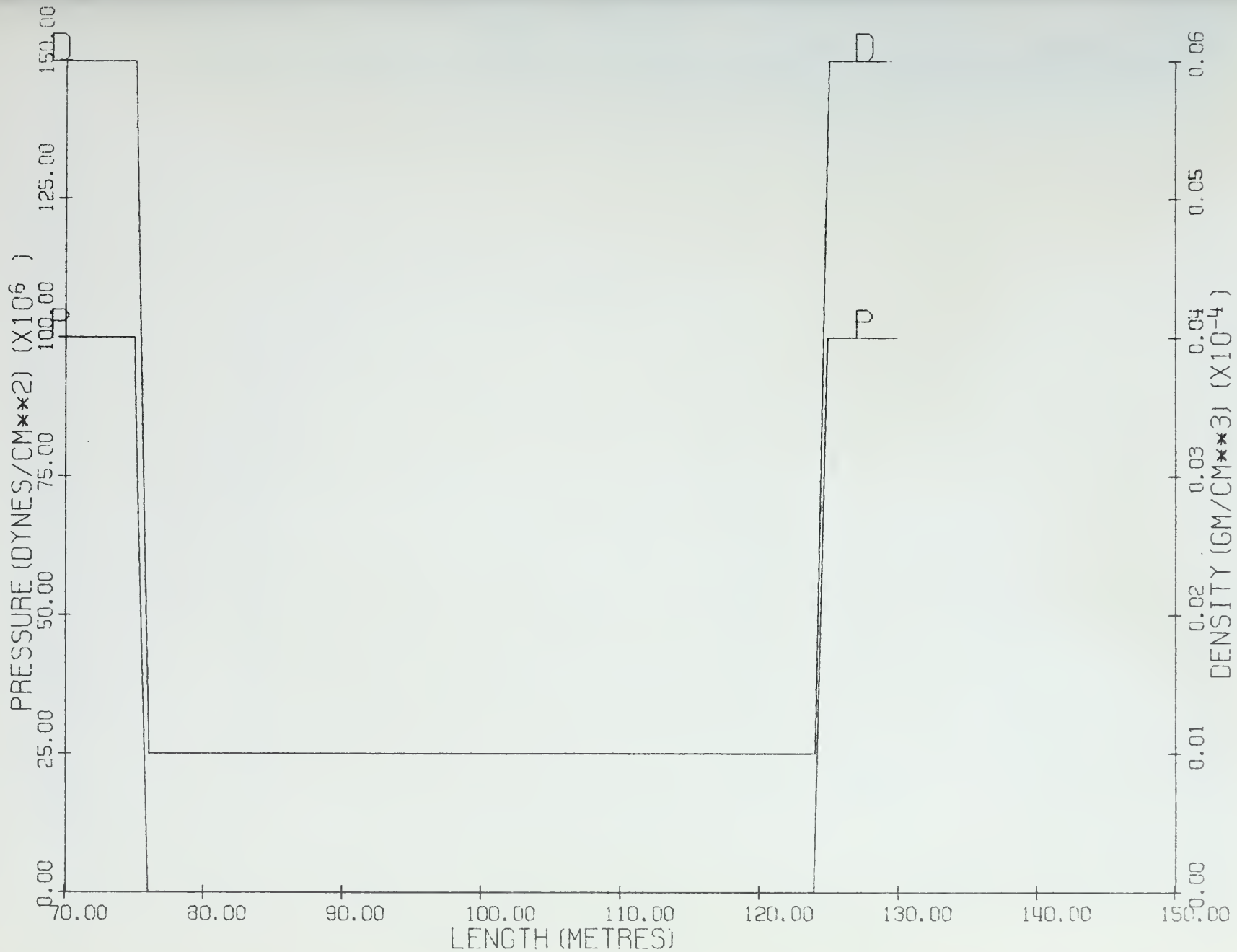

Figure 83. 6B Exact, Time = 0. Sec.

Figure 84. 6B Exact, Time = 0. Sec.

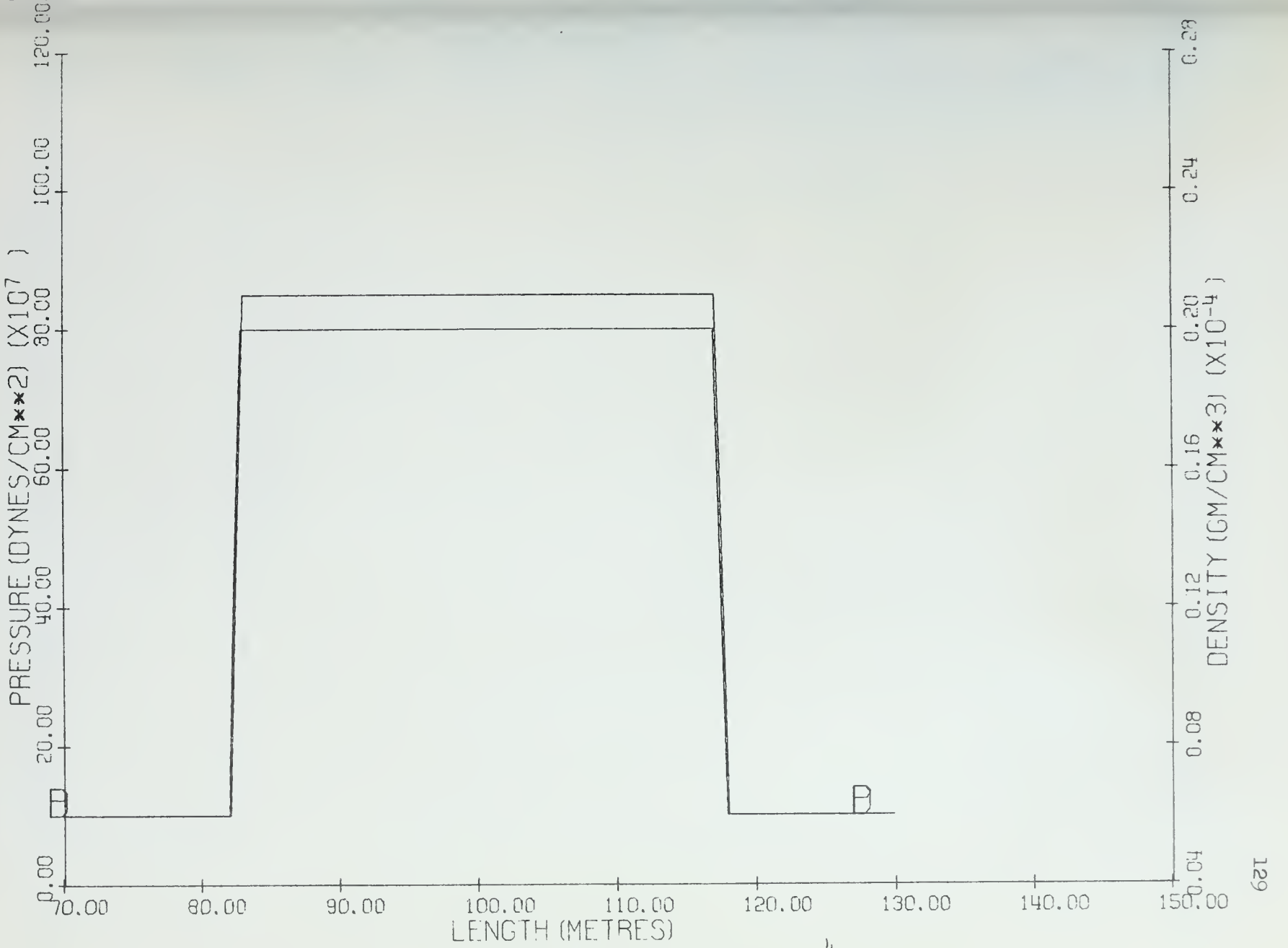

Figure 85. 6B Exact, Time = 7. X 10^{-4} Sec.

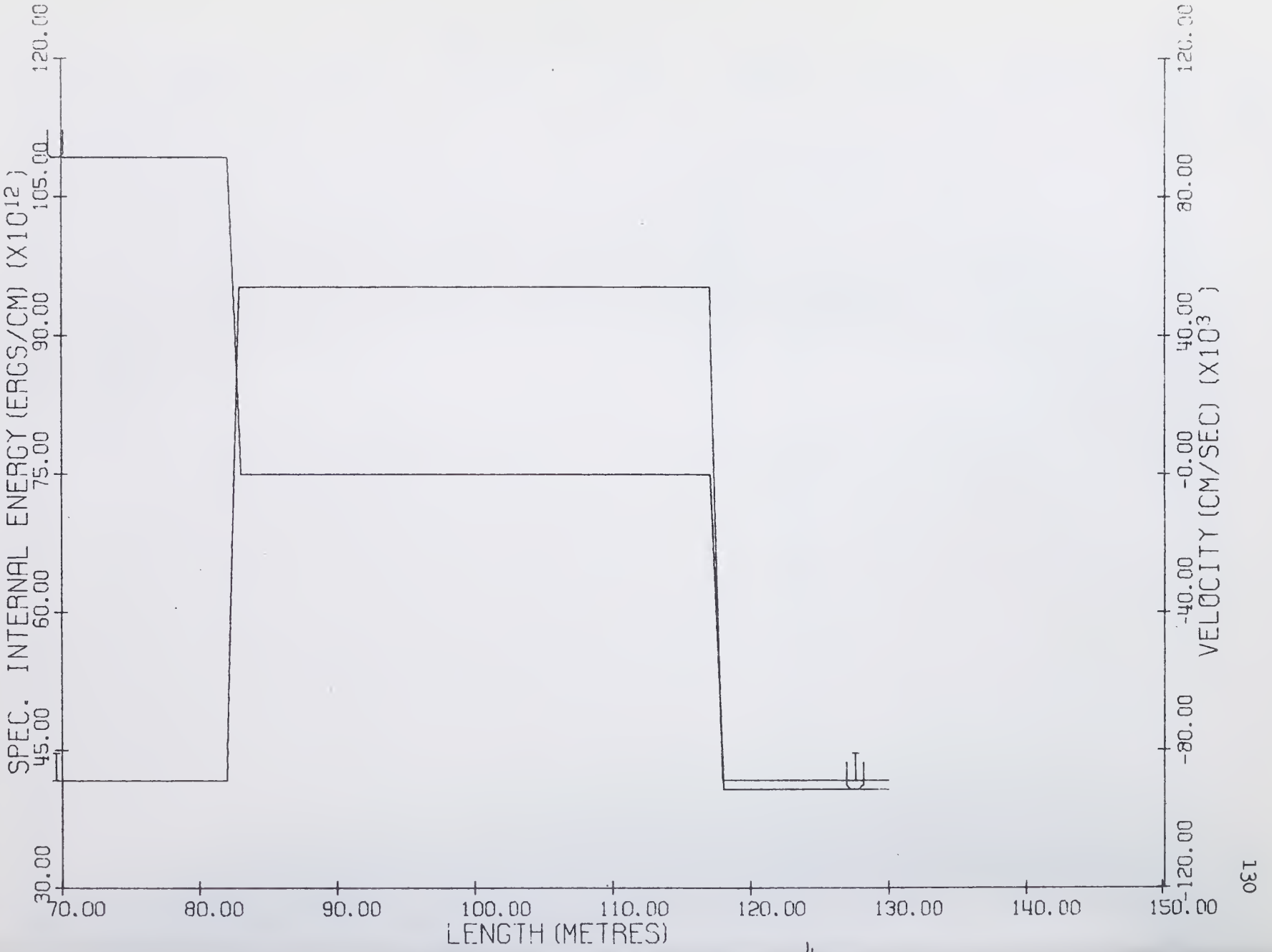

Figure 86. 6B Exact, Time = 7. X 10^{-4} Sec.

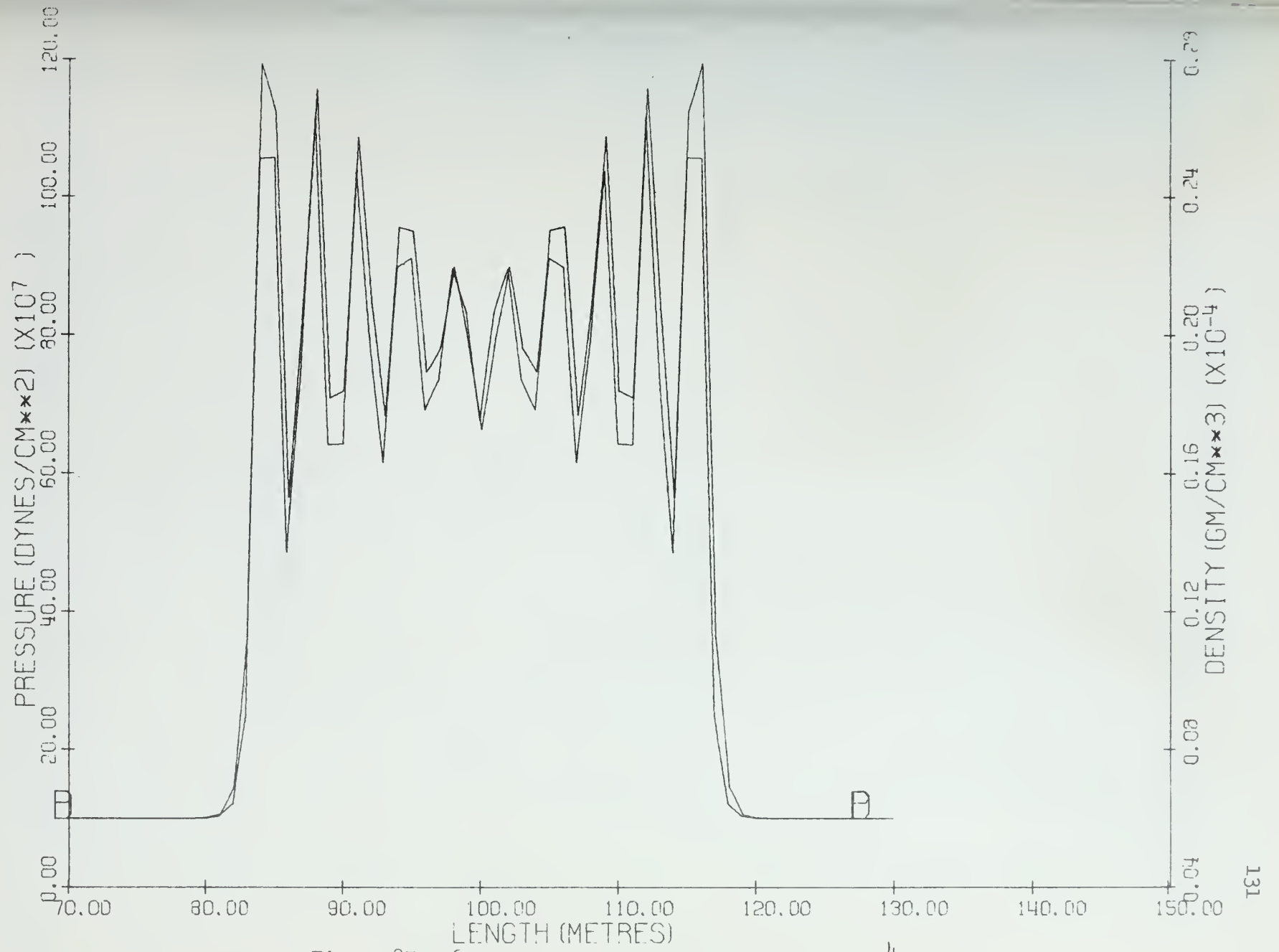

Figure 87. 6B Continuous Rezone, Time = 7. X 10^{-4} Sec.

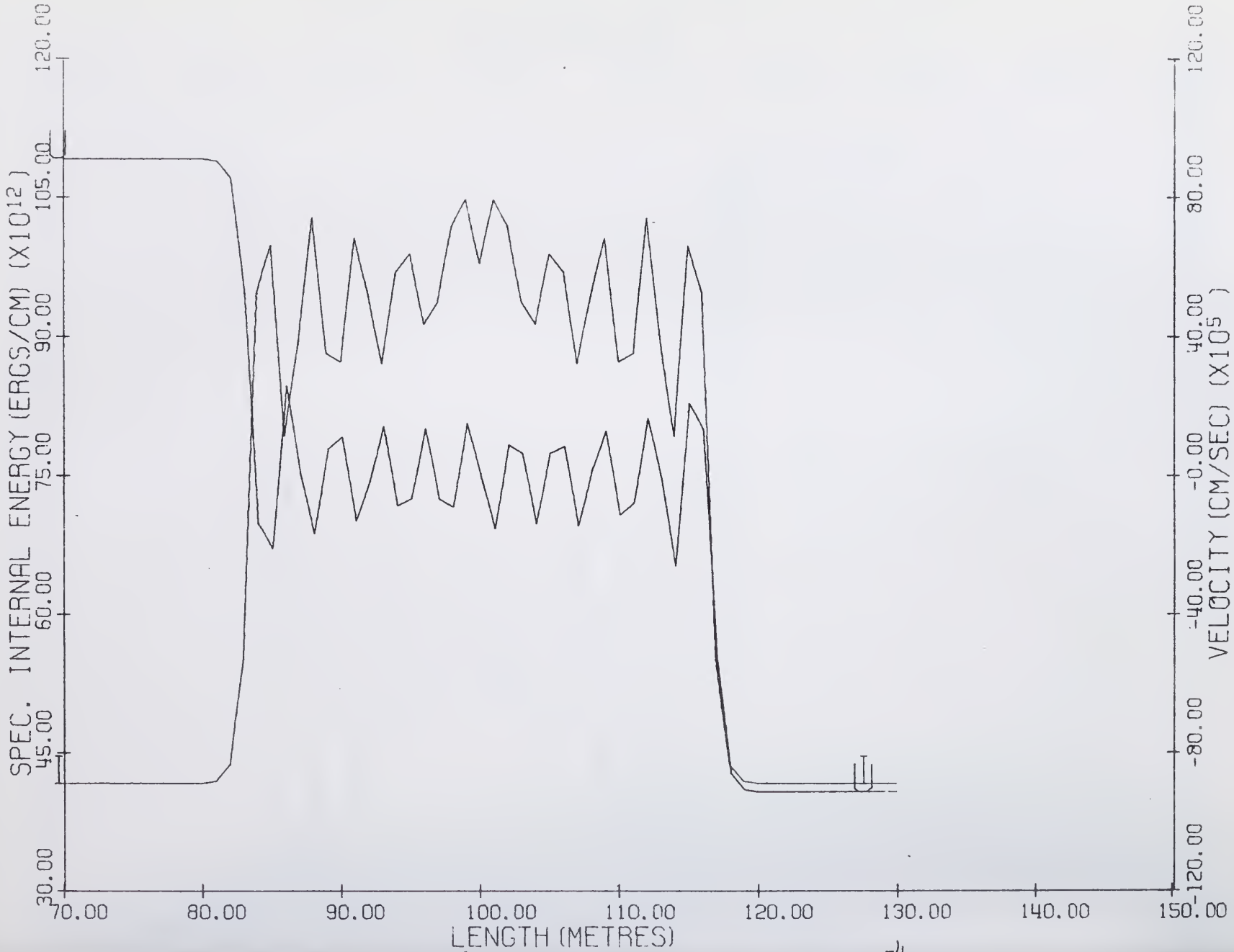

Figure 88. 6B Continuous Rezone, Time = 7. X 10^{-4} Sec.

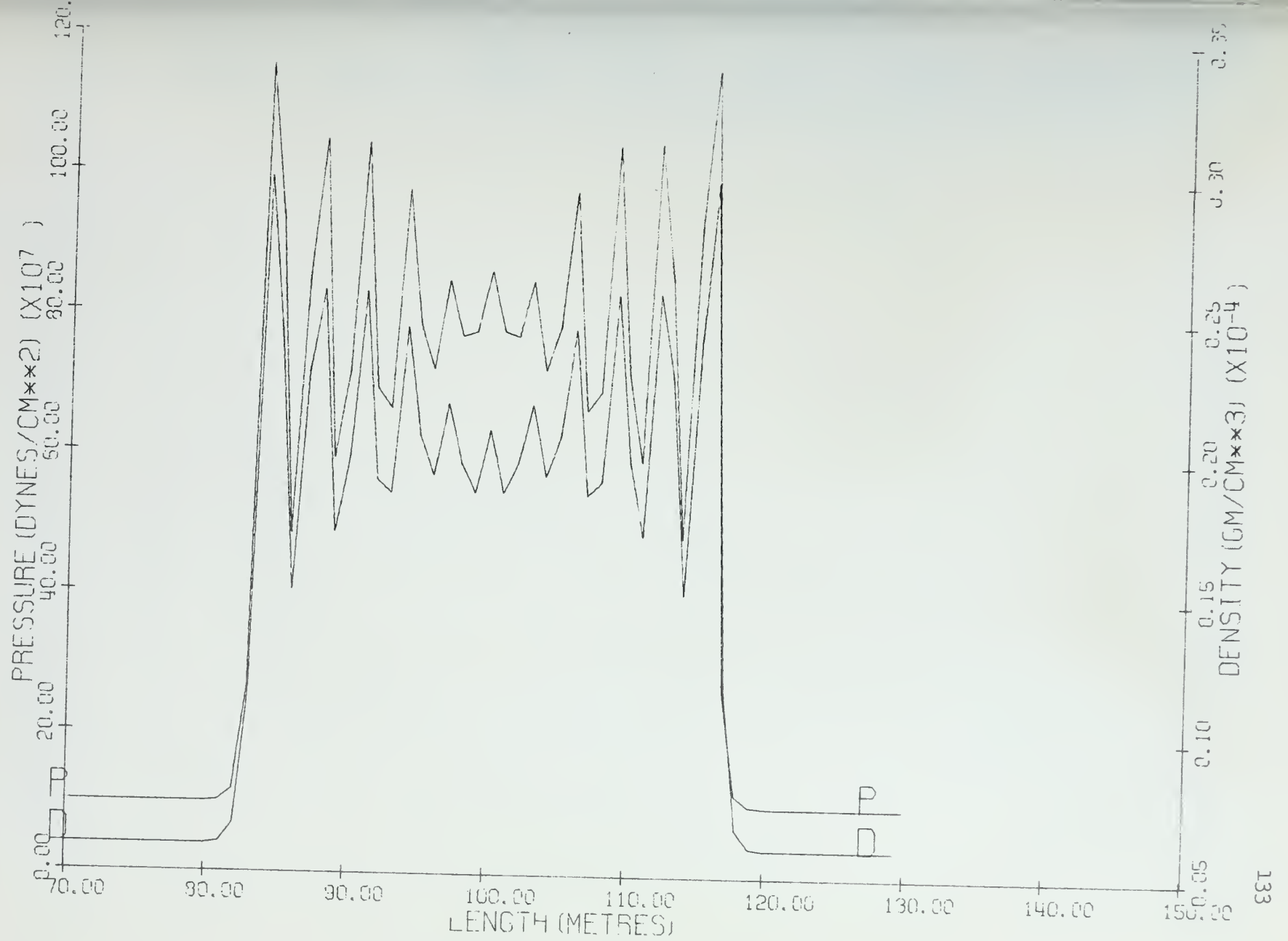

Figure 89. 6B OIL, Time = 7. X 10^{-4} Sec.

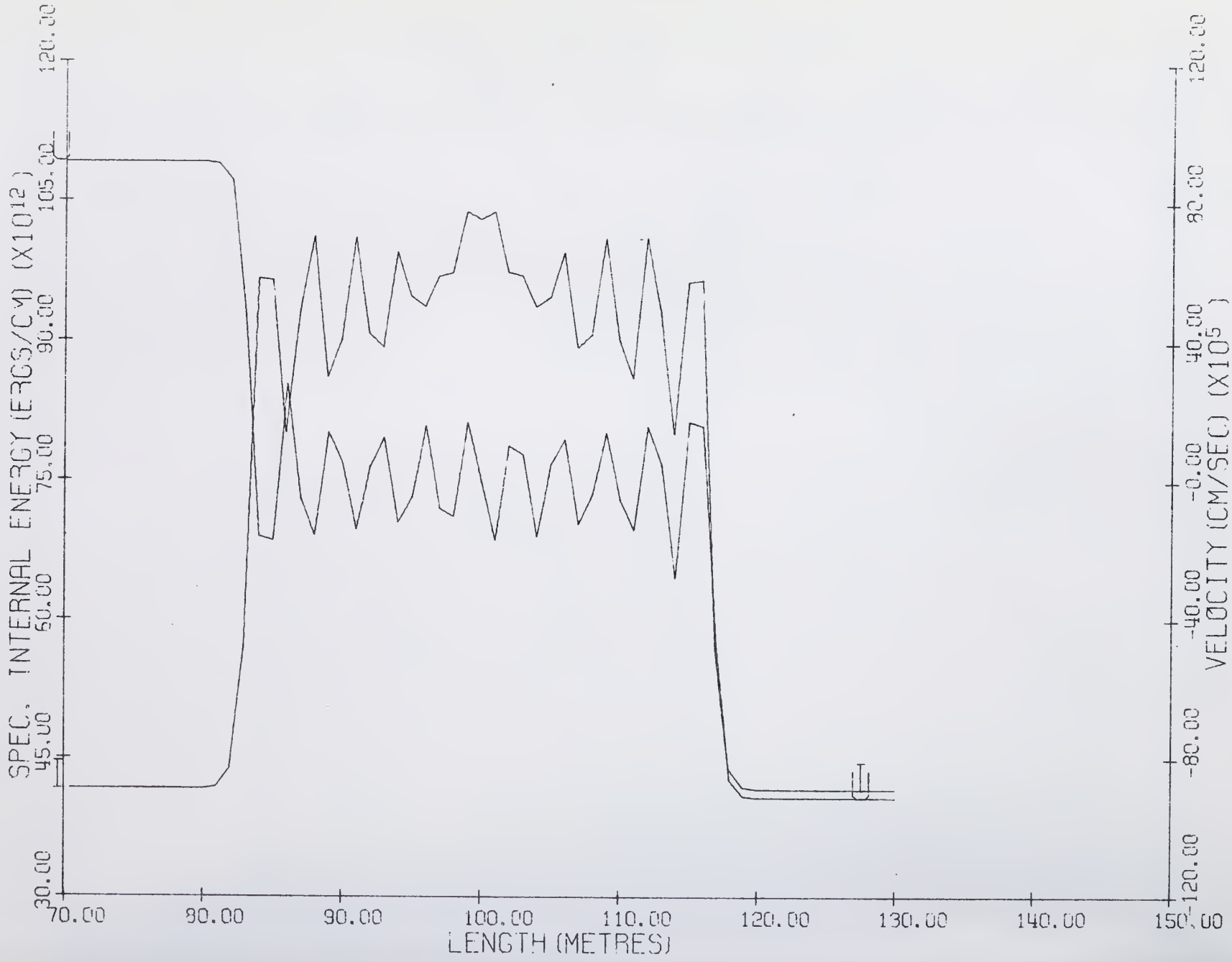

Figure 90. 6B OIL, Time = 7. X 10^{-4} Sec.

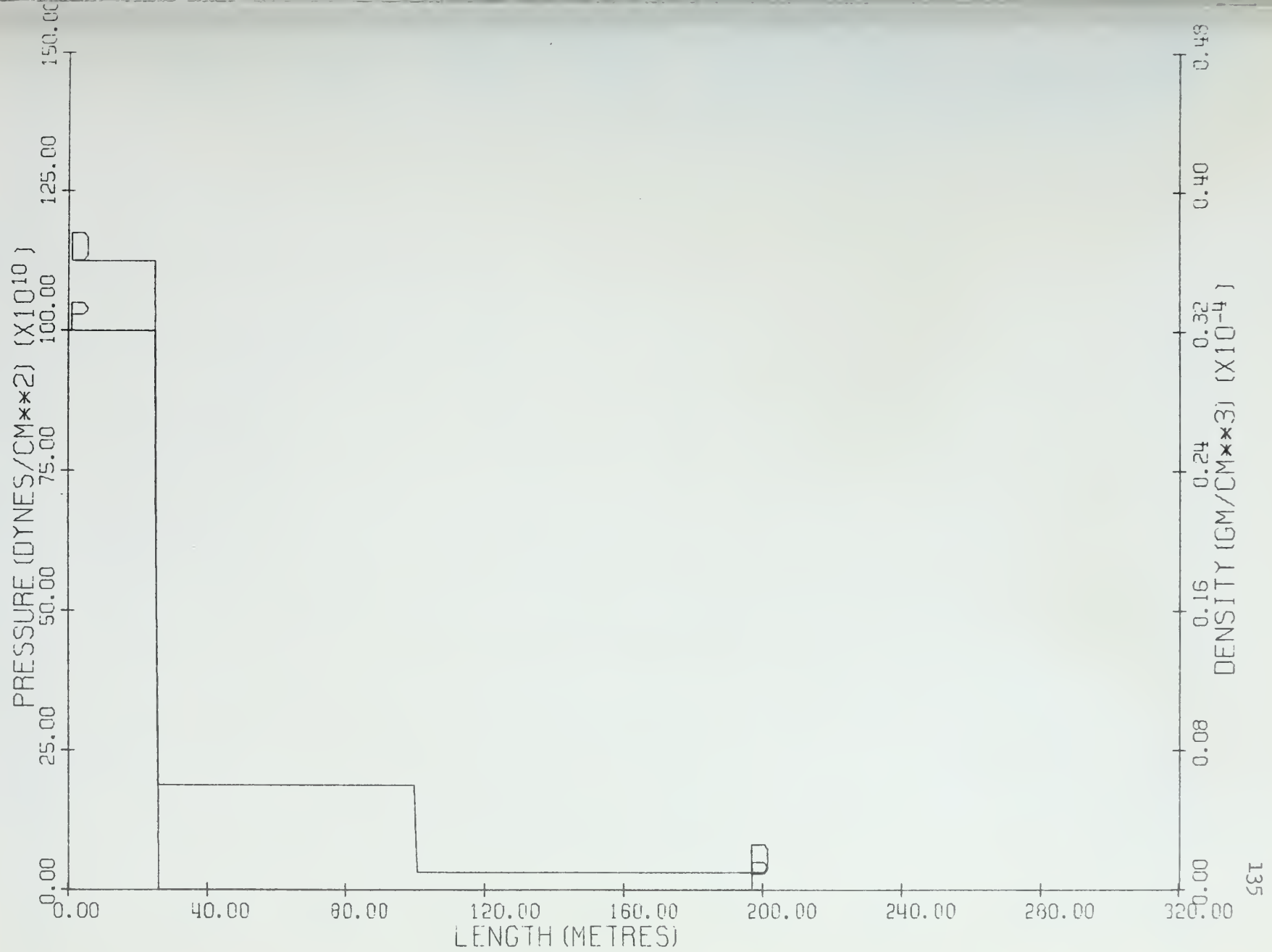

Figure 91. 7A Exact, Time = 0. Sec.

Figure 92. 7A Exact, Time = 0. Sec.

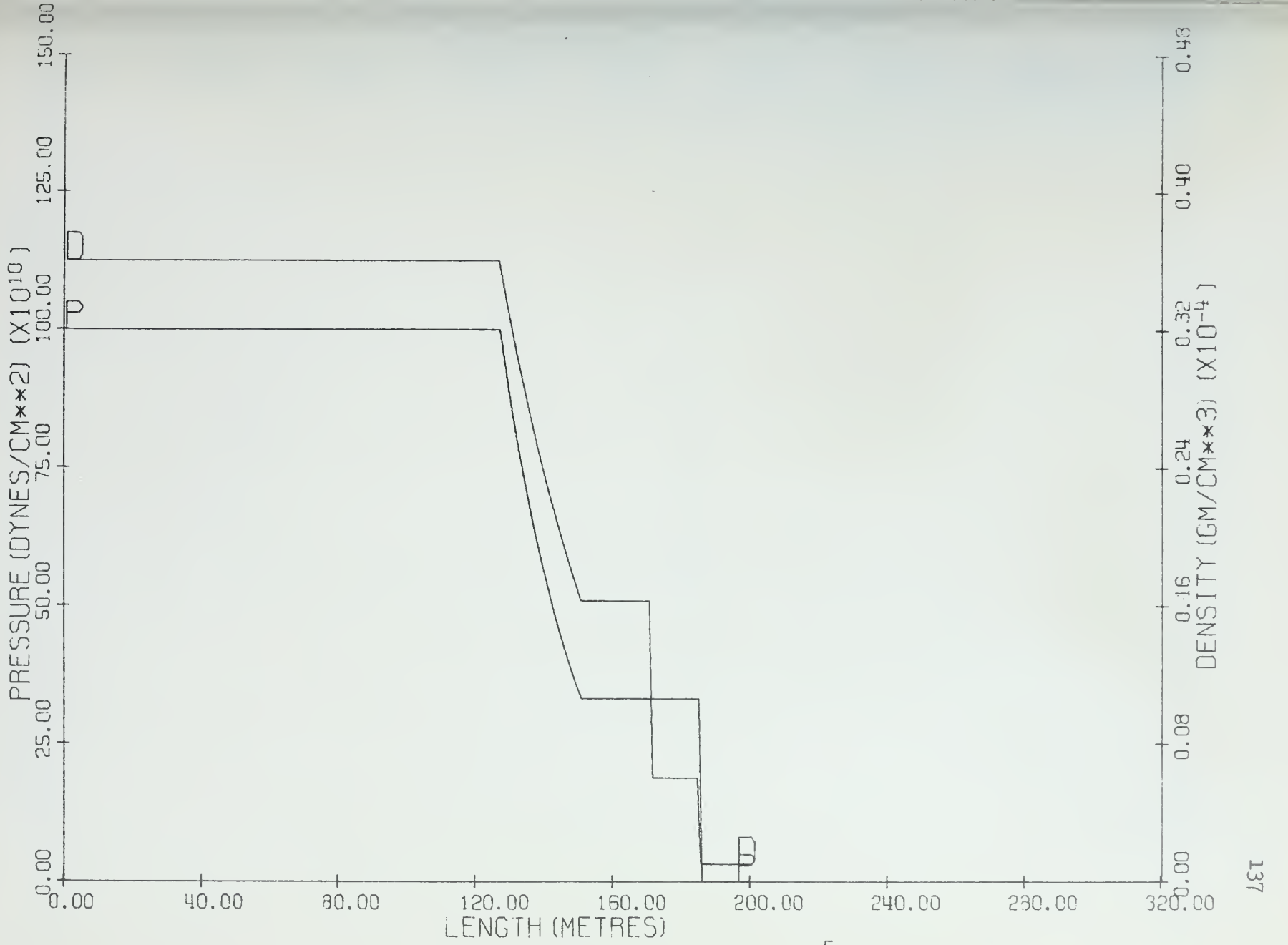

Figure 93. 7A Exact, Time = 3. X 10^{-5} Sec.

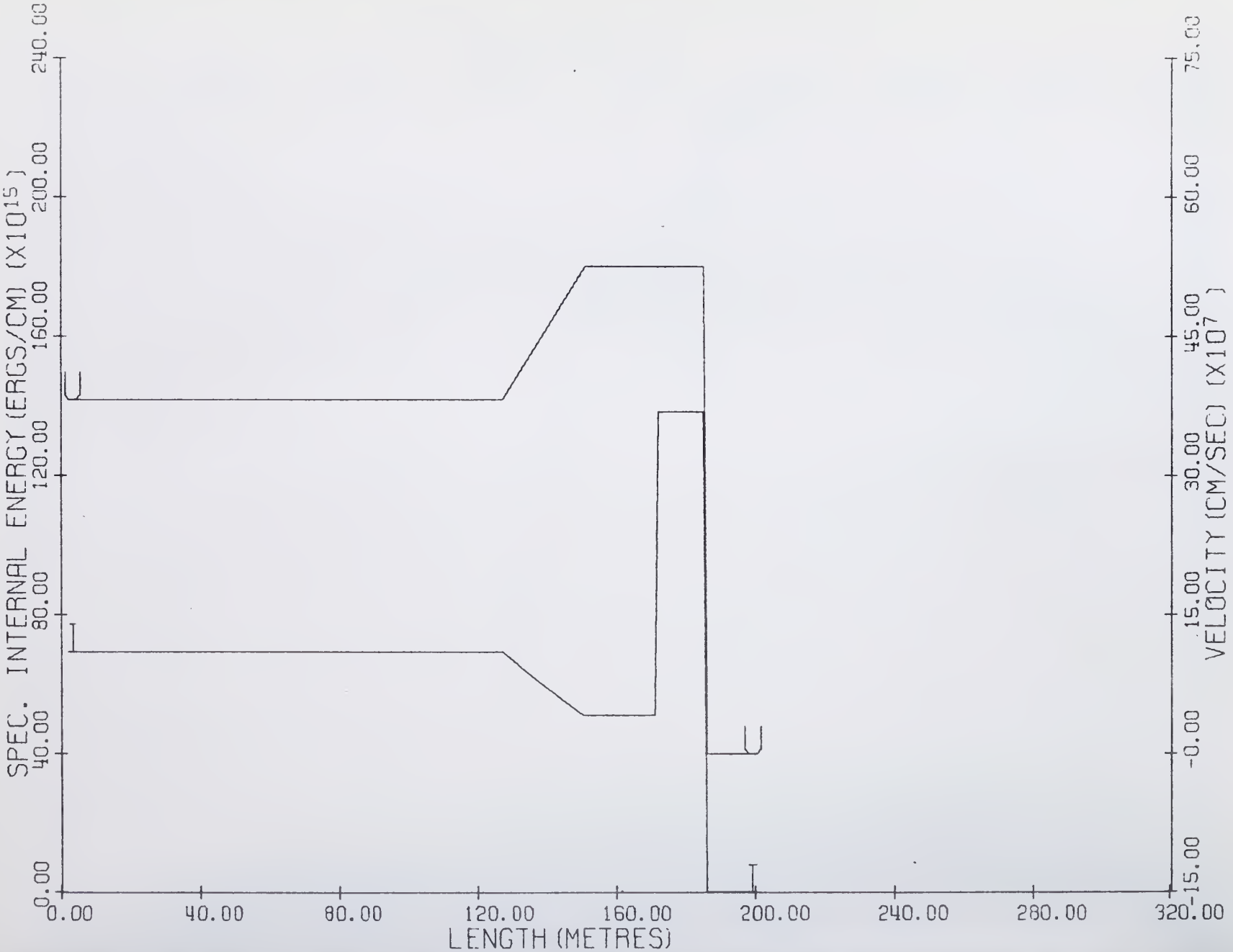

Figure 94. 7A Exact, Time = 3. X 10^{-5} Sec.

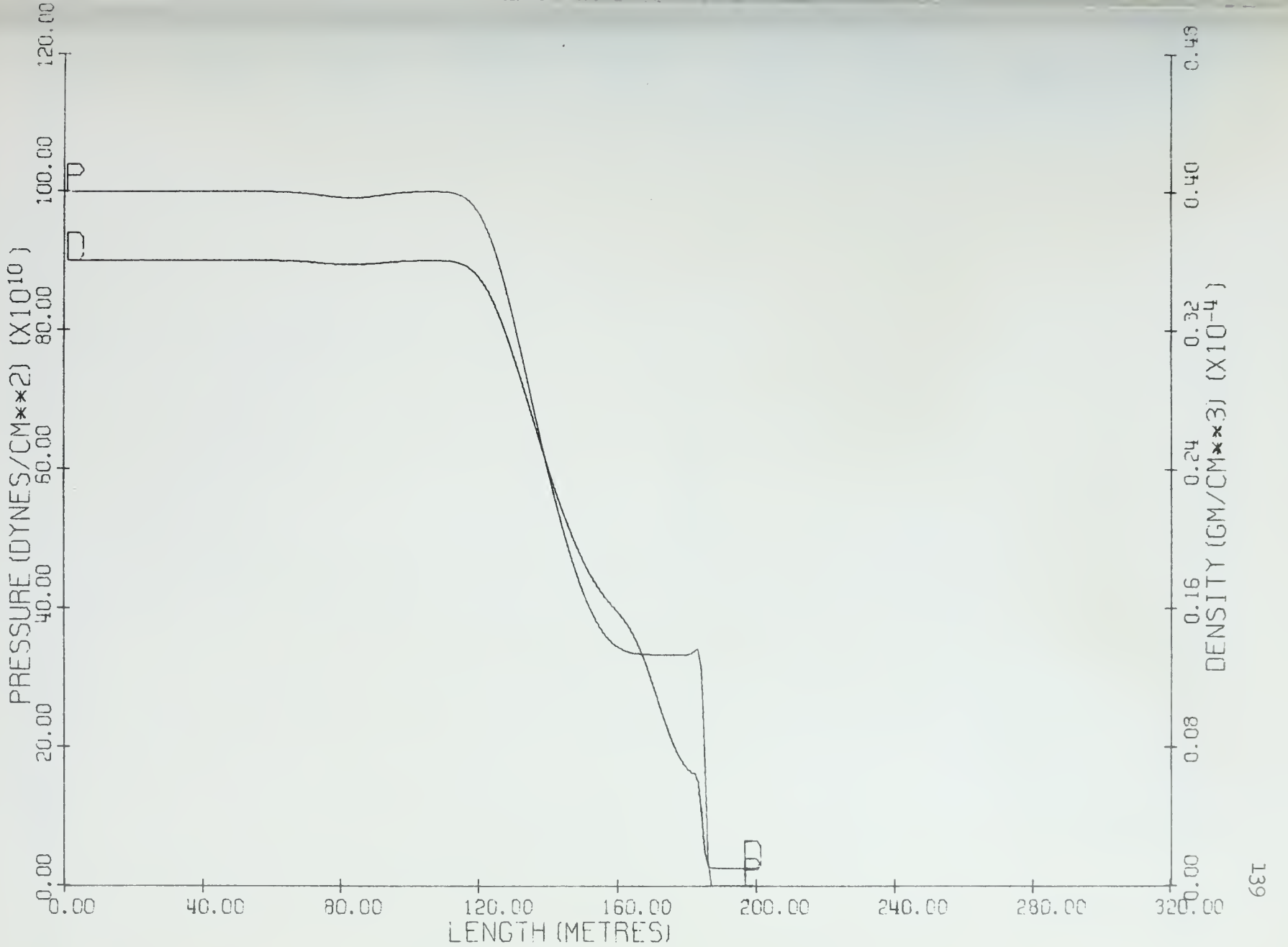

Figure 95. 7A Continuous Rezone, Time = 3. X 10^{-5} Sec.

Figure 96. 7A Continuous Rezone, Time = 3. X 10^{-5} Sec.

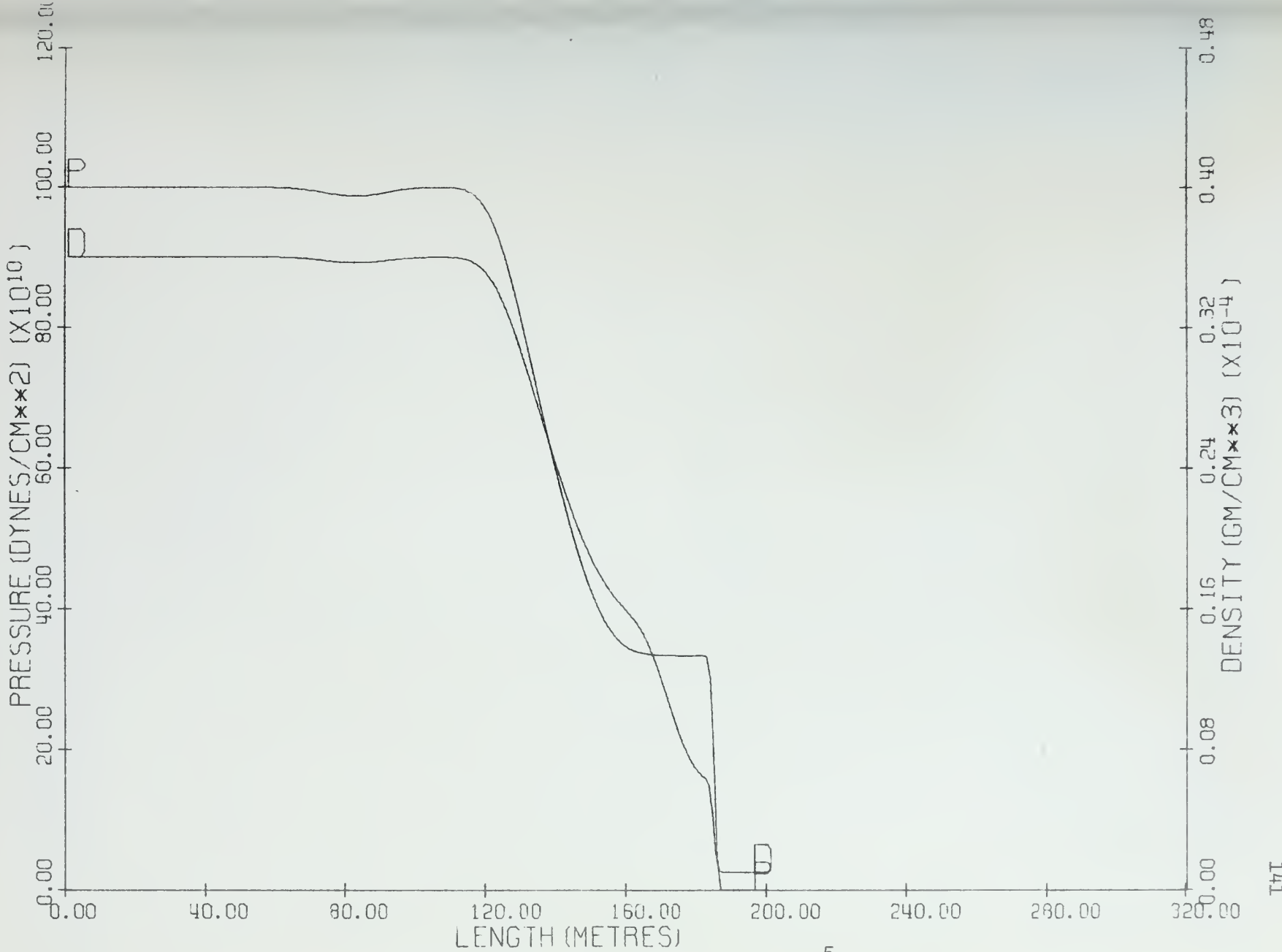

Figure 97. 7A OIL, Time = 3. X 10^{-5} Sec.

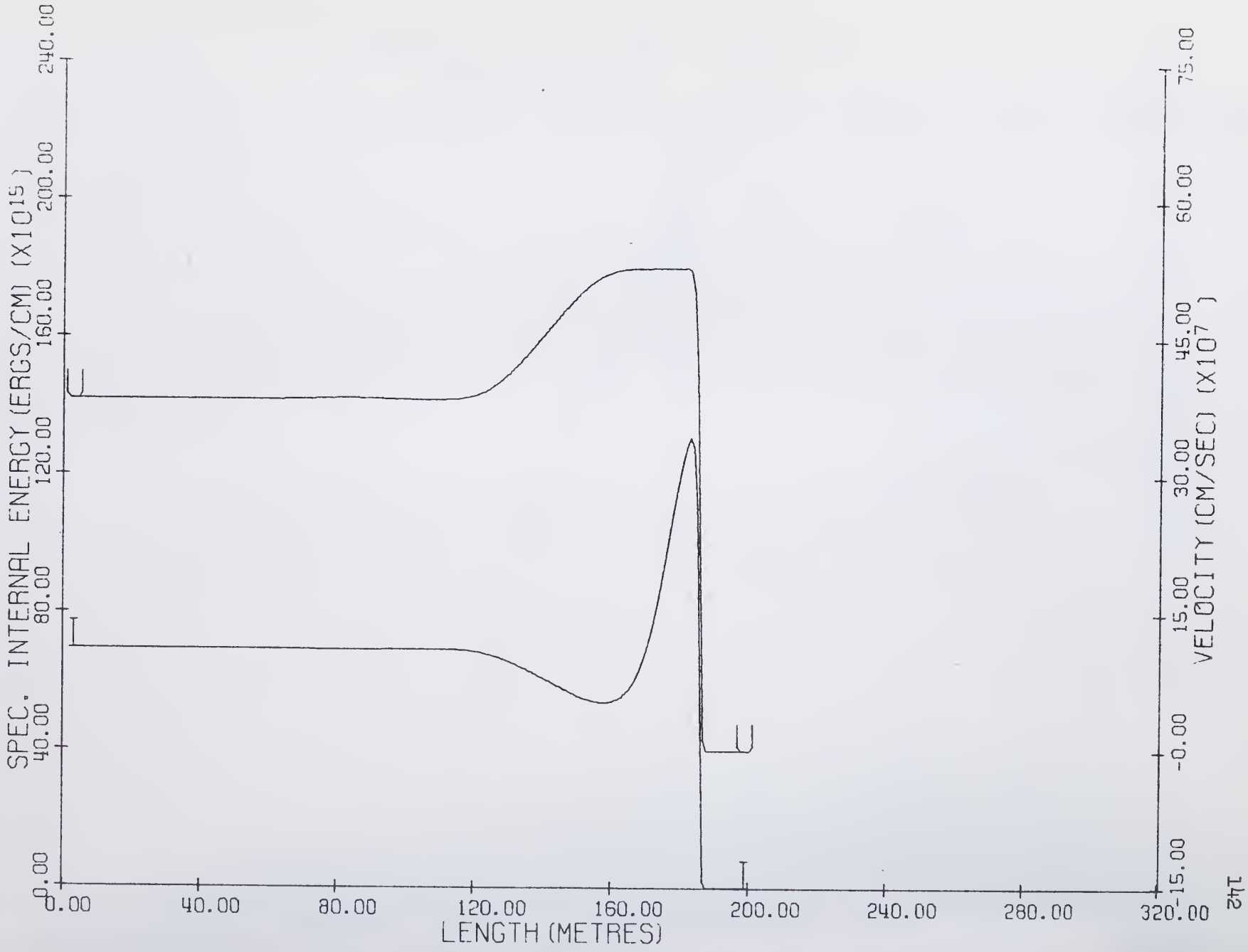

Figure 98. 7A OIL, Time = 3. X 10^{-5} Sec.

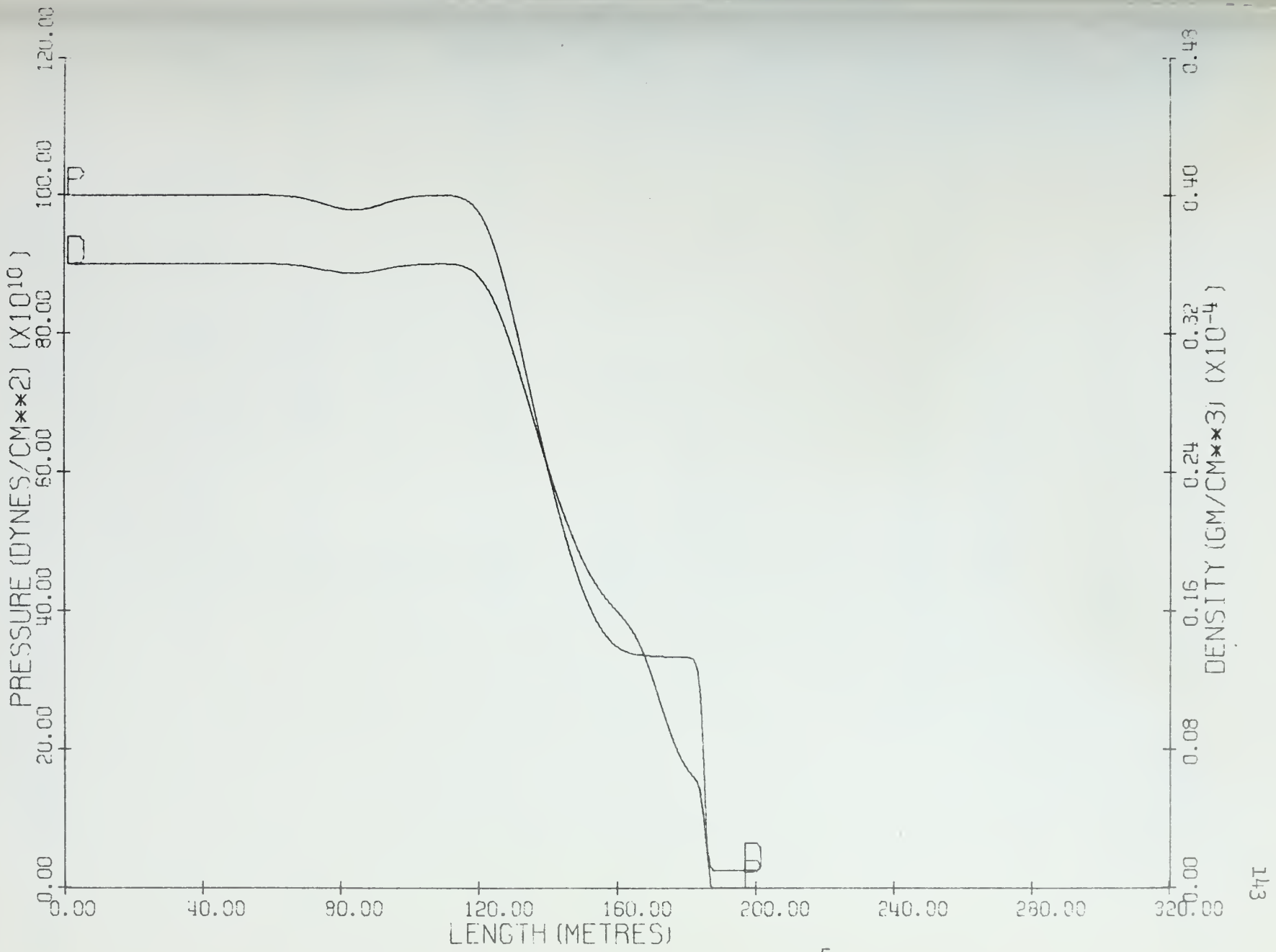

Figure 99. 7A Donor, Time = 3. X 10^{-5} Sec.

Figure 100. 7A Donor. Time = 3 x 10^{-5} Sec

APPENDIX B

DERIVATIONS OF ORDERS OF TRUNCATION ERRORS

Conservation of Mass

(a) Continuous Rezone

It is necessary to find expressions for $\tilde{U}_{i-\frac{1}{2}}^{n}$

From equation (12)

$$\tilde{U}_i^n = U_i^n - (P_{i+1}^n - P_{i-1}^n) \frac{\Delta t}{2\rho_i^n \Delta x}$$

Therefore $$\tilde{U}_i^n = U_i^n - \left[\frac{\partial P}{\partial x}\Big|_i + O(\Delta x^2)\right] \frac{\Delta t}{\rho_i^n} \qquad (17)$$

Hence $$\tilde{U}_{i-\frac{1}{2}}^{n} = U_{i-\frac{1}{2}}^{n} - \frac{\Delta t}{\rho_i^n} \frac{\partial P}{\partial x}\Big|_i + O(\Delta x \Delta t) \qquad (18)$$

noting that $\frac{1}{1-E} \simeq 1 + E$ if $E \ll 1$

Also $$\tilde{U}_{i+\frac{1}{2}}^{n} = U_{i+\frac{1}{2}}^{n} - \frac{\Delta t}{\rho_i^n} \frac{\partial P}{\partial x}\Big|_i + O(\Delta x \Delta t) \qquad (19)$$

Therefore

$$\tilde{U}_{i+\frac{1}{2}}^{n} - \tilde{U}_{i-\frac{1}{2}}^{n} = \frac{\partial U}{\partial x}\Big|_i \Delta x + O(\Delta x^3) + O(\Delta x \Delta t) \qquad (20)$$

In general $\Delta M_{i+\frac{1}{2}}^{n} = \rho_{i+\frac{1}{2}}^{n} U_{i+\frac{1}{2}}^{*n} \Delta t$

Hence $$\Delta M_{i+\frac{1}{2}}^{n+1} = \frac{\rho_i^n \tilde{U}_{i+\frac{1}{2}}^{n+1} \Delta t}{1 + (\tilde{U}_{i+\frac{1}{2}}^{n+1} - \tilde{U}_{i-\frac{1}{2}}^{n+1}) \frac{\Delta t}{\Delta x}}$$

$$= \frac{\rho_i^n \tilde{U}_{i+\frac{1}{2}}^{n+1} \Delta t}{1 + \frac{\partial U}{\partial x}\Big|_i \Delta t + O(\Delta t^2) + O(\Delta x^2 \Delta t)}$$

from equation (20)

Therefore

$$\Delta M_{i+\frac{1}{2}}^{n+1} = \rho_i^n \Delta t \left[U_{i+\frac{1}{2}}^{n+1} - \Delta t \left[\frac{1}{\rho_i^n} \frac{\partial P}{\partial x}\Big|_i + U_i^n \frac{\partial U}{\partial x}\Big|_i \right] + O(\Delta x \Delta t) + O(\Delta t^2) \right] \quad (21)$$

from equation (19)

Also $$\Delta M_{i-\frac{1}{2}}^{n+1} = \rho_{i-1}^n \Delta t \left[U_{i-\frac{1}{2}}^{n+1} - \Delta t \left[\frac{1}{\rho_{i-1}^n} \frac{\partial P}{\partial x}\Big|_i + U_{i-1}^n \frac{\partial U}{\partial x}\Big|_{i-1} \right] + O(\Delta x \Delta t) + O(\Delta t^2) \right]$$

The equation of continuity is

$$M_i^{n+1} - M_i^n = \Delta M_{i-\frac{1}{2}}^{n+1} - \Delta M_{i+\frac{1}{2}}^{n+1}$$

Therefore

$$\frac{M_i^{n+1} - M_i^n}{\Delta t} = \rho_{i-1}^n U_{i-\frac{1}{2}}^{n+1} - \rho_i^n U_{i+\frac{1}{2}}^{n+1} + O(\Delta t^2) + O(\Delta x \Delta t)$$

$$= \rho_{i-1}^{n} U_{i-1}^{n} - \rho_i^n U_i^n + O(\Delta x^2) + O(\Delta t^2) + O(\Delta x \Delta t)$$

Therefore

$$\frac{\rho_i^{n+1} - \rho_i^n}{\Delta t} + \frac{(\rho U)_i^n - (\rho U)_{i-1}^n}{\Delta x}$$

$$= \frac{\partial \rho}{\partial t} + \frac{\partial \rho U}{\partial x} + O(\Delta x) + O(\Delta t) + O\left(\frac{\Delta t^2}{\Delta x}\right)$$

(b) OIL

$$\Delta M_{i+\frac{1}{2}}^{n_1} = \frac{\rho_i^n \Delta t \ \tilde{U}_{i+\frac{1}{2}}^{n_1}}{1 + (\tilde{U}_{i+1}^{n} - \tilde{U}_i^n) \frac{\Delta t}{\Delta x}} \tag{22}$$

$$= \frac{\rho_i^n \Delta t \ \tilde{U}_{i+\frac{1}{2}}^{n_1}}{1 + \frac{\partial U}{\partial x} \Big|_{i+\frac{1}{2}}^{n_1} \Delta t + O(\Delta x^2 \Delta t) + O(\Delta t^2)}$$

Therefore

$$\Delta M_{i+\frac{1}{2}}^{n_1} = \rho_i^n \Delta t \left[U_{i+\frac{1}{2}}^{n_1} - \Delta t \left[\frac{1}{\rho_i^n} \frac{\partial P}{\partial x} \Big|_i + U_i^n \frac{\partial U}{\partial x} \Big|_i \right] + O(\Delta x \Delta t) + O(\Delta t^2) \right] \tag{23}$$

Since equation (23) is identical to equation (21), the rest of the calculation for OIL is the same as for continuous rezone.

(c) Donor $\Delta M_{i-\frac{1}{2}}^{n_1} = \rho_{i-1}^n \tilde{U}_{i-1}^n \Delta t$

Also $\rho_i^n \tilde{U}_i^n = \rho_i^n U_i^n - \left[P_{i+1}^n - P_{i-1}^n \right] \frac{\Delta t}{2\Delta x}$

from equation (12)

Therefore

$$\frac{\rho_i^{n+1} - \rho_i^n}{\Delta t} + \frac{\rho_i^n U_i^n - \rho_{i-1}^n U_{i-1}^n}{\Delta x} = \Delta t \left.\frac{\partial^2 \rho}{\partial x^2}\right|_{i-\frac{1}{2}}$$

Therefore

$$\frac{\rho_i^{n+1} - \rho_i^n}{\Delta t} + \frac{\rho_i^n U_i^n - \rho_{i-1}^n U_{i-1}^n}{\Delta x} = \frac{\partial \rho}{\partial t} + \frac{\partial \rho U}{\partial x} + O(\Delta t) + O(\Delta x)$$

Conservation of Momentum

(a) donor

The form of the conservation of momentum equation which will be used is

$$\frac{\partial \rho U}{\partial t} + \frac{\partial \rho U^2}{\partial x} + \frac{\partial P}{\partial x} = 0$$

The finite difference equation used is

$$M_i^{n+1} U_i^{n+1} = M_i^n \tilde{U}_i^n + \Delta M_{i-\frac{1}{2}}^n \tilde{U}_{i-1} - \Delta M_{i+\frac{1}{2}}^n \tilde{U}_i \qquad (24)$$

Therefore

$$\frac{M_i^{n+1} U_i^{n+1} - M_i^n U_i^n}{\Delta t} = \rho_{i-1}^n \tilde{U}_{i-1}^2 - \rho_i^n \tilde{U}_i^2 - \frac{(P_{i+1}^n - P_{i-1}^n)}{2}$$

Therefore

$$\frac{\rho_i^{n+1} U_i^{n+1} - \rho_i^n U_i^n}{\Delta t} + \frac{P_{i+1}^n - P_{i-1}^n}{2\,\Delta x} = \frac{\rho_{i-1} \tilde{U}_{i-1}^2 - \rho_i \tilde{U}_i^2}{\Delta x} \qquad (25)$$

The right hand side equals

$$\frac{\rho_{i-1}^{n}\left[U_{i-1}^{n}-\left\{\frac{\partial P}{\partial x}\Big|_{i-1}+O(\Delta x^2)\right\}\frac{\Delta t}{\rho_{i-1}^{n}}\right]^2-\rho_i^n\left[U_i^n-\left\{\frac{\partial P}{\partial x}\Big|_{i}+O(\Delta x^2)\right\}\frac{\Delta t}{\rho_i^n}\right]^2}{\Delta x}$$

from equation (17)

$$=\frac{\rho_{i-1}^{n}\,(U_{i-1}^{n})^2-\rho_i^n\,(U_i^n)^2}{\Delta x}+O(\Delta t)$$

Therefore

$$\frac{\rho_i^{n+1}\,U_i^{n+1}-\rho_i^n\,U_i^n}{\Delta t}+\frac{\rho_i^n\,(U_i^n)^2-\rho_{i-1}^{n}\,(U_{i-1}^{n})^2}{\Delta x}+\frac{P_{i+1}^{n}-P_{i-1}^{n}}{2\Delta x}$$

$$=\frac{\partial \rho U}{\partial t}+\frac{\partial \rho U^2}{\partial x}+\frac{\partial P}{\partial x}+O(\Delta x)+O(\Delta t)$$

(b) continuous rezone

$$\tilde{U}_i^n\,\Delta M_{i+\frac{1}{2}}=\rho_i^n\,\Delta t\left[U_{i+\frac{1}{2}}^{n}-\Delta t\left\{\frac{1}{\rho_i^n}\frac{\partial P}{\partial x}\Big|_i+U_i^n\frac{\partial U}{\partial x}\Big|_i\right\}+O(\Delta x\Delta t)+O(\Delta t^2)\right]\left[-\left\{\frac{\partial P}{\partial x}\Big|_i+O(\Delta x^2)\right\}\frac{\Delta t}{\rho_i^n}+U_i^n\right]$$

from equations (17) and (21)

$$\frac{\rho_i^{n+1} U_i^{n+1} - \rho_i^n U_i^n}{\Delta t} + \frac{P_{i+1}^n - P_{i-1}^n}{2\Delta x} = \frac{\Delta M_{i-\frac{1}{2}}^n \tilde{U}_{i-1}^n - \Delta M_{i+\frac{1}{2}}^n \tilde{U}_i^n}{\Delta x \Delta t}$$

from equation (25)

The right hand side equals

$$\frac{\rho_{i-1}^n}{\Delta x} \left[U_{i-\frac{1}{2}}^n U_{i-1}^n - \Delta t\, U_{i-1}^n \left\{ \frac{1}{\rho_{i-1}^n} \frac{\partial P}{\partial x}\Big|_i + U_{i-1}^n \frac{\partial U}{\partial x}\Big|_{i-1} \right\} \right.$$

$$\left. - U_{i-\frac{1}{2}}^n \left\{ \frac{\partial P}{\partial x}\Big|_{i-1} + O(\Delta x^2) \right\} \frac{\Delta t}{\rho_{i-1}^n} + O(\Delta x \Delta t) + O(\Delta t^2) \right]$$

$$- \frac{\rho_i^n}{\Delta x} \left[U_{i+\frac{1}{2}}^n U_i^n - \Delta t U_i^n \left\{ \frac{1}{\rho_i^n} \frac{\partial P}{\partial x}\Big|_i + U_i^n \frac{\partial U}{\partial x}\Big|_i \right\} \right.$$

$$\left. - U_{i+\frac{1}{2}}^n \left\{ \frac{\partial P}{\partial x}\Big|_i + O(\Delta x^2) \right\} \frac{\Delta t}{\rho_i^n} + O(\Delta x \Delta t) + O(\Delta t^2) \right]$$

$$= \left[\frac{1}{\Delta x} \left\{ \rho_{i-1}^n U_{i-\frac{1}{2}}^n U_{i-1}^n - \rho_i^n U_{i+\frac{1}{2}}^n U_i^n \right\} + O(\Delta t) + O\left(\frac{\Delta t^2}{\Delta x}\right) \right.$$

$$+ \frac{\Delta t}{\Delta x} \left\{ - U_{i-1}^n \left\{ \frac{\partial P}{\partial x}\Big|_i + \rho_{i-1}^n U_{i-1}^n \frac{\partial U}{\partial x}\Big|_{i-1} \right\} \right.$$

$$+ U_i^n \left\{ \frac{\partial P}{\partial x}\Big|_i + \rho_i^n U_i^n \frac{\partial U}{\partial x}\Big|_i \right\}$$

$$\left. \left. - U_{i-\frac{1}{2}}^n \left\{ \frac{\partial P}{\partial x}\Big|_{i-1} + O(\Delta x^2) \right\} + U_{i+\frac{1}{2}}^n \left\{ \frac{\partial P}{\partial x}\Big|_i + O(\Delta x^2) \right\} \right\} \right]$$

$$= \frac{-\partial \rho U^2}{\partial x} + O(\Delta x) + O(\Delta t)$$

$$+ O\left(\frac{\Delta t^2}{\Delta x}\right)$$

Hence, equation (25) for continuous rezone becomes

$$\frac{\rho_i^{n+1} U_i^{n+1} - \rho_i^n U_i^n}{\Delta t} + \frac{\rho_i^n (U_i^n)^2 - \rho_{i-1}^n (U_{i-1}^n)^2}{\Delta x} + \frac{P_{i+1}^n - P_{i-1}^n}{2\Delta x}$$

$$= \frac{\partial \rho U}{\partial t} + \frac{\partial \rho U^2}{\partial x} + \frac{\partial P}{\partial x} + O(\Delta x) + O(\Delta t) + O\left(\frac{\Delta t^2}{\Delta x}\right)$$

(c) OIL

Since equation (23) is identical to equation (21) and the $\tilde{U}_i^n$ (i an integer) for continuous rezone and OIL are equal, the calculation for OIL is the same as for continuous rezone.

Conservation of Energy

The form of the conservation of energy equation which will be used is

$$\frac{\partial \rho E}{\partial t} + \frac{\partial \rho EU}{\partial x} + \frac{\partial PU}{\partial x} = 0$$

It can be seen that

$$\tilde{E}_i^n = E_i^n - \frac{\rho_i^n \Delta t}{\rho_i^n \Delta x\, 4}\left[U_{i+1}^n + \tilde{U}_{i+1}^n - U_{i-1}^n - \tilde{U}_{i-1}^n\right]$$

$$- \frac{U_i^n \Delta t}{2\rho_i^n \Delta x}\left(P_{i+1}^n - P_{i-1}^n\right) + \frac{\Delta t^2}{8(\rho_i^n)^2 \Delta x^2}\left(P_{i+1}^n - P_{i-1}^n\right)^2$$

The conservation of energy equation in finite difference form is

$$M_i^{n+1} E_i^{n+1} = M_i^n \tilde{E}_i^n + \Delta M_{i-\frac{1}{2}}^n \tilde{E}_{i-1}^n - \Delta M_{i+\frac{1}{2}}^n \tilde{E}_i^n$$

$$\text{or} \quad \frac{M_i^{n+1} E_i^{n+1} - M_i^n E_i^n}{\Delta t} = \left[\begin{array}{l} -\frac{P_i^n}{4}\left[U_{i+1}^n + \tilde{U}_{i+1}^n - U_{i-1}^n - \tilde{U}_{i-1}^n\right] \\ -\frac{U_i^n}{2}\left(P_{i+1}^n - P_{i-1}^n\right) \\ +\frac{\Delta t}{8\rho_i^n \Delta x}\left(P_{i+1}^n - P_{i-1}^n\right)^2 \\ +\rho_{i-1}^n U_{i-\frac{1}{2}}^{*n} \tilde{E}_{i-1}^n - \rho_i^n U_{i+\frac{1}{2}}^{*n} \tilde{E}_i^n \end{array}\right]$$

$$\text{Hence} \quad \frac{M_i^{n+1} E_i^{n+1} - M_i^n E_i^n}{\Delta t} = \left[\begin{array}{l} -\frac{\partial PU}{\partial x}\Big|_i^n \Delta x + \rho_{i-1}^n U_{i-\frac{1}{2}}^{*n} \tilde{E}_{i-1}^n \\ \quad - \rho_i^n U_{i+\frac{1}{2}}^{*n} \tilde{E}_i^n \\ \quad + O(\Delta x^2) + O(\Delta x \Delta t) \end{array}\right] \qquad (26)$$

(a) Donor

$$U^{*n}_{i-\frac{1}{2}} = U^{n}_{i-1} \text{ and } U^{*n}_{i+\frac{1}{2}} = U^{n}_{i}$$

Hence $\rho^{n}_{i-1}\, U^{*n}_{i-\frac{1}{2}}\, \tilde{E}^{n}_{i-1} - \rho^{n}_{i}\, U^{*n}_{i+\frac{1}{2}}\, \tilde{E}^{n}_{i} =$

$$\rho^{n}_{i-1}\, U^{n}_{i-1} \left[E^{n}_{i-1} - \frac{P^{n}_{i-1}\,\Delta t}{\rho^{n}_{i-1}\,\Delta x\, 4} \left(U^{n}_{i} + \tilde{U}^{n}_{i} - U^{n}_{i-2} - \tilde{U}^{n}_{i-2}\right) - \frac{U^{n}_{i-1}\,\Delta t}{2\rho^{n}_{i-1}\Delta x} \left(P^{n}_{i} - P^{n}_{i-2}\right) + O(\Delta t^{2}) \right]$$

$$- \rho^{n}_{i}\, U^{n}_{i} \left[E^{n}_{i} - \frac{P^{n}_{i}\,\Delta t}{\rho^{n}_{i}\,\Delta x\, 4} \left(U^{n}_{i+1} + \tilde{U}^{n}_{i+1} - U^{n}_{i-1} - \tilde{U}^{n}_{i-1}\right) - \frac{U^{n}_{i}\,\Delta t}{2\rho^{n}_{i}\,\Delta x} \left(P^{n}_{i+1} - P^{n}_{i-1}\right) + O(\Delta t^{2}) \right]$$

$$= \rho^{n}_{i-1}\, U^{n}_{i-1}\, E^{n}_{i-1} - \rho^{n}_{i}\, U^{n}_{i}\, E^{n}_{i} + O(\Delta t^{2}) + O(\Delta x \Delta t)$$

Hence equation (26) becomes

$$\frac{\rho^{n+1}_{i}\, E^{n+1}_{i} - \rho^{n}_{i}\, E^{n}_{i}}{\Delta t} + \frac{\partial PU}{\partial x}\Big|^{n}_{i} + \frac{(\rho EU)^{n}_{i} - (\rho EU)^{n}_{i-1}}{\Delta x}$$

$$= O(\Delta t) + O\left(\frac{\Delta t^{2}}{\Delta x}\right)$$

Therefore

$$\frac{(\rho E)_i^{n+1} - (\rho E)_i^n}{\Delta t} + \frac{(\rho EU)_i^n - (\rho EU)_{i-1}^n}{\Delta x} + \frac{(PU)_i^n - (PU)_{i-1}^n}{\Delta x}$$

$$= \frac{\partial \rho E}{\partial t} + \frac{\partial \rho EU}{\partial x} + \frac{\partial PU}{\partial x}$$

$$+ O(\Delta t) + O(\Delta x) + O\left(\frac{\Delta t^2}{\Delta x}\right)$$

(b) continuous rezone

$$\rho_i^n U_{i+\frac{1}{2}}^{*n_1} \tilde{E}_i^n = \rho_i^n \left[U_{i+\frac{1}{2}}^{n_1} - \Delta t \left\{ \frac{1}{2\rho_i^n} \frac{\partial P}{\partial x} \Big|_{i+\frac{1}{2}} + U_{i+\frac{1}{2}}^{n_1} \frac{\partial U}{\partial x} \Big|_i \right\} \right] \times$$

$$\left[\begin{array}{l} E_i^n - \dfrac{P_i^n \Delta t}{\rho_i^n \Delta x \; 4} \left(U_{i+1}^n + \tilde{U}_{i+1}^n - U_{i-1}^n - \tilde{U}_{i-1}^n \right) \\ \\ \quad - \dfrac{U_i^n \Delta t}{2\rho_i^n \Delta x} \left(P_{i+1}^n - P_{i-1}^n \right) + O(\Delta t^2) \end{array} \right]$$

Hence, the right hand side of equation (26) becomes

$$- \frac{\partial PU}{\partial x} \Big|_i^n \Delta x + O(\Delta x^2) + O(\Delta x \Delta t)$$

$$+ \left[U_{i-1}^n + \frac{\partial U}{\partial x} \Big|_{i-1} \frac{\Delta x}{2} - \Delta t \left\{ \frac{1}{2\rho_{i-1}^n} \frac{\partial P}{\partial x} \Big|_{i-\frac{1}{2}} + U_{i-\frac{1}{2}}^{n_1} \frac{\partial U}{\partial x} \Big|_{i-1} \right\} \right] \times$$

$$+ O(\Delta x \Delta t) + O(\Delta t^2) + O(\Delta x^2)$$

$$\left[\rho_{i-1}^{n}\, E_{i-1}^{n} - \frac{P_{i-1}^{n}\,\Delta t}{4\Delta x}\,[U_i^n + \tilde{U}_i^n - U_{i-2}^n - \tilde{U}_{i-2}^n] - \frac{U_{i-1}^{n}}{2\Delta x}\,(P_i^n - P_{i-2}^n)\,\Delta t + O(\Delta t^2)\right]$$

$$-\left[U_i^n + \frac{\partial U}{\partial x}\Big|_i \frac{\Delta x}{2} - \Delta t\left\{\frac{1}{2\rho_i^n}\frac{\partial P}{\partial x}\Big|_{i+\frac{1}{2}} + U_{i+\frac{1}{2}}^{n}\frac{\partial U}{\partial x}\Big|_i\right\} + O(\Delta x\Delta t) + O(\Delta t^2) + O(\Delta x^2)\right] \times$$

$$\left[\rho_i^n\, E_i^n - \frac{P_i^n\,\Delta t}{4\Delta x}\,[U_{i+1}^n + \tilde{U}_{i+1}^n - U_{i-1}^n - \tilde{U}_{i-1}^n] - U_i\,\frac{(P_{i+1}^n - P_{i-1}^n)\,\Delta t}{2\Delta x} + O(\Delta t^2)\right]$$

Hence, it can be seen that

$$\frac{M_i^{n+1}\, E_i^{n+1} - M_i^n\, E_i^n}{\Delta t} + \frac{\partial PU}{\partial x}\Big|_i \Delta x + \rho_i^n\, E_i^n\, U_i^n - \rho_{i-1}^n\, E_{i-1}^n\, U_{i-1}^n$$

$$= O(\Delta t^2) + O(\Delta x^2) + O(\Delta t\Delta x)$$

Therefore

$$\frac{(\rho E)_i^{n+1} - (\rho E)_i^n}{\Delta t} + \frac{(\rho EU)_i^n - (\rho EU)_{i-1}^n}{\Delta x} + \frac{(PU)_i^n - (PU)_{i-1}^n}{\Delta x}$$

$$= \frac{\partial \rho E}{\partial t} + \frac{\partial \rho EU}{\partial x} + \frac{\partial PU}{\partial x} + O(\Delta x) + O(\Delta t) + O(\frac{\Delta t^2}{\Delta x})$$

(c) OIL

As stated previously, the mass transport terms for continuous rezone and OIL are equal. Also, the $\tilde{E}_i^n$ (i an integer) for continuous rezone and OIL are equal and hence the calculations of the order of the error for OIL and continuous rezone are the same.

LIST OF REFERENCES

[1] Evans, M. W., and Harlow, F. H., "The Particle-in-Cell Method for Hydrodynamic Calculations", Los Alamos Scientific Laboratory Report No. LA-2139 (1957).

[2] Hicks, Darrell, "Hydrocode Test Problems", Air Force Weapons Laboratory Report No. AFWL-TR-67-127 (1968).

[3] Hicks, Darrell and Pelzl, Robert, "Comparison between a Von Neumann-Richtmyer Hydrocode (AFWL's PUFF) and a Lax-Wendroff Hydrocode", Air Force Weapons Laboratory Report No. AFWL-TR-68-112 (1968).

[4] Von Neumann, J., and Richtmyer, R., "A Method for the Numerical Calculation of Hydrodynamic Shocks", J. Appl. Phys., Vol. 21 (1950), P. 232.

[5] Hicks, Darrell, "The Convergence of Numerical Solutions of Hydrodynamic Shock Problems", Air Force Weapons Laboratory Report No. AFWL-TR-69-20 (1969), p. 32.

[6] Landshoff, R., "A Numerical Method for Treating Fluid Flow in the Presence of Shocks", Los Alamos Scientific Laboratory Report No. LA-1930 (1955).

[7] Bjork, R., Brooks, N., and Papetti, R., "A Numerical Technique for Solution of Multidimensional Hydrodynamic Problems", Rand Corporation Report No. RM-2628-PR (1963).

[8] Kaplan, M. A., and Papetti, R. A., "An Analysis of the Two Dimensional Particle-in-Cell Method", Rand Corporation Report No. RM-4876-PR (1966).

[9] Amsden, Anthony A., "The Particle-in-Cell Method for the Calculation of the Dynamics of Compressible Fluids", Los Alamos Scientific Laboratory Report No. LA-3466 (1966), p. 25.

[10] Johnson, W. E., "OIL: A Continuous Two-Dimensional Eulerian Hydrodynamic Code", General Dynamics Corporation, General Atomic Division Report No. GAMD 5580 (1965), p. 23.

[11] Rich, Marvin, "A Method for Eulerian Fluid Dynamics", Los Alamos Scientific Laboratory Report No. LAMS-2826 (1962).

[12] Schulz, William D., "Two-Dimensional Lagrangian Hydrodynamic Difference Equations", Meth. Comp. Phys., Vol. 3 (1964), p. 1.

UNCLASSIFIED

Security Classification

DOCUMENT CONTROL DATA - R & D

(Security classification of title, body of abstract and indexing annotation must be entered when the overall report is classified)

ORIGINATING ACTIVITY *(Corporate author)*

epartment of Computer Science
niversity of Illinois at Urbana-Champaign
rbana, Illinois 61801

2a. REPORT SECURITY CLASSIFICATION

UNCLASSIFIED

2b. GROUP

REPORT TITLE

N ANALYSIS OF SOME EULERIAN METHODS FOR ONE DIMENSIONAL,
NVISCID, COMPRESSIBLE HYDRODYNAMICS

DESCRIPTIVE NOTES *(Type of report and inclusive dates)*

esearch Report

AUTHOR(S) *(First name, middle initial, last name)*

anley J. Flowerdew

REPORT DATE	7a. TOTAL NO. OF PAGES	7b. NO. OF REFS
eptember 22, 1969	163	12

CONTRACT OR GRANT NO.	9a. ORIGINATOR'S REPORT NUMBER(S)
-26-15-305 PROJECT NO. AF 30(602)4144	DCS Report No. 352
	9b. OTHER REPORT NO(S) *(Any other numbers that may be assigned this report)*

DISTRIBUTION STATEMENT

ualified requesters may obtain copies of this report from DCS.

SUPPLEMENTARY NOTES	12. SPONSORING MILITARY ACTIVITY
ONE	Rome Air Development Center Griffiss Air Force Base Rome, New York 13440

ABSTRACT

The description and comparison of several explicit differencing schemes for the solution of the inviscid, non-thermal-conducting, single-material, one-dimensional equations of compressible hydrodynamics is included in this report. The comparison was based on the plots obtained from a series of one dimensional test problems which are included in APPENDIX A.

D FORM 1 NOV 65 1473

UNCLASSIFIED

Security Classification

14. KEY WORDS	LINK A		LINK B		LINK C	
	ROLE	WT	ROLE	WT	ROLE	WT
explicit differencing schemes						
one-dimensional, inviscid, compressible hydrodynamics						
Eulerian methods						
particle-in-cell method						